

HEP Physics Opportunities Using Reactor Antineutrinos: A Snowmass 2021 White Paper Submission

Abstract

Nuclear reactors are uniquely powerful, abundant, and flavor-pure sources of antineutrinos that continue to play a vital role in the US neutrino physics program. The US reactor antineutrino physics community is a diverse interest group encompassing many detection technologies and many particle physics topics, including Standard Model and short-baseline oscillations, BSM physics searches, and reactor flux and spectrum modelling. The community's aims offer strong complimentary with numerous aspects of the wider US neutrino program and have direct relevance to most of the topical sub-groups composing the Snowmass 2021 Neutrino Frontier. Reactor neutrino experiments also have a direct societal impact and have become a strong workforce and technology development pipeline for DOE National Laboratories and universities.

This white paper, prepared as a submission to the Snowmass 2021 community organizing exercise, will survey the state of the reactor antineutrino physics field and summarize the ways in which current and future reactor antineutrino experiments can play a critical role in advancing the field of particle physics in the next decade. As it is directed towards the Snowmass 2021 Neutrino Frontier, Sections 4 through 9 are organized around specific Topical Groups within that Frontier, with the relevant Topical Group specified in each Section's title. Finally, to enable quick reference to the document's main themes, two to four 'Key Takeaways' are provided at the beginning of each Section.

O. A. Akindele,¹ J. M. Berryman,^{2,3} N. S. Bowden,¹ R. Carr,⁴ A. J. Conant,⁵ P. Huber,⁶
T. J. Langford,⁷ J. M. Link,⁶ B. R. Littlejohn,⁸ G. Fernandez-Moroni,^{9,10} J. P. Ochoa-Ricoux,¹¹
C. Roca,¹ S. Schoppmann,^{12,3} L. Strigari,¹³ J. Xu,¹ C. Zhang,¹⁴ and X. Zhang¹
(White Paper Editors)

C. Awe,^{15,16} P. S. Barbeau,^{15,16} A. Haghghat,^{6,17} S. C. Li,⁶
J. M. Link,⁶ V. Mascolino,¹⁷ T. Subedi,⁶ and K. Walkup⁶
(The CHANDLER Collaboration)

P. S. Barbeau,^{15,16} E. P. Bernard,¹ N. S. Bowden,¹ I. Jovanovic,¹⁸ J. W. Kingston,^{19,1} E. Mizrachi,^{20,1}
E. Pantic,¹⁹ T. J. Pershing,¹ S. V. Pereverzev,¹ C. G. Prior,^{15,16} R. Smith,²¹ J. Xu,¹ and A. Bernstein¹
(The CHILLAX development team)

A. Aguilar-Arevalo,²² N. Avalos,²³ J. Bernal,²⁴ X. Bertou,²³ C. Bonifazi,^{25,26} G. Cancelo,⁹
V. G. P. B. de Carvalho,²⁵ B. A. Cervantes-Vergara,²² C. Chavez,²⁴ J. C. D'Olivo,²² J. M. De
Egea,²⁴ J. C. dos Anjos,²⁷ J. Estrada,⁹ A. R. Fernandez Neto,²⁸ G. Fernandez-Moroni,^{9,10}
A. Foguel,²⁵ R. Ford,⁹ J. Gasanego,²⁹ J. Gonzalez-Cuevas,²⁴ A. Haghghat,^{6,17} S. Hernandez,⁹
F. Izraelevitch,²⁹ B. Kilminster,³⁰ K. Kuk,⁹ P. Lemos,²⁵ H. P. Lima Jr.,²⁷ M. Makler,^{27,26}
F. Marinho,³¹ K. Maslova,²⁵ L. H. Mendes,²⁵ J. Molina,²⁴ M. M. Montero,²² P. Mota,²⁷
I. Nasteva,²⁵ A. C. Oliveira,²⁵ E. Paolini,¹⁰ L. Paulucci,³² D. Rodrigues,³³ C. Romero,²⁴
Y. Sarkis,²² M. S. Haro,²³ A. Soto,¹⁰ D. Stalder,²⁴ J. Tiffenberg,⁹ C. Torres,²⁴ and P. Z. Ventura²⁵
(The CONNIE Collaboration)

A. Bonhomme,³⁴ C. Buck,³⁴ J. Hakenmüller,³⁴ M. Lindner,³⁴
W. Maneschg,³⁴ E. Sanchez Garcia,³⁴ and T. Rink³⁴
(on behalf of The CONUS Collaboration)

F. P. An,³⁵ W. D. Bai,³⁶ A. B. Balantekin,³⁷ M. Bishai,¹⁴ S. Blyth,³⁸ G. F. Cao,³⁹ J. Cao,³⁹ J. F. Chang,³⁹
Y. Chang,⁴⁰ H. S. Chen,³⁹ H. Y. Chen,⁴¹ S. M. Chen,⁴¹ Y. Chen,^{42,36} Y. X. Chen,⁴³ J. Cheng,³⁹
Z. K. Cheng,³⁶ J. J. Cherwinka,³⁷ M. C. Chu,⁴⁴ J. P. Cummings,⁴⁵ O. Dalager,¹¹ F. S. Deng,⁴⁶ Y. Y. Ding,³⁹
M. V. Diwan,¹⁴ T. Dohnal,⁴⁷ D. Dolzhikov,⁴⁸ J. Dove,⁴⁹ D. A. Dwyer,⁵⁰ J. P. Gallo,⁸ M. Gonchar,⁴⁸
G. H. Gong,⁴¹ H. Gong,⁴¹ W. Q. Gu,¹⁴ J. Y. Guo,³⁶ L. Guo,⁴¹ X. H. Guo,⁵¹ Y. H. Guo,⁵² Z. Guo,⁴¹
R. W. Hackenburg,¹⁴ A. Haghghat,^{6,17} S. Hans,^{14,*} M. He,³⁹ K. M. Heeger,⁷ Y. K. Heng,³⁹ Y. K. Hor,³⁶
Y. B. Hsiung,³⁸ B. Z. Hu,³⁸ J. R. Hu,³⁹ T. Hu,³⁹ Z. J. Hu,³⁶ H. X. Huang,⁵³ J. H. Huang,³⁹ X. T. Huang,⁵⁴
Y. B. Huang,⁵⁵ P. Huber,⁶ D. E. Jaffe,¹⁴ K. L. Jen,⁵⁶ X. L. Ji,³⁹ X. P. Ji,¹⁴ D. Jones,⁵⁷ L. Kang,⁵⁸
S. H. Kettell,¹⁴ S. Kohn,²¹ M. Kramer,^{50,21} T. J. Langford,⁷ J. Lee,⁵⁰ J. H. C. Lee,⁵⁹ R. T. Lei,⁵⁸
R. Leitner,⁴⁷ J. K. C. Leung,⁵⁹ F. Li,³⁹ H. L. Li,³⁹ J. J. Li,⁴¹ Q. J. Li,³⁹ R. H. Li,³⁹ S. Li,⁵⁸ S. C. Li,⁶
W. D. Li,³⁹ X. N. Li,³⁹ X. Q. Li,⁶⁰ Y. F. Li,³⁹ Z. B. Li,³⁶ H. Liang,⁴⁶ C. J. Lin,⁵⁰ G. L. Lin,⁵⁶ S. Lin,⁵⁸
J. J. Ling,³⁶ J. M. Link,⁶ L. Littenberg,¹⁴ B. R. Littlejohn,⁸ J. C. Liu,³⁹ J. L. Liu,⁶¹ J. X. Liu,³⁹ C. Lu,⁶²
H. Q. Lu,³⁹ K. B. Luk,^{21,50} B. Z. Ma,⁵⁴ X. B. Ma,⁴³ X. Y. Ma,³⁹ Y. Q. Ma,³⁹ R. C. Mandujano,¹¹
C. Marshall,⁵⁰ K. T. McDonald,⁶² R. D. McKeown,^{63,64} Y. Meng,⁶¹ J. Napolitano,⁵⁷ D. Naumov,⁴⁸
E. Naumova,⁴⁸ T. M. T. Nguyen,⁵⁶ J. P. Ochoa-Ricoux,¹¹ A. Olshevskiy,⁴⁸ H.-R. Pan,³⁸ J. Park,⁶
S. Patton,⁵⁰ J. C. Peng,⁴⁹ C. S. J. Pun,⁵⁹ F. Z. Qi,³⁹ M. Qi,⁶⁵ X. Qian,¹⁴ N. Raper,³⁶ J. Ren,⁵³
C. Morales Revoco,¹¹ R. Rosero,¹⁴ B. Roskovec,¹¹ X. C. Ruan,⁵³ J. L. Sun,⁶⁶ T. Tmej,⁴⁷ K. Treskov,⁴⁸
W.-H. Tse,⁴⁴ C. E. Tull,⁵⁰ B. Viren,¹⁴ V. Vorobel,⁴⁷ C. H. Wang,⁴⁰ J. Wang,³⁶ M. Wang,⁵⁴
N. Y. Wang,⁵¹ R. G. Wang,³⁹ W. Wang,^{36,64} X. Wang,⁶⁷ Y. Wang,⁶⁵ Y. F. Wang,³⁹ Z. Wang,³⁹
Z. Wang,⁴¹ Z. M. Wang,³⁹ H. Y. Wei,¹⁴ L. H. Wei,³⁹ L. J. Wen,³⁹ K. Whisnant,⁶⁸ C. G. White,⁸
H. L. H. Wong,^{21,50} E. Worcester,¹⁴ D. R. Wu,³⁹ Q. Wu,⁵⁴ W. J. Wu,³⁹ D. M. Xia,⁶⁹ Z. Q. Xie,³⁹

Z. Z. Xing,³⁹ H. K. Xu,³⁹ J. L. Xu,³⁹ T. Xu,⁴¹ T. Xue,⁴¹ C. G. Yang,³⁹ L. Yang,⁵⁸ Y. Z. Yang,⁴¹
H. F. Yao,³⁹ M. Ye,³⁹ M. Yeh,¹⁴ B. L. Young,⁶⁸ H. Z. Yu,³⁶ Z. Y. Yu,³⁹ B. B. Yue,³⁶ V. Zavadskiy,⁴⁸
S. Zeng,³⁹ Y. Zeng,³⁶ L. Zhan,³⁹ C. Zhang,¹⁴ F. Y. Zhang,⁶¹ H. H. Zhang,³⁶ J. L. Zhang,⁶⁵ J. W. Zhang,³⁹
Q. M. Zhang,⁵² S. Q. Zhang,³⁶ X. T. Zhang,³⁹ Y. M. Zhang,³⁶ Y. X. Zhang,⁶⁶ Y. Y. Zhang,⁶¹ Z. J. Zhang,⁵⁸
Z. P. Zhang,⁴⁶ Z. Y. Zhang,³⁹ J. Zhao,³⁹ R. Z. Zhao,³⁹ L. Zhou,³⁹ H. L. Zhuang,³⁹ and J. H. Zou³⁹

(The Daya Bay Collaboration)

T. Abrahão,^{70,71} H. Almazan,⁷² J.C. dos Anjos,⁷⁰ S. Appel,⁷³ J.C. Barriere,⁷⁴ I. Bekman,⁷⁵
T.J.C. Bezerra,⁷⁶ L. Bezrukov,⁷⁷ E. Blucher,⁷⁸ T. Brugière,⁷⁹ C. Buck,⁷² J. Busenitz,⁸⁰ A. Cabrera,^{71,81,82}
M. Cerrada,⁸³ E. Chauveau,⁸⁴ P. Chimenti,⁷⁰ O. Corpacci,⁷⁴ J.V. Dawson,⁷¹ Z. Djurcic,⁸⁵ A. Etenko,⁸⁶
H. Furuta,⁸⁷ I. Gil-Botella,⁸³ A. Givaudan,⁷¹ H. Gomez,^{71,74} L.F.G. Gonzalez,⁸⁸ M.C. Goodman,⁸⁵
T. Hara,⁸⁹ J. Haser,⁷² D. Hellwig,⁷⁵ A. Hourlier,⁷¹ M. Ishitsuka,⁹⁰ J. Jochum,⁹¹ C. Jollet,⁸⁴ K. Kale,^{84,79}
M. Kaneda,⁹⁰ M. Karakac,⁷¹ T. Kawasaki,⁹² E. Kemp,⁸⁸ D. Kryn,⁷¹ M. Kuze,⁹⁰ T. Lachenmaier,⁹¹
C.E. Lane,⁹³ T. Lasserre,^{74,71} C. Lastoria,⁸³ D. Lhuillier,⁷⁴ H.P. Lima Jr,⁷⁰ M. Lindner,⁷²
J.M. López-Castaño,⁸³ J.M. LoSecco,⁹⁴ B. Lubsandorzhev,⁷⁷ J. Maeda,^{95,89} C. Mariani,⁹⁶ J. Maricic,⁹³
J. Martino,⁷⁶ T. Matsubara,⁹⁵ G. Mention,⁷⁴ A. Meregaglia,⁸⁴ T. Miletic,⁹³ R. Milincic,⁹³ A. Minotti,⁷⁴
D. Navas-Nicolás,^{71,83,82} P. Novella,⁸³ L. Oberauer,⁷³ M. Obolensky,⁷¹ A. Onillon,⁷⁴ A. Oralbaev,⁸⁶
C. Palomares,⁸³ I.M. Pepe,⁷⁰ G. Pronost,⁷⁶ J. Reichenbacher,⁸⁰ B. Reinhold,⁷² S. Schönert,⁷³
S. Schoppmann,⁷² L. Scola,⁷⁴ R. Sharankova,⁹⁰ V. Sibille,⁷⁴ V. Sinev,⁷⁷ M. Skorokhvatov,⁸⁶ P. Soldin,⁷⁵
A. Stahl,⁷⁵ I. Stancu,⁸⁰ L.F.F. Stokes,⁹¹ F. Suekane,^{87,71} S. Sukhotin,⁸⁶ T. Sumiyoshi,⁹⁵ Y. Sun,⁸⁰
C. Veysièrre,⁷⁴ B. Viaud,⁷⁶ M. Vivier,⁷⁴ S. Wagner,^{71,70} C. Wiebusch,⁷⁵ G. Yang,⁸⁵ and F. Yermia⁷⁶

(The Double Chooz Collaboration)

T. Anderson,⁹⁷ E. Anderssen,¹² M. Askins,^{12,3} A. J. Bacon,⁹⁸ Z. Bagdasarian,^{12,3}
A. Baldoni,⁹⁷ N. Barros,^{99,100} L. Bartoszek,¹⁰¹ A. Bat,¹⁰² M. Bergevin,¹ A. Bernstein,¹
E. Blucher,⁷⁸ J. Boissevain,¹⁰¹ R. Bonventre,¹² D. Brown,¹² E. J. Callaghan,^{12,3}
D. F. Cowen,⁹⁷ S. Dazeley,¹ M. Diwan,¹⁴ K. Frankiewicz,¹⁰³ C. Grant,¹⁰³ T. Kaptanoglu,^{12,3}
J.R. Klein,⁹⁸ C. Kraus,^{104,105} T. Kroupa,⁹⁸ B. Land,^{12,3,98} L. Lebanowski,⁹⁸ V. Lozza,^{99,100}
A. Marino,¹⁰⁶ A. Mastbaum,¹⁰⁷ C. Mauger,⁹⁸ S. Naugle,⁹⁸ M. Newcomer,⁹⁸ A. Nikolica,⁹⁸
G. D. Orebi Gann,^{12,3} L. Pickard,¹⁰⁸ J. Saba,¹² S. Schoppmann,^{12,3} J. Sensenig,⁹⁸ M. Smiley,^{12,3}
H. Steiger,^{109,110} R. Svoboda,¹⁰⁸ E. Tiras,^{102,111} W. H. Trzaska,¹¹² R. van Berg,^{98,101}
G. Wendel,⁹⁷ M. Wetstein,¹¹³ M. Wurm,¹⁰⁹ G. Yang,^{12,3} M. Yeh,¹⁴ and E.D. Zimmerman¹⁰⁶

(The EOS team)

A. Abusleme,¹¹⁴ T. Adam,¹¹⁵ S. Ahmad,¹¹⁶ R. Ahmed,¹¹⁶ S. Aiello,¹¹⁷ M. Akram,¹¹⁶ A. Aleem,¹¹⁶
T. Alexandros,¹¹⁸ F. P. An,¹¹⁹ Q. An,⁴⁶ G. Andronico,¹¹⁷ N. Anfimov,⁴⁸ V. Antonelli,¹²⁰ T. Antoshkina,⁴⁸
B. Asavapibhop,¹²¹ J. P. A. M. de André,¹¹⁵ D. Auguste,¹²² W. Bai,³⁶ N. Balashov,⁴⁸ W. Baldini,¹²³
A. Barresi,¹²⁴ D. Basilico,¹²⁰ E. Baussan,¹¹⁵ M. Bellato,¹²⁵ A. Bergnoli,¹²⁵ T. Birkenfeld,¹¹⁸ S. Blin,¹²²
D. Blum,¹²⁶ S. Blyth,³⁸ A. Bolshakova,⁴⁸ M. Bongrand,¹²² C. Bordereau,^{127,40} D. Breton,¹²²
A. Brigatti,¹²⁰ R. Brugnera,¹²⁸ R. Bruno,¹¹⁷ A. Budano,¹²⁹ Jose Busto,¹³⁰ A. Cabrera,¹²² B. Caccianiga,¹²⁰
H. Cai,¹³¹ X. Cai,³⁹ Y. K. Cai,³⁹ Z. Y. Cai,³⁹ R. Callegari,¹²⁸ A. Cammi,¹³² A. Campeny,¹¹⁴ C. Y. Cao,³⁹
G. F. Cao,³⁹ J. Cao,³⁹ R. Caruso,¹¹⁷ C. Cerna,¹²⁷ C. Chan,⁵⁶ J. F. Chang,³⁹ Y. Chang,⁴⁰ P. P. Chen,¹³³
P. A. Chen,³⁸ S. Chen,¹³⁴ X. Chen,¹³⁵ Y. Chen,⁴³ Y. Chen,³⁶ Z. Chen,³⁹ Z. Chen,³⁶ J. Cheng,⁴³
Y. Cheng,¹³⁶ Y. C. Cheng,³⁸ A. Chetverikov,⁴⁸ D. Chiesa,¹²⁴ P. Chimenti,¹³⁷ Z. Chu,³⁹ A. Chukanov,⁴⁸
G. Claverie,¹²⁷ C. Clementi,¹³⁸ B. Clerboux,¹³⁹ S. Di Lorenzo,¹²² D. Corti,¹²⁵ F. D. Corso,¹²⁵
O. Dalager,¹¹ C. De La Taille,¹²² Z. Deng,¹³⁴ Z. Y. Deng,³⁹ W. Depnering,¹⁴⁰ M. Diaz,¹¹⁴ X. F. Ding,¹²⁰
Y. Y. Ding,³⁹ B. Dirgantara,¹⁴¹ S. Dmitrievsky,⁴⁸ T. Dohnal,⁴⁷ D. Dolzhikov,⁴⁸ G. Donchenko,¹⁴²
J. M. Dong,¹³⁴ E. Doroshkevich,¹⁴³ W. Dou,¹³⁴ M. Dracos,¹¹⁵ F. Druillolle,¹²⁷ R. Du,³⁹ S. X. Du,¹⁴⁴

S. Dusini,¹²⁵ M. Dvorak,⁴⁷ T. Enqvist,¹⁴⁵ A. Fabbri,¹²⁹ U. Fahrenholz,¹⁴⁶ D. H. Fan,¹⁴⁷ L. Fan,³⁹
 J. Fang,³⁹ W. X. Fang,³⁹ M. Fargetta,¹¹⁷ D. Fedoseev,⁴⁸ Z. Fei,³⁹ L. C. Feng,⁵⁶ Q. C. Feng,¹⁴⁸
 F. Ferraro,¹²⁰ R. Ford,¹²⁰ A. Fournier,¹²⁷ H. N. Gan,¹⁴⁹ F. Gao,¹¹⁸ A. Garfagnini,¹²⁸ A. Gavrikov,⁴⁸
 M. Giammarchi,¹²⁰ N. Giudice,¹¹⁷ M. Gonchar,⁴⁸ G. Gong,¹³⁴ H. Gong,¹³⁴ Y. Gornushkin,⁴⁸
 A. Göttel,^{150,118} M. Grassi,¹²⁸ V. Gromov,⁴⁸ M. Gu,³⁹ X. Gu,¹⁴⁴ Y. Gu,¹⁵¹ M. Y. Guan,³⁹ Y. D. Guan,³⁹
 N. Guardone,¹¹⁷ C. Guo,³⁹ J. Y. Guo,³⁶ W. L. Guo,³⁹ X. H. Guo,⁵¹ Y. H. Guo,¹⁵⁰ C. Hagner,¹⁵² R. Han,¹³⁶
 Y. Han,³⁶ M. He,³⁹ W. He,³⁹ T. Heinz,¹²⁶ P. Hellmuth,¹²⁷ Y. K. Heng,³⁹ R. Herrera,¹¹⁴ Y. K. Hor,³⁶
 S. J. Hou,³⁹ Y. Hsiung,³⁸ B. Z. Hu,³⁸ H. Hu,³⁶ J. R. Hu,³⁹ J. Hu,³⁹ S. Y. Hu,⁵³ T. Hu,³⁹ Y. X. Hu,³⁹
 Z. J. Hu,³⁶ G. H. Huang,³⁹ H. X. Huang,⁵³ K. X. Huang,³⁶ W. H. Huang,⁵⁴ X. Huang,³⁹ X. T. Huang,⁵⁴
 Y. B. Huang,⁵⁵ J. Q. Hui,¹⁵³ L. Huo,¹⁴⁸ W. Huo,⁴⁶ C. Huss,¹²⁷ S. Hussain,¹¹⁶ A. Ioannisian,¹⁵⁴
 R. Isocrate,¹²⁵ B. Jelmini,¹²⁸ I. Jeria,¹¹⁴ X. L. Ji,³⁹ H. H. Jia,⁶⁰ J. J. Jia,¹³¹ S. Y. Jian,⁵³ D. Jiang,⁴⁶
 W. Jiang,³⁹ X. S. Jiang,³⁹ X. P. Jing,³⁹ C. Jollet,¹²⁷ J. Joutsenvaara,¹⁴⁵ L. Kalousis,¹¹⁵ P. Kampmann,^{150,118}
 L. Kang,¹³³ R. Karaparambil,¹⁵⁵ N. Kazarian,¹⁵⁴ A. Khatun,¹⁵⁶ K. Khosonthongkee,¹⁴¹ D. Korablev,⁴⁸
 K. Kouzakov,¹⁴² A. Krasnoperov,⁴⁸ N. Kutovskiy,⁴⁸ P. Kuusiniemi,¹⁴⁵ T. Lachenmaier,¹²⁶ C. Landini,¹²⁰
 S. Leblanc,¹²⁷ V. Lebrin,¹⁵⁵ F. Lefevre,¹⁵⁵ R. Lei,¹³³ R. Leitner,⁴⁷ J. Leung,⁵⁶ D. Z. Li,³⁹ D. Li,¹⁴⁴ F. Li,³⁹
 F. Li,¹³⁴ H. Li,³⁶ G. S. Li,³⁹ H. L. Li,³⁹ M. Z. Li,³⁹ M. Li,⁴³ N. Li,⁶⁷ N. Li,³⁹ Q. J. Li,⁶⁷ R. H. Li,³⁹
 R. Li,¹⁵³ S. F. Li,¹³³ T. Li,³⁶ T. Li,⁵⁴ W. D. Li,³⁹ W. G. Li,³⁹ X. M. Li,⁵³ X. N. Li,³⁹ X. L. Li,⁵³
 Y. Li,¹³³ Y. C. Li,³⁹ Y. F. Li,³⁹ Z. Li,³⁹ Z. H. Li,³⁹ Z. B. Li,³⁶ Z. Y. Li,³⁶ Z. H. Li,¹³¹ H. Liang,⁴⁶
 H. Liang,⁵³ J. J. Liao,³⁶ A. Limphirat,¹⁴¹ G. L. Lin,⁵⁶ S. X. Lin,¹³³ T. Lin,³⁹ J. J. Ling,³⁶ I. Lippi,¹²⁵
 F. Liu,⁴³ H. D. Liu,¹⁴⁴ H. T. Liu,¹³¹ H. B. Liu,⁵⁵ H. J. Liu,¹⁵⁷ H. T. Liu,³⁶ H. Liu,¹⁵¹ J. L. Liu,^{153,158}
 J. C. Liu,³⁹ M. Liu,¹⁵⁷ Q. Liu,¹⁵⁹ Q. Liu,⁴⁶ R. X. Liu,^{150,118} S. B. Liu,⁴⁶ S. L. Liu,³⁹ X. W. Liu,³⁶
 X. Liu,⁵⁵ Y. Liu,³⁹ Y. Liu,³⁹ A. Lokhov,¹⁴² P. Lombardi,¹²⁰ C. Lombardo,¹⁶⁰ K. Loo,¹⁴⁰ C. Lu,¹⁶¹
 H. Q. Lu,³⁹ J. B. Lu,¹⁶² J. G. Lu,³⁹ P. Z. Lu,³⁶ S. X. Lu,¹⁴⁴ B. Lubsandorzhev,¹⁴³ S. Lubsandorzhev,¹⁴³
 L. Ludhova,^{150,118} A. Lukanov,¹⁴³ D. B. Luo,³⁹ F. J. Luo,³⁹ G. Luo,³⁶ S. Luo,¹⁶³ W. M. Luo,³⁹
 X. J. Luo,³⁹ V. Lyashuk,¹⁴³ B. Z. Ma,⁵⁴ B. Ma,¹⁴⁴ Q. M. Ma,³⁹ S. Ma,³⁹ X. Y. Ma,³⁹ X. B. Ma,⁴³
 J. Maalmi,¹²² M. Magoni,¹²⁰ J. Y. Mai,³⁶ Y. Malyshev,⁴⁸ R. C. Mandujano,¹¹ F. Mantovani,¹²³
 X. Mao,¹³⁶ Y. J. Mao,¹⁶⁴ S. M. Mari,¹²⁹ F. Marini,¹²⁸ C. Martellini,¹²⁹ G. Martin-Chassard,¹²²
 A. Martini,¹⁶⁵ M. Mayer,¹⁴⁶ D. Mayilyan,¹⁵⁴ I. Mednieks,¹⁶⁶ A. Meinus,¹⁴⁰ Y. Meng,¹⁵³
 A. Meregaglia,¹²⁷ E. Meroni,¹²⁰ D. Meyhöfer,¹⁵² M. Mezzetto,¹²⁵ J. Miller,¹⁴⁹ L. Miramonti,¹²⁰
 M. C. Molla,¹³⁹ P. Montini,¹²⁹ M. Montuschi,¹²³ A. Müller,¹²⁶ M. Nastasi,¹²⁴ D. V. Naumov,⁴⁸
 E. Naumova,⁴⁸ D. Navas-Nicolas,¹²² I. Nemchenok,⁴⁸ T. M. T. Nguyen,⁵⁶ F. P. Ning,³⁹ Z. Ning,³⁹
 H. Nunokawa,¹⁶⁷ L. Oberauer,¹⁴⁶ J. P. Ochoa-Ricoux,^{11,114} A. Olshevskiy,⁴⁸ D. Orestano,¹²⁹ F. Ortica,¹³⁸
 R. Othegraven,¹⁴⁰ A. Paoloni,¹⁶⁵ S. Parmeggiano,¹²⁰ Y. Pei,³⁹ L. Pelicci,^{150,118} N. Pelliccia,¹³⁸ A. Peng,¹⁵⁷
 H. Peng,⁴⁶ Y. Peng,³⁹ Z. Y. Peng,³⁹ F. Perrot,¹²⁷ P. A. Petitjean,¹³⁹ F. Petrucci,¹²⁹ O. Pilarczyk,¹⁴⁰
 L. F. Piñeres Rico,¹¹⁵ A. Popov,¹⁴² P. Poussot,¹¹⁵ E. Previtali,¹²⁴ F. Qi,³⁹ M. Qi,⁶⁵ S. Qian,³⁹ X. H. Qian,³⁹
 Z. Qian,³⁹ H. Qiao,¹⁶⁴ Z. H. Qin,³⁹ S. K. Qiu,¹⁵⁷ G. Ranucci,¹²⁰ N. Raper,³⁶ R. Rasheed,¹²⁷ A. Re,¹²⁰
 H. Rebber,¹⁵² A. Rebi,¹²⁷ M. Redchuk,^{125,128} B. Ren,¹³³ J. Ren,⁵³ B. Ricci,¹²³ M. Rifai,^{150,118}
 M. Roche,¹²⁷ N. Rodphai,¹²¹ A. Romani,¹³⁸ B. Roskovec,⁴⁷ X. Ruan,⁵³ S. Rujirawat,¹⁴¹ A. Rybnikov,⁴⁸
 A. Sadovsky,⁴⁸ P. Saggese,¹²⁰ G. Salamanna,¹²⁹ S. Sanfilippo,¹²⁹ A. Sangka,¹⁶⁸ U. Sawangwit,¹⁶⁸
 J. Sawatzki,¹⁴⁶ M. Schever,^{150,118} C. Schwab,¹¹⁵ K. Schweizer,¹⁴⁶ A. Selyunin,⁴⁸ A. Serafini,¹²³
 G. Settanta,¹⁵⁰ M. Settimo,¹⁵⁵ Z. Shao,¹⁶⁹ V. Sharov,⁴⁸ A. Shaydurova,⁴⁸ J. Shi,³⁹ Y. Shi,³⁹ V. Shutov,⁴⁸
 A. Sidorenkov,¹⁴³ F. Šimkovic,¹⁵⁶ C. Sirignano,¹²⁸ J. Siripak,¹⁴¹ M. Sisti,¹²⁴ M. Slupecki,¹⁴⁵
 M. Smirnov,³⁶ O. Smirnov,⁴⁸ T. Sogo-Bezerra,¹⁵⁵ J. Songwadhana,¹⁴¹ B. Soonthornthum,¹⁶⁸
 A. Sotnikov,⁴⁸ O. Sramek,⁴⁷ W. Sreethawong,¹⁴¹ A. Stahl,¹¹⁸ L. Stanco,¹²⁵ K. Stankevich,¹⁴²
 D. Stefanik,¹⁵⁶ H. Steiger,¹⁴⁶ J. Steinmann,¹¹⁸ T. Sterr,¹²⁶ M. R. Stock,¹⁴⁶ V. Strati,¹²³ A. Studenikin,¹⁴²
 J. Su,³⁶ S. F. Sun,⁴³ X. L. Sun,³⁹ Y. J. Sun,⁴⁶ Y. Z. Sun,³⁹ N. Suwonjandee,¹²¹ M. Szelezniak,¹¹⁵ J. Tang,³⁶
 Q. Tang,³⁶ Q. Tang,¹⁵⁷ X. Tang,³⁹ V. T. Hariharan,¹⁵² E. Theisen,¹⁴⁰ A. Tietzsch,¹²⁶ I. Tkachev,¹⁴³

T. Tmej,⁴⁷ M. D. C. Torri,¹²⁰ K. Treskov,⁴⁸ A. Triossi,¹¹⁵ G. Troni,¹¹⁴ W. Trzaska,¹⁴⁵ C. Tuve,¹¹⁷ N. Ushakov,¹⁴³ V. Vedin,¹⁶⁶ G. Verde,¹¹⁷ M. Vialkov,¹⁴² B. Viaud,¹⁵⁵ C. M. Vollbrecht,^{118,150} C. Volpe,¹²² K. Von Sturm,¹²⁸ V. Vorobel,⁴⁷ D. Voronin,¹⁴³ L. Votano,¹⁶⁵ P. Walker,¹¹⁴ C. Wang,¹³³ C. H. Wang,⁴⁰ E. Wang,¹⁴⁴ G. Wang,¹⁴⁸ J. Wang,⁴⁶ J. Wang,³⁶ L. Wang,³⁹ M. F. Wang,³⁹ M. Wang,⁵⁴ M. Wang,¹⁵⁷ R. G. Wang,³⁹ S. G. Wang,¹⁶⁴ W. Wang,⁶⁵ W. Wang,³⁶ W. S. Wang,³⁹ X. Wang,⁶⁷ X. Y. Wang,³⁶ Y. F. Wang,³⁹ Y. G. Wang,¹³¹ Y. Wang,¹³⁴ Y. Wang,¹⁴⁷ Y. Wang,³⁹ Y. F. Wang,³⁹ Y. Q. Wang,¹³⁴ Y. Wang,⁶⁵ Z. Wang,¹³⁴ Z. Wang,³⁹ Z. M. Wang,³⁹ Z. Y. Wang,¹³⁴ A. Watcharangkool,¹⁶⁸ W. Wei,³⁹ W. Wei,¹⁴⁴ W. L. Wei,³⁹ Y. D. Wei,¹³³ K. Wen,³⁹ L. J. Wen,³⁹ J. Weng,¹³⁴ C. Wiebusch,¹¹⁸ S. C. F. Wong,³⁶ B. Wonsak,¹⁵² D. Wu,³⁹ Q. Wu,⁵⁴ Z. Wu,³⁹ M. Wurm,¹⁴⁰ J. Wurtz,¹¹⁵ C. Wysotzki,¹¹⁸ Y. F. Xi,¹⁶¹ D. M. Xia,⁶⁹ X. Xiao,³⁶ X. C. Xie,⁵⁵ Y. G. Xie,³⁹ Z. Q. Xie,³⁹ Z. Xin,³⁹ Z. Z. Xing,³⁹ B. Xu,¹³⁴ C. Xu,¹⁵⁷ D. L. Xu,^{158,153} F. R. Xu,¹⁵¹ H. K. Xu,³⁹ J. L. Xu,³⁹ J. Xu,⁵¹ M. H. Xu,³⁹ Y. Xu,⁶⁰ B. J. Yan,³⁹ Q. Yan,¹⁵⁹ T. Yan,¹⁴¹ W. Q. Yan,³⁹ X. B. Yan,³⁹ Y. P. Yan,¹⁴¹ C. G. Yang,³⁹ C. F. Yang,⁵⁵ H. Yang,³⁹ J. Yang,¹⁴⁴ L. Yang,¹³³ X. Y. Yang,³⁹ Y. . Yang,¹³⁹ Y. F. Yang,³⁹ H. F. Yao,³⁹ J. X. Ye,³⁹ M. Ye,³⁹ Z. P. Ye,¹⁵⁸ F. Yermia,¹⁵⁵ Z. Y. You,³⁶ B. X. Yu,³⁹ C. Y. Yu,¹³³ C. X. Yu,⁶⁰ H. Z. Yu,³⁶ M. Yu,¹³¹ X. H. Yu,⁶⁰ Z. Y. Yu,³⁹ Z. Z. Yu,³⁹ C. Yuan,³⁶ C. Z. Yuan,³⁹ Y. Yuan,¹⁶⁴ Z. X. Yuan,¹³⁴ B. B. Yue,³⁶ N. Zafar,¹¹⁶ V. Zavadskyi,⁴⁸ S. Zeng,³⁹ T. X. Zeng,³⁹ Y. D. Zeng,³⁶ L. Zhan,³⁹ A. Q. Zhang,¹³⁴ B. Zhang,¹⁴⁴ B. T. Zhang,³⁹ F. Y. Zhang,¹⁵³ G. Q. Zhang,³⁹ H. H. Zhang,³⁶ J. L. Zhang,⁶⁵ J. W. Zhang,³⁹ J. Zhang,⁵⁵ J. Zhang,³⁹ J. B. Zhang,¹⁴⁸ J. Zhang,³⁹ M. Zhang,³⁹ P. Zhang,³⁹ Q. M. Zhang,¹⁶⁹ S. Zhang,³⁶ S. Zhang,³⁶ T. Zhang,¹⁵³ X. M. Zhang,³⁹ X. Zhang,³⁹ X. T. Zhang,³⁹ Y. Zhang,³⁹ Y. H. Zhang,³⁹ Y. Y. Zhang,³⁹ Y. P. Zhang,³⁹ Y. Y. Zhang,¹⁵³ Y. M. Zhang,³⁶ Z. Y. Zhang,¹³¹ Z. J. Zhang,¹³³ F. Y. Zhao,¹³⁵ J. Zhao,³⁹ R. Zhao,³⁶ R. Zhao,³⁹ S. J. Zhao,¹⁴⁴ D. Q. Zheng,¹⁵¹ H. Zheng,¹³³ Y. H. Zheng,¹⁵⁹ W. R. Zhong,¹⁵¹ J. Zhou,⁵³ L. Zhou,³⁹ N. Zhou,⁴⁶ S. Zhou,³⁹ T. Zhou,³⁹ X. Zhou,¹³¹ J. Zhu,³⁶ J. S. Zhu,¹¹⁹ K. F. Zhu,¹⁶⁹ K. J. Zhu,³⁹ Z. H. Zhu,³⁹ B. Zhuang,³⁹ H. L. Zhuang,³⁹ L. Zong,¹³⁴ J. H. Zou,³⁹ and S. Zwickel¹⁴⁶

(The JUNO Collaboration)

J. dos Anjos,⁷⁰ L. Asquith,¹⁷⁰ J.-L. Beney,¹⁷¹ T. J. C. Bezerra,¹⁷⁰ M. Bongrand,¹⁷¹ C. Bourgeois,¹⁷² D. Brasse,⁷⁹ D. Breton,¹⁷² M. Briere,¹⁷² J. Busto,¹⁷³ A. Cabrera,¹⁷² A. Cadiou,¹⁷¹ E. Calvo,⁸³ H. Carduner,¹⁷¹ V. Chaumat,¹⁷² E. Chauveau,¹⁷⁴ M. Chen,¹⁷⁵ P. Chimenti,¹⁷⁶ F. Dal Corso,¹⁷⁷ A. Dahmane,⁷⁹ S. Dusini,¹⁷⁷ A.D. Earle,¹⁷⁰ C. Frigerio-Martins,¹⁷⁶ J. Galán,¹⁷⁸ J.A. García,¹⁷⁸ R. Gazzini,¹⁷² A. Gibson,¹⁷⁰ D. Giovagnoli,⁷⁹ P. Govoni,^{179,180} M. Grassi,¹⁸¹ W.C. Griffith,¹⁷⁰ F. Haddad,¹⁷¹ J. Hartnell,¹⁷⁰ A. Hourlier,⁷⁹ G. Hull,¹⁷² I. Irastorza,¹⁷⁸ L. Koch,¹⁸² P. Laniéce,¹⁷² P. Lasorak,¹⁷⁰ C. Lefevre,¹⁷⁵ F. Lefevre,¹⁷¹ P. Loaiza,¹⁷² G. Luzon,¹⁷⁸ J. Maalmi,¹⁷² F. Mantovani,^{183,184} C. Marquet,¹⁷⁴ M. Martinez,¹⁷⁸ J. Martino,¹⁷¹ L. Menard,¹⁷² D. Navas-Nicolás,¹⁷² H. Nunokawa,¹⁸⁵ M. Obolensky,¹⁷² J. P. Ochoa-Ricoux,¹¹ C. Palomares,⁸³ P. Pillot,¹⁷¹ J. C. C. Porter,¹⁷⁰ M. S. Pravikoff,¹⁷⁴ M. Roche,¹⁷⁴ B. Roskovec,¹⁸⁶ M.L. Sarsa,¹⁷⁸ S. Schoppmann,¹⁸² A. Serafini,^{177,181} L. Simard,¹⁷² M. Sisti,¹⁷⁹ D. Stocco,¹⁷¹ V. Strati,^{183,184} J.-S. Stutzmann,¹⁷¹ F. Suekane,¹⁸⁷ M.-A. Verdier,¹⁷² A. Verdugo,⁸³ B. Viaud,¹⁷¹ A. Weber,¹⁸² and F. Yermia¹⁷¹

(The LiquidO Consortium)

B. C. Rasco¹⁸⁸ and K. P. Rykaczewski¹⁸⁸

(on behalf of The MTAS Collaboration)

B. Y. Han,¹⁸⁹ E. J. Jeon,¹⁹⁰ Y. Jeong,¹⁹¹ H. S. Jo,¹⁹² D. K. Kim,¹⁹² J. Y. Kim,¹⁹³ J. G. Kim,¹⁹⁴ Y. D. Kim,^{190,193,195} Y. J. Ko,¹⁹⁰ H. M. Lee,¹⁸⁹ M. H. Lee,^{190,195} J. Lee,¹⁹⁰ C. S. Moon,¹⁹² Y. M. Oh,¹⁹⁰ H. K. Park,¹⁹⁶ K. S. Park,¹⁹⁰ S. H. Seo,¹⁹⁰ K. Siyeon,¹⁹¹ G. M. Sun,¹⁸⁹ Y. S. Yoon,¹⁹⁷ and I. Yu¹⁹⁴

(The NEOS Collaboration)

G. Angloher,¹⁹⁸ A. Bento,^{198,199} L. Canonica,¹⁹⁸ F. Cappella,²⁰⁰ L. Cardani,²⁰⁰ N. Casali,²⁰⁰

R. Cerulli,^{201,202} I. Colantoni,^{203,200} A. Cruciani,²⁰⁰ G. del Castello,^{204,200} A. Erhart,²⁰⁵ M. Friedl,²⁰⁶
A. Garai,¹⁹⁸ V.M. Ghete,²⁰⁶ C. Goupy,⁷⁴ V. Guidi,^{207,208} D. Hauff,^{198,209} M. Kaznacheeva,²⁰⁵
A. Kinast,²⁰⁵ L. Klinkenberg,²⁰⁵ H. Kluck,²⁰⁶ A. Langenkämper,²⁰⁵ T. Lasserre,^{74,71} D. Lhuillier,⁷⁴
M. Mancuso,¹⁹⁸ B. Mauri,⁷⁴ A. Mazzolari,²⁰⁸ E. Mazzucato,⁷⁴ H. Neyrial,⁷⁴ C. Nones,⁷⁴
L. Oberauer,²⁰⁵ A. Onillon,⁷⁴ T. Ortmann,²⁰⁵ L. Pattavina,^{210,205} F. Petricca,¹⁹⁸ W. Potzel,²⁰⁵
F. Pröbst,¹⁹⁸ F. Pucci,¹⁹⁸ F. Reindl,^{206,211} R. Rogly,⁷⁴ J. Rothe,²⁰⁵ V. Savu,⁷⁴ N. Schermer,²⁰⁵
J. Schieck,^{206,211} S. Schönert,²⁰⁵ C. Schwertner,^{206,211} L. Scola,⁷⁴ L. Stodolsky,¹⁹⁸ R. Strauss,²⁰⁵
C. Tomei,²⁰⁰ K. v. Mirbach,²⁰⁵ M. Vignati,^{204,200} M. Vivier,⁷⁴ V. Wagner,²⁰⁵ and A. Wex²⁰⁵

(The NUCLEUS Collaboration)

H. Abele,²¹¹ M. del Gallo Roccagiovine,^{204,200} S. Dorer,²¹¹
A. Doblhammer,²¹¹ E. Jericha,²¹¹ L. Peters,²⁰⁵ and G. Soum⁷⁴

(Associated to the NUCLEUS Collaboration)

M. Andriamirado,⁸ A. B. Balantekin,³⁷ C. D. Bass,²¹² D. E. Bergeron,²¹³ E. P. Bernard,¹ N. S. Bowden,¹
C. D. Bryan,²¹⁴ R. Carr,⁴ T. Classen,¹ A. J. Conant,⁵ G. Deichert,²¹⁴ A. Delgado,^{188,215} M. V. Diwan,¹⁴
M. J. Dolinski,⁹³ A. Erickson,²¹⁶ B. T. Foust,⁷ J. K. Gaison,⁷ A. Galindo-Uribarri,^{188,215} C. E. Gilbert,¹⁸⁸
S. Gokhale,¹⁴ C. Grant,²¹⁷ S. Hans,¹⁴ A. B. Hansell,²¹⁸ K. M. Heeger,⁷ B. Heffron,^{188,215}
D. E. Jaffe,¹⁴ S. Jayakumar,⁹³ X. Ji,¹⁴ D. C. Jones,⁵⁷ O. Kzylova,⁹³ P. Kunkle,²¹⁷ C. E. Lane,⁹³
T. J. Langford,⁷ J. LaRosa,²¹³ B. R. Littlejohn,⁸ X. Lu,^{188,215} J. Maricic,²¹⁹ M. P. Mendenhall,¹
A. M. Meyer,²¹⁹ R. Milincic,²¹⁹ P. E. Mueller,¹⁸⁸ H. P. Mumm,²¹³ J. Napolitano,⁵⁷ R. Neilson,⁹³
J. A. Nikkel,⁷ S. Nour,²¹³ J. L. Palomino,⁸ D. A. Pushin,²²⁰ X. Qian,¹⁴ C. Roca,¹ R. Rosero,¹⁴
M. Searles,²¹⁴ P. T. Surukuchi,⁷ F. Sutanto,¹ M. A. Tyra,²¹³ R. L. Varner,¹⁸⁸ D. Venegas-Vargas,^{188,215}
P. B. Weatherly,⁹³ J. Wilhelmi,⁷ A. Woolverton,²²⁰ M. Yeh,¹⁴ C. Zhang,¹⁴ and X. Zhang¹

(The PROSPECT Collaboration)

H. I. Jang,²²¹ J. S. Jang,²²² S. H. Jeon,¹⁹⁴ K. K. Joo,²²³ D. E. Jung,¹⁹⁴ J. Y. Kim,²²³
S. B. Kim,¹⁹⁴ S. Y. Kim,²²⁴ W. Kim,¹⁹² E. Kwon,¹⁹⁴ H. G. Lee,²²⁴ W. J. Lee,²²⁴
I. T. Lim,²²³ D. H. Moon,²²³ M. Y. Pac,²²⁵ R. G. Park,²²³ H. Seo,²²⁴ J. W. Seo,¹⁹⁴
C. D. Shin,²²³ B. S. Yang,²²⁴ J. Yoo,²²⁴ S. G. Yoon,²²⁶ I. S. Yeo,²²⁵ and I. Yu¹⁹⁴

(The RENO Collaboration)

C. Augier,²²⁷ J. Billard,²²⁷ A. Broniatowski,²²⁸ M. Calvo,²²⁹ A. Cazes,²²⁷ C. Chang,²³⁰ M. Chapellier,²²⁸
G. Chemin,²³¹ M. De Jesus,²²⁷ L. Dumoulin,²²⁸ E. Figueroa-Feliciano,²³² J. A. Formaggio,²³³ J. Gascon,²²⁷
A. Giuiani,²²⁸ J. Goupy,²²⁹ C. Goy,²³¹ P. Harrington,²³³ S. T. Heine,²³³ S. A. Hertel,²³⁴ Z. Hong,²³⁵
Y. Jin,²³⁶ A. Juillard,²²⁷ J. Lamblin,²³¹ H. Lattaud,²²⁷ A. Lubashevskiy,²³⁷ P. de Marcillac,²²⁸
S. Marnieros,²²⁸ A. Monfardini,²²⁹ W. Oliver,²³³ E. Olivieri,²²⁸ K. J. Palladino,²³⁸ D. Poda,²²⁸ J. S. Real,²³¹
J. S. Ricol,²³¹ A. Robert,²³⁹ S. Rozov,²³⁷ V. Sanglard,²²⁷ T. Salagnac,²²⁷ B. Schmidt,²³² V. Sibille,^{233,227}
J. Stachurska,²³³ A. Stutz,²³¹ W. Van De Ponteselee,²³³ L. Winslow,²³³ E. Yakushev,²³⁷ and D. Zinatulina²³⁷

(The Ricochet Collaboration)

O. A. Akindede,¹ N. S. Bowden,¹ L. Carman,¹ T. Classen,¹ S. Dazeley,¹ M. Ford,¹
V. A. Li,¹ M. P. Mendenhall,¹ C. Roca,¹ F. Sutanto,¹ N. Zaitseva,¹ and X. Zhang¹

(The ROADSTR Near-Field Working Group)

W. Beaumont,²⁴⁰ S. Binet,²⁴¹ I. Bolognino,²⁴² M. Bongrand,²⁴² J. Borg,²⁴³ V. Buridon,²⁴⁴
H. Chanal,²⁴¹ B. Coupé,²⁴⁵ P. Crochet,²⁴¹ D. Cussans,²⁴⁶ A. De Roeck,^{240,247} D. Durand,²⁴⁴
M. Fallot,²⁴² D. Galbinski,²⁴³ S. Gallego,²⁴⁴ L. Giot,²⁴² B. Guillon,²⁴⁴ D. Henaff,²⁴²

S. Hayashida,²⁴³ B. Hosseini,²⁴³ S. Kalcheva,²⁴⁵ G. Lehaut,²⁴⁴ I. Michiels,²⁴⁸ S. Monteil,²⁴¹
D. Newbold,^{246,249} N. Roy,²⁵⁰ D. Ryckbosch,²⁴⁸ H. Rejeb Sfar,²⁴⁰ L. Simard,^{250,251}
A. Vacheret,²⁴³ G. Vandierendonck,²⁴⁸ S. Van Dyck,²⁴⁵ N. van Remortel,²⁴⁰ S. Vercaemer,²⁴⁰
M. Verstraeten,²⁴⁰ B. Viaud,²⁴² A. Weber,^{252,249} M. Yeresko,²⁴¹ and and F. Yermia.²⁴²

(The SoLid Collaboration)

A. Bonhomme,^{34,74} C. Buck,³⁴ P. del Amo Sanchez,²⁵³ I. El Atmani,⁷⁴ L. Labit,²⁵³ J. Lamblin,²⁵⁴
A. Letourneau,⁷⁴ D. Lhuillier,⁷⁴ M. Licciardi,²⁵⁴ M. Lindner,³⁴ T. Materna,⁷⁴ H. Pessard,²⁵³ J.-S. Réal,²⁵⁴
J.-S. Ricol,²⁵⁴ R. Rogly,⁷⁴ V. Savu,⁷⁴ S. Schoppmann,³⁴ T. Soldner,²⁵⁵ A. Stutz,²⁵⁴ and M. Vialat²⁵⁵

(The STEREO Collaboration)

M. Askins,^{3,12} Z. Bagdasarian,^{3,12} N. Barros,^{98,99,100} E.W. Beier,⁹⁸ A. Bernstein,¹ M. Böhles,¹⁰⁹
E. Blucher,⁷⁸ R. Bonventre,¹² E. Bourret,¹² E. J. Callaghan,^{3,12} J. Caravaca,^{3,12} M. Diwan,¹⁴ S.T. Dye,²⁵⁶
J. Eisch,²⁵⁷ A. Elagin,⁷⁸ T. Enqvist,¹¹² U. Fahrenholz,¹¹⁰ V. Fischer,¹⁰⁸ K. Frankiewicz,¹⁰³ C. Grant,¹⁰³
D. Guffanti,¹⁰⁹ C. Hagner,²⁵⁸ A. Hallin,²⁵⁹ C. M. Jackson,²⁶⁰ R. Jiang,⁷⁸ T. Kaptanoglu,^{3,12} J.R. Klein,⁹⁸
Yu. G. Kolomensky,^{3,12} C. Kraus,^{104,105} F. Krennrich,¹¹³ T. Kutter,²⁶¹ T. Lachenmaier,²⁶² B. Land,^{3,12,98}
K. Lande,⁹⁸ L. Lebanowski,⁹⁸ J.G. Learned,²⁵⁶ V.A. Li,¹ V. Lozza,^{99,100} L. Ludhova,^{263,75}
M. Malek,²⁶⁴ S. Manecki,^{105,265,104} J. Maneira,^{99,100} J. Maricic,²⁵⁶ J. Martyn,¹⁰⁹ A. Mastbaum,¹⁰⁷
C. Mauger,⁹⁸ M. Mayer,¹¹⁰ J. Migenda,²⁶⁶ F. Moretti,¹² J. Napolitano,²⁶⁷ B. Naranjo,²⁶⁸ S. Naugle,⁹⁸
M. Nieslony,¹⁰⁹ L. Oberauer,¹¹⁰ G. D. Orebi Gann,^{3,12} J. Ouellet,²⁶⁹ T. Pershing,¹⁰⁸ S.T. Petcov,²⁷⁰
L. Pickard,¹⁰⁸ R. Rosero,¹⁴ M. C. Sanchez,¹¹³ J. Sawatzki,¹¹⁰ S. Schoppmann,^{3,12} S.H. Seo,¹⁹⁰
M. Smiley,^{3,12} M. Smy,²⁷¹ A. Stahl,⁷⁵ H. Steiger,^{109,110} M. R. Stock,¹¹⁰ H. Sunej,¹⁴ R. Svoboda,¹⁰⁸
E. Tiras,^{102,111} W. H. Trzaska,¹¹² M. Tzanov,²⁶¹ M. Vagins,²⁷¹ C. Vilela,²⁷² Z. Wang,²⁷³ J. Wang,²⁷⁴
M. Wetstein,¹¹³ M.J. Wilking,²⁷² L. Winslow,²⁶⁹ P. Wittich,²⁷⁵ B. Wonsak,²⁵⁸ E. Worcester,^{14,272}
M. Wurm,¹⁰⁹ G. Yang,²⁷² M. Yeh,¹⁴ E.D. Zimmerman,¹⁰⁶ S. Zsoldos,^{3,12} and K. Zuber²⁷⁶

(The THEIA Collaboration)

A. Algora,²⁷⁷ A. Beloeuvre,²⁴² M. Estienne,²⁴² M. Fallot,²⁴²
L. Giot,²⁴² R. Kean,²⁴² A. Porta,²⁴² and J. L. Tain²⁷⁷

(The Valencia-Nantes TAGS Collaboration)

J. I. Collar,²⁷⁸ Z. Djurcic,²⁷⁹ A. Erlandson,²⁸⁰ M. Foxe,²⁶⁰ S. Gariazzo,²⁸¹ M.V.
Garzelli,²⁸² C. Giunti,²⁸³ S. Hedges,¹ I. Jovanovic,¹⁸ J. Learned,²¹⁹ C. M. Lewis,²⁷⁸
J. LoSecco,²⁸⁴ X. Mougeot,²⁸⁵ J. Newby,⁵ K. Ni,²⁸⁶ R. Pestes,⁶ and L. Périssé⁷⁴

¹Lawrence Livermore National Laboratory, Livermore, CA 94550, USA

²Institute for Nuclear Theory, University of Washington, Seattle, WA 98195, USA

³Department of Physics, University of California at Berkeley, Berkeley, CA 94720-7300, USA

⁴Department of Physics, United States Naval Academy, Annapolis, MD, USA

⁵Oak Ridge National Laboratory, Oak Ridge, TN, USA

⁶Center for Neutrino Physics, Virginia Tech, Blacksburg, Virginia 24061

⁷Wright Laboratory and Department of Physics, Yale University, New Haven, Connecticut 06520, USA

⁸Department of Physics, Illinois Institute of Technology, Chicago, Illinois 60616

⁹Fermi National Accelerator Laboratory, Batavia, IL, United States

¹⁰Instituto de Investigaciones en Ingeniería Eléctrica, Departamento de Ingeniería Eléctrica y Computadoras, Universidad Nacional del Sur (UNS) - CONICET, Bahía Blanca, Argentina

- ¹¹*Department of Physics and Astronomy, University of California, Irvine, California 92697*
- ¹²*Lawrence Berkeley National Laboratory, 1 Cyclotron Road, Berkeley, CA 94720-8153, USA*
- ¹³*Texas A&M University, College Station, TX 77843, USA*
- ¹⁴*Brookhaven National Laboratory, Upton, New York 11973, USA*
- ¹⁵*Department of Physics, Duke University, Durham, NC 27708*
- ¹⁶*Triangle Universities Nuclear Laboratory, Durham, NC 27708*
- ¹⁷*Nuclear Engineering Program, Virginia Tech, Falls Church, Virginia 22043*
- ¹⁸*University of Michigan, Ann Arbor, MI, USA*
- ¹⁹*Department of Physics, University of California at Davis, Davis, California 95616, USA*
- ²⁰*University of Maryland, Department of Physics, College Park, MD 20742*
- ²¹*Department of Physics, University of California, Berkeley, California 94720*
- ²²*Universidad Nacional Autónoma de México, Ciudad de México, México*
- ²³*Centro Atómico Bariloche and Instituto Balseiro, Comisión Nacional de Energía Atómica (CNEA), Consejo Nacional de Investigaciones Científicas y Técnicas (CONICET), Universidad Nacional de Cuyo (UNCUYO), San Carlos de Bariloche, Argentina.*
- ²⁴*Facultad de Ingeniería - Universidad Nacional de Asunción, Asunción, Paraguay*
- ²⁵*Universidade Federal do Rio de Janeiro, Instituto de Física, Rio de Janeiro, RJ, Brazil*
- ²⁶*International Center for Advanced Studies & Instituto de Ciencias Físicas, ECyT-UNSAM and CONICET, Buenos Aires, Argentina*
- ²⁷*Centro Brasileiro de Pesquisas Físicas, Rio de Janeiro, RJ, Brazil*
- ²⁸*Centro Federal de Educação Tecnológica Celso Suckow da Fonseca, Angra dos Reis, RJ, Brazil*
- ²⁹*Universidad Nacional de San Martín (UNSAM), Comisión Nacional de Energía Atómica (CNEA), Consejo Nacional de Investigaciones Científicas y Técnicas (CONICET), Argentina*
- ³⁰*Universität Zürich Physik Institut, Zurich, Switzerland*
- ³¹*Universidade Federal de São Carlos, Araras, SP, Brazil*
- ³²*Universidade Federal do ABC, Santo André, SP, Brazil*
- ³³*Departamento de Física, FCEN, Universidad de Buenos Aires and IFIBA, CONICET, Buenos Aires, Argentina*
- ³⁴*Max-Planck-Institut für Kernphysik, Saupfercheckweg 1, 69117 Heidelberg, Germany*
- ³⁵*Institute of Modern Physics, East China University of Science and Technology, Shanghai*
- ³⁶*Sun Yat-Sen (Zhongshan) University, Guangzhou*
- ³⁷*University of Wisconsin, Madison, Wisconsin 53706*
- ³⁸*Department of Physics, National Taiwan University, Taipei*
- ³⁹*Institute of High Energy Physics, Beijing*
- ⁴⁰*National United University, Miao-Li*
- ⁴¹*Department of Engineering Physics, Tsinghua University, Beijing*
- ⁴²*Shenzhen University, Shenzhen*
- ⁴³*North China Electric Power University, Beijing*
- ⁴⁴*Chinese University of Hong Kong, Hong Kong*
- ⁴⁵*Siena College, Loudonville, New York 12211*
- ⁴⁶*University of Science and Technology of China, Hefei*

- ⁴⁷*Charles University, Faculty of Mathematics and Physics, Prague*
- ⁴⁸*Joint Institute for Nuclear Research, Dubna, Moscow Region*
- ⁴⁹*Department of Physics, University of Illinois at Urbana-Champaign, Urbana, Illinois 61801*
- ⁵⁰*Lawrence Berkeley National Laboratory, Berkeley, California 94720*
- ⁵¹*Beijing Normal University, Beijing*
- ⁵²*Department of Nuclear Science and Technology, School of Energy and Power Engineering, Xi'an Jiaotong University, Xi'an*
- ⁵³*China Institute of Atomic Energy, Beijing*
- ⁵⁴*Shandong University, Jinan*
- ⁵⁵*Guangxi University, No.100 Daxue East Road, Nanning*
- ⁵⁶*Institute of Physics, National Chiao-Tung University, Hsinchu*
- ⁵⁷*Department of Physics, College of Science and Technology, Temple University, Philadelphia, Pennsylvania 19122*
- ⁵⁸*Dongguan University of Technology, Dongguan*
- ⁵⁹*Department of Physics, The University of Hong Kong, Pokfulam, Hong Kong*
- ⁶⁰*School of Physics, Nankai University, Tianjin*
- ⁶¹*Department of Physics and Astronomy, Shanghai Jiao Tong University, Shanghai Laboratory for Particle Physics and Cosmology, Shanghai*
- ⁶²*Joseph Henry Laboratories, Princeton University, Princeton, New Jersey 08544*
- ⁶³*California Institute of Technology, Pasadena, California 91125*
- ⁶⁴*College of William and Mary, Williamsburg, Virginia 23187*
- ⁶⁵*Nanjing University, Nanjing*
- ⁶⁶*China General Nuclear Power Group, Shenzhen*
- ⁶⁷*College of Electronic Science and Engineering, National University of Defense Technology, Changsha*
- ⁶⁸*Iowa State University, Ames, Iowa 50011*
- ⁶⁹*Chongqing University, Chongqing*
- ⁷⁰*Centro Brasileiro de Pesquisas Físicas, Rio de Janeiro, RJ, 22290-180, Brazil*
- ⁷¹*APC, Université de Paris, CNRS, Astroparticule et Cosmologie, F-75006, Paris*
- ⁷²*Max-Planck-Institut für Kernphysik, 69117 Heidelberg, Germany*
- ⁷³*Physik Department, Technische Universität München, 85748 Garching, Germany*
- ⁷⁴*IRFU, CEA, Université Paris-Saclay, 91191 Gif-sur-Yvette, France*
- ⁷⁵*III. Physikalisches Institut, RWTH Aachen University, 52056 Aachen, Germany*
- ⁷⁶*SUBATECH, CNRS/IN2P3, Université de Nantes, IMT-Atlantique, 44307 Nantes, France*
- ⁷⁷*Institute of Nuclear Research of the Russian Academy of Sciences, Moscow 117312, Russia*
- ⁷⁸*The Enrico Fermi Institute, The University of Chicago, Chicago, Illinois 60637, USA*
- ⁷⁹*IPHC, CNRS/IN2P3, Université de Strasbourg, 67037 Strasbourg, France*
- ⁸⁰*Department of Physics and Astronomy, University of Alabama, Tuscaloosa, Alabama 35487, USA*
- ⁸¹*LNCA Underground Laboratory, CNRS/IN2P3-CEA, Chooz, France*
- ⁸²*IJC Laboratory, CNRS/IN2P3, Université Paris-Saclay, Orsay, France*
- ⁸³*Centro de Investigaciones Energéticas, Medioambientales y Tecnológicas, CIEMAT, 28040, Madrid, Spain*
- ⁸⁴*Université de Bordeaux, CNRS/IN2P3, CENBG, F-33175 Gradignan, France*

- ⁸⁵Argonne National Laboratory, Argonne, Illinois 60439, USA
- ⁸⁶NRC Kurchatov Institute, 123182 Moscow, Russia
- ⁸⁷Research Center for Neutrino Science, Tohoku University, Sendai 980-8578, Japan
- ⁸⁸Universidade Estadual de Campinas-UNICAMP, Campinas, SP, 13083-970, Brazil
- ⁸⁹Department of Physics, Kobe University, Kobe, 657-8501, Japan
- ⁹⁰Department of Physics, Tokyo Institute of Technology, Tokyo, 152-8551, Japan
- ⁹¹Kepler Center for Astro and Particle Physics, Universität Tübingen, 72076 Tübingen, Germany
- ⁹²Department of Physics, Kitasato University, Sagamihara, 252-0373, Japan
- ⁹³Department of Physics, Drexel University, Philadelphia, Pennsylvania 19104, USA
- ⁹⁴University of Notre Dame, Notre Dame, Indiana 46556, USA
- ⁹⁵Department of Physics, Tokyo Metropolitan University, Tokyo, 192-0397, Japan
- ⁹⁶Center for Neutrino Physics, Virginia Tech, Blacksburg, Virginia 24061, USA
- ⁹⁷Pennsylvania State University, University Park, PA 16802, USA
- ⁹⁸Department of Physics and Astronomy, University of Pennsylvania, Philadelphia, PA 19104-6396
- ⁹⁹Universidade de Lisboa, Faculdade de Ciências (FCUL), Departamento de Física, Campo Grande, Edifício C8, 1749-016 Lisboa, Portugal
- ¹⁰⁰Laboratório de Instrumentação e Física Experimental de Partículas (LIP), Av. Prof. Gama Pinto, 2, 1649-003, Lisboa, Portugal
- ¹⁰¹Bartoszek Engineering, Aurora, IL 60506, USA
- ¹⁰²Department of Physics, Erciyes University, 38030, Kayseri, Turkey
- ¹⁰³Boston University, Department of Physics, Boston, MA 02215, USA
- ¹⁰⁴SNOLAB, Creighton Mine 9, 1039 Regional Road 24, Sudbury, ON P3Y 1N2, Canada
- ¹⁰⁵Laurentian University, Department of Physics, 935 Ramsey Lake Road, Sudbury, ON P3E 2C6, Canada
- ¹⁰⁶University of Colorado at Boulder, Department of Physics, Boulder, Colorado, USA
- ¹⁰⁷Department of Physics and Astronomy, Rutgers, The State University of New Jersey, 136 Frelinghuysen Road, Piscataway, NJ 08854-8019 USA
- ¹⁰⁸University of California, Davis, 1 Shields Avenue, Davis, CA 95616, USA
- ¹⁰⁹Institute of Physics and Excellence Cluster PRISMA, Johannes Gutenberg-Universität Mainz, 55099 Mainz, Germany
- ¹¹⁰Physics Department, Technische Universität München, 85748 Garching, Germany
- ¹¹¹Department of Physics and Astronomy, The University of Iowa, Iowa City, Iowa, USA
- ¹¹²Department of Physics, University of Jyväskylä, Finland
- ¹¹³Department of Physics and Astronomy, Iowa State University, Ames, IA 50011, USA
- ¹¹⁴Pontificia Universidad Católica de Chile, Santiago, Chile
- ¹¹⁵IPHC, Université de Strasbourg, CNRS/IN2P3, F-67037 Strasbourg, France
- ¹¹⁶Pakistan Institute of Nuclear Science and Technology, Islamabad, Pakistan
- ¹¹⁷INFN Catania and Dipartimento di Fisica e Astronomia dell Università di Catania, Catania, Italy
- ¹¹⁸III. Physikalisches Institut B, RWTH Aachen University, Aachen, Germany
- ¹¹⁹East China University of Science and Technology, Shanghai, China
- ¹²⁰INFN Sezione di Milano and Dipartimento di Fisica dell Università di Milano, Milano, Italy

- ¹²¹*Department of Physics, Faculty of Science, Chulalongkorn University, Bangkok, Thailand*
- ¹²²*IJCLab, Université Paris-Saclay, CNRS/IN2P3, 91405 Orsay, France*
- ¹²³*Department of Physics and Earth Science, University of Ferrara and INFN Sezione di Ferrara, Ferrara, Italy*
- ¹²⁴*INFN Milano Bicocca and University of Milano Bicocca, Milano, Italy*
- ¹²⁵*INFN Sezione di Padova, Padova, Italy*
- ¹²⁶*Eberhard Karls Universität Tübingen, Physikalisches Institut, Tübingen, Germany*
- ¹²⁷*Université de Bordeaux, CNRS, CENBG-IN2P3, F-33170 Gradignan, France*
- ¹²⁸*Dipartimento di Fisica e Astronomia dell'Università di Padova and INFN Sezione di Padova, Padova, Italy*
- ¹²⁹*University of Roma Tre and INFN Sezione Roma Tre, Roma, Italy*
- ¹³⁰*Centre de Physique des Particules de Marseille, Marseille, France*
- ¹³¹*Wuhan University, Wuhan, China*
- ¹³²*INFN Milano Bicocca and Politecnico di Milano, Milano, Italy*
- ¹³³*Dongguan University of Technology, Dongguan, China*
- ¹³⁴*Tsinghua University, Beijing, China*
- ¹³⁵*Institute of Modern Physics, Chinese Academy of Sciences, Lanzhou, China*
- ¹³⁶*Beijing Institute of Spacecraft Environment Engineering, Beijing, China*
- ¹³⁷*Universidade Estadual de Londrina, Londrina, Brazil*
- ¹³⁸*INFN Sezione di Perugia and Dipartimento di Chimica, Biologia e Biotecnologie dell'Università di Perugia, Perugia, Italy*
- ¹³⁹*Université Libre de Bruxelles, Brussels, Belgium*
- ¹⁴⁰*Institute of Physics and EC PRISMA⁺, Johannes-Gutenberg Universität Mainz, Mainz, Germany*
- ¹⁴¹*Suranaree University of Technology, Nakhon Ratchasima, Thailand*
- ¹⁴²*Lomonosov Moscow State University, Moscow, Russia*
- ¹⁴³*Institute for Nuclear Research of the Russian Academy of Sciences, Moscow, Russia*
- ¹⁴⁴*School of Physics and Microelectronics, Zhengzhou University, Zhengzhou, China*
- ¹⁴⁵*University of Jyväskylä, Department of Physics, Jyväskylä, Finland*
- ¹⁴⁶*Technische Universität München, München, Germany*
- ¹⁴⁷*Wuyi University, Jiangmen, China*
- ¹⁴⁸*Harbin Institute of Technology, Harbin, China*
- ¹⁴⁹*Universidad Tecnica Federico Santa Maria, Valparaiso, Chile*
- ¹⁵⁰*Forschungszentrum Jülich GmbH, Nuclear Physics Institute IKP-2, Jülich, Germany*
- ¹⁵¹*Jinan University, Guangzhou, China*
- ¹⁵²*Institute of Experimental Physics, University of Hamburg, Hamburg, Germany*
- ¹⁵³*School of Physics and Astronomy, Shanghai Jiao Tong University, Shanghai, China*
- ¹⁵⁴*Yerevan Physics Institute, Yerevan, Armenia*
- ¹⁵⁵*SUBATECH, Université de Nantes, IMT Atlantique, CNRS-IN2P3, Nantes, France*
- ¹⁵⁶*Comenius University Bratislava, Faculty of Mathematics, Physics and Informatics, Bratislava, Slovakia*
- ¹⁵⁷*The Radiochemistry and Nuclear Chemistry Group in University of South China, Hengyang, China*
- ¹⁵⁸*Tsung-Dao Lee Institute, Shanghai Jiao Tong University, Shanghai, China*
- ¹⁵⁹*University of Chinese Academy of Sciences, Beijing, China*

- ¹⁶⁰*INFN Catania and Centro Siciliano di Fisica Nucleare e Struttura della Materia, Catania, Italy*
- ¹⁶¹*Institute of Hydrogeology and Environmental Geology,
Chinese Academy of Geological Sciences, Shijiazhuang, China*
- ¹⁶²*Jilin University, Changchun, China*
- ¹⁶³*Xiamen University, Xiamen, China*
- ¹⁶⁴*School of Physics, Peking University, Beijing, China*
- ¹⁶⁵*Laboratori Nazionali di Frascati dell'INFN, Roma, Italy*
- ¹⁶⁶*Institute of Electronics and Computer Science, Riga, Latvia*
- ¹⁶⁷*Pontificia Universidade Catolica do Rio de Janeiro, Rio, Brazil*
- ¹⁶⁸*National Astronomical Research Institute of Thailand, Chiang Mai, Thailand*
- ¹⁶⁹*Xi'an Jiaotong University, Xi'an, China*
- ¹⁷⁰*Department of Physics and Astronomy, University of Sussex, Falmer, Brighton BN1 9QH, United Kingdom*
- ¹⁷¹*Subatech, CNRS/IN2P3, Nantes Université, IMT-Atlantique, 44307 Nantes, France*
- ¹⁷²*IJCLab, CNRS/IN2P3, Université Paris-Saclay, Université
de Paris, 15 rue Georges Clémenceau, 91400 Orsay, France*
- ¹⁷³*Aix Marseille Univ, CNRS/IN2P3, CPPM, Marseille, France*
- ¹⁷⁴*Université de Bordeaux, CNRS, LP2i, F-33170 Gradignan, France*
- ¹⁷⁵*Department of Physics, Engineering Physics & Astronomy,
Queen's University, Kingston, Ontario K7L3N6, Canada*
- ¹⁷⁶*Departamento de Física, Universidade Estadual de Londrina, Rodovia Celso Garcia Cid, PR
445 Km 380, Campus Universitário Cx. Postal 10.011, CEP 86.057-970, Londrina – PR, Brazil*
- ¹⁷⁷*INFN, Sezione di Padova, via Marzolo 8, I-35131 Padova, Italy*
- ¹⁷⁸*University of Zaragoza, Facultad de Ciencias, Departamento de Física, Pedro Cerbuna 12, 50009, Zaragoza*
- ¹⁷⁹*INFN, Sezione di Milano-Bicocca, I-20126 Milano, Italy*
- ¹⁸⁰*Dipartimento di Fisica, Università di Milano-Bicocca, I-20126 Milano, Italy*
- ¹⁸¹*Dipartimento di Fisica e Astronomia, Università di Padova, via Marzolo 8, I-35131 Padova, Italy*
- ¹⁸²*Johannes Gutenberg Universität Mainz, Institut für Physik, Staudingerweg 7, 55128 Mainz, Germany*
- ¹⁸³*INFN, Ferrara Section, Via Saragat 1, 44122 Ferrara, Italy*
- ¹⁸⁴*Department of Physics and Earth Sciences, University of Ferrara, Via Saragat 1, 44122 Ferrara, Italy*
- ¹⁸⁵*Department of Physics, Pontificia Universidade Católica do
Rio de Janeiro, C.P. 38097, 22451-900, Rio de Janeiro, Brazil*
- ¹⁸⁶*Institute of Particle and Nuclear Physics Faculty of Mathematics and Physics,
Charles University, V Holešovičkách 2 180 00 Prague 8, Czech Republic*
- ¹⁸⁷*RCNS, Tohoku University, 6-3 AzaAoba, Aramaki, Aoba-ku, 980-8578, Sendai, Japan*
- ¹⁸⁸*Physics Division, Oak Ridge National Laboratory, Oak Ridge, TN, USA*
- ¹⁸⁹*Neutron Science Division, Korea Atomic Energy Research Institute, Daejeon, 34057, Korea*
- ¹⁹⁰*Center for Underground Physics, Institute for Basic Science (IBS), Daejeon, 34126, Korea*
- ¹⁹¹*Department of Physics, Chung-Ang University, Seoul, 06974, Korea*
- ¹⁹²*Department of Physics, Kyungpook National University, Daegu 41566, Korea*
- ¹⁹³*Department of Physics and Astronomy, Sejong University, Seoul, 05006, Korea*
- ¹⁹⁴*Department of Physics, SungKyun Kwan University, Suwon, 16419, Korea*

- ¹⁹⁵*IBS School, University of Science and Technology (UST), Daejeon, 34113, Korea*
- ¹⁹⁶*Department of Accelerator Science, Korea University, Sejong, 30019, Korea*
- ¹⁹⁷*Center for Ionizing Radiation, Korea Research Institute of Standards and Science, Daejeon, 34113, Korea*
- ¹⁹⁸*Max-Planck-Institut für Physik, D-80805 München, Germany*
- ¹⁹⁹*CIUC, Departamento de Física, Universidade de Coimbra, P3004 516 Coimbra, Portugal*
- ²⁰⁰*Istituto Nazionale di Fisica Nucleare – Sezione di Roma, Roma I-00185, Italy*
- ²⁰¹*Istituto Nazionale di Fisica Nucleare – Sezione di Roma "Tor Vergata", Roma I-00133, Italy*
- ²⁰²*Dipartimento di Fisica, Università di Roma "Tor Vergata", Roma I-00133, Italy*
- ²⁰³*Consiglio Nazionale delle Ricerche, Istituto di Nanotecnologia, Roma I-00185, Italy*
- ²⁰⁴*Dipartimento di Fisica, Sapienza Università di Roma, Roma I-00185, Italy*
- ²⁰⁵*Physik-Department and Excellence Cluster ORIGINS, Technische Universität München, D-85748 Garching, Germany*
- ²⁰⁶*Institut für Hochenergiephysik der Österreichischen Akademie der Wissenschaften, A-1050 Wien, Austria*
- ²⁰⁷*Dipartimento di Fisica, Università di Ferrara, I-44122 Ferrara, Italy*
- ²⁰⁸*Istituto Nazionale di Fisica Nucleare – Sezione di Ferrara, I-44122 Ferrara, Italy*
- ²⁰⁹*Present address: Eberhard-Karls-Universität Tübingen, D-72076 Tübingen, Germany*
- ²¹⁰*Istituto Nazionale di Fisica Nucleare – Laboratori Nazionali del Gran Sasso, Assergi (L'Aquila) I-67100, Italy*
- ²¹¹*Atominstytut, Technische Universität Wien, A-1020 Wien, Austria*
- ²¹²*Department of Physics, Le Moyne College, Syracuse, NY, USA*
- ²¹³*National Institute of Standards and Technology, Gaithersburg, MD, USA*
- ²¹⁴*High Flux Isotope Reactor, Oak Ridge National Laboratory, Oak Ridge, TN, USA*
- ²¹⁵*Department of Physics and Astronomy, University of Tennessee, Knoxville, TN, USA*
- ²¹⁶*George W. Woodruff School of Mechanical Engineering, Georgia Institute of Technology, Atlanta, GA USA*
- ²¹⁷*Department of Physics, Boston University, Boston, MA, USA*
- ²¹⁸*Department of Physics, Susquehanna University, Selinsgrove, PA, USA*
- ²¹⁹*Department of Physics & Astronomy, University of Hawaii, Honolulu, HI, USA*
- ²²⁰*Institute for Quantum Computing and Department of Physics and Astronomy, University of Waterloo, Waterloo, ON, Canada*
- ²²¹*Department of Fire Safety, Seoyeong University, Gwangju 61268, Korea*
- ²²²*GIST College, Gwangju Institute of Science and Technology, Gwangju 61005, Korea*
- ²²³*Institute for Universe and Elementary Particles, Chonnam National University, Gwangju 61186, Korea*
- ²²⁴*Department of Physics and Astronomy, Seoul National University, Seoul 08826, Korea*
- ²²⁵*Institute for High Energy Physics, Dongshin University, Naju 58245, Korea*
- ²²⁶*Department of Physics, KAIST, Daejeon 34141, Korea*
- ²²⁷*Institut de Physique Nucléaire de Lyon (IPNL), France*
- ²²⁸*Centre de Sciences Nucléaires et de Sciences de la Matière (CSNSM), France*
- ²²⁹*Institut Neel PI at Neel Institute Grenoble, France*
- ²³⁰*Argonne National Laboratory, USA*
- ²³¹*Laboratoire de Physique Subatomique et de Cosmologie (LPSC), France*
- ²³²*Northwestern University, USA*

- ²³³Massachusetts Institute of Technology, USA
- ²³⁴University of Massachusetts at Amherst, USA
- ²³⁵University of Toronto, Canada
- ²³⁶CNRS, Univ. Paris-Saclay, France
- ²³⁷Joint Institute for Nuclear Research (JINR), Russian Federation
- ²³⁸University of Oxford, United Kingdom
- ²³⁹Institut Laue Langevin, Grenoble, France
- ²⁴⁰Universiteit Antwerpen, Antwerpen, Belgium
- ²⁴¹Université Clermont Auvergne, CNRS/IN2P3, LPC, Clermont-Ferrand, France
- ²⁴²SUBATECH, CNRS/IN2P3, Université de Nantes, Ecole des Mines de Nantes, Nantes, France
- ²⁴³Imperial College London, Department of Physics, London, United Kingdom
- ²⁴⁴Normandie Univ, ENSICAEN, UNICAEN, CNRS/IN2P3, LPC Caen, 14000 Caen, France
- ²⁴⁵SCK-CEN, Belgian Nuclear Research Centre, Mol, Belgium
- ²⁴⁶University of Bristol, Bristol, UK
- ²⁴⁷CERN, 1211 Geneva 23, Switzerland
- ²⁴⁸Universiteit Gent, Gent, Belgium
- ²⁴⁹STFC, Rutherford Appleton Laboratory, Harwell Oxford, and Daresbury Laboratory
- ²⁵⁰LAL, Univ Paris-Sud, CNRS/IN2P3, Université Paris-Saclay, Orsay, France
- ²⁵¹Institut Universitaire de France, F-75005 Paris, France
- ²⁵²University of Oxford, Oxford, UK
- ²⁵³Univ. Grenoble Alpes, Université Savoie Mont Blanc, CNRS/IN2P3, LAPP, 74000 Annecy, France
- ²⁵⁴Univ. Grenoble Alpes, CNRS, Grenoble INP, LPSC-IN2P3, 38000 Grenoble, France
- ²⁵⁵Institut Laue-Langevin, CS 20156, 38042 Grenoble Cedex 9, France
- ²⁵⁶University of Hawai'i at Manoa, Honolulu, Hawai'i 96822, USA
- ²⁵⁷Fermi National Accelerator Laboratory, Batavia, IL 60510, USA
- ²⁵⁸Institut für Experimentalphysik, Universität Hamburg, 22761 Hamburg, Germany
- ²⁵⁹University of Alberta, Department of Physics, 4-181 CCIS, Edmonton, AB T6G 2E1, Canada
- ²⁶⁰Pacific Northwest National Laboratory, Richland, WA 99352, USA
- ²⁶¹Department of Physics and Astronomy, Louisiana State University, Baton Rouge, LA 70803
- ²⁶²Kepler Center for Astro and Particle Physics, Universität Tübingen, 72076 Tübingen, Germany
- ²⁶³Forschungszentrum Jülich, Institute for Nuclear Physics, Wilhelm-Johnen-Straße 52425 Jülich, Germany
- ²⁶⁴University of Sheffield, Physics & Astronomy, Western Bank, Sheffield S10 2TN, UK
- ²⁶⁵Queen's University, Department of Physics, Engineering Physics & Astronomy, Kingston, ON K7L 3N6, Canada
- ²⁶⁶King's College London, Department of Physics, Strand Building, Strand, London WC2R 2LS, UK
- ²⁶⁷Department of Physics, Temple University, Philadelphia, PA, USA
- ²⁶⁸University of California Los Angeles, Department of Physics & Astronomy, 475 Portola Plaza, Los Angeles, CA 90095-1547, USA
- ²⁶⁹Massachusetts Institute of Technology, Department of Physics and Laboratory for Nuclear Science, 77 Massachusetts Ave Cambridge, MA 02139, USA
- ²⁷⁰SISSA/INFN, Via Bonomea 265, I-34136 Trieste, Italy ,

- Kavli IPMU (WPI), University of Tokyo, 5-1-5 Kashiwanoha, 277-8583 Kashiwa, Japan*
- ²⁷¹*University of California, Irvine, Department of Physics, CA 92697, Irvine, USA*
- ²⁷²*State University of New York at Stony Brook, Department of Physics and Astronomy, Stony Brook, New York, USA*
- ²⁷³*Department of Engineering Physics, Tsinghua University, Beijing 100084, China*
- ²⁷⁴*Department of Physics, South Dakota School of Mines and Technology, Rapid City, SD 57701, USA*
- ²⁷⁵*Cornell University, Ithaca, NY, USA*
- ²⁷⁶*Institut für Kern und Teilchenphysik, TU Dresden, Zellescher Weg 19, 01069, Dresden, Germany*
- ²⁷⁷*Instituto de Física Corpuscular, CSIC-Universitat de Valencia, E-46071 Valencia, Spain*
- ²⁷⁸*University of Chicago, Chicago, IL 60637, USA*
- ²⁷⁹*Argonne National Laboratory, Lemont, IL, United States*
- ²⁸⁰*Canadian Nuclear Laboratories Ltd., Chalk River, ON, K0J 1J0, Canada*
- ²⁸¹*Istituto Nazionale di Fisica Nucleare (INFN),
Sezione di Torino, Via P. Giuria 1, I-10125 Torino, Italy*
- ²⁸²*University of Hamburg, II Institute for Theoretical Physics,
Luruper Chaussee 149, D-22761 Hamburg, Germany*
- ²⁸³*Istituto Nazionale di Fisica Nucleare (INFN),
Sezione di Torino, Via P. Giuria 1, I-10125 Torino, Italy*
- ²⁸⁴*University of Notre Dame du Lac, Notre Dame, IN 46556-5670*
- ²⁸⁵*Université Paris-Saclay, CEA, List, Laboratoire National
Henri Becquerel (LNE-LNHB), F-91120 Palaiseau, France*
- ²⁸⁶*University of California San Diego, La Jolla, 92093, CA*

* Now at Department of Chemistry and Chemical Technology, Bronx Community College, Bronx, New York 10453

Contents

1	Introduction	18
1.1	Key Takeaways	18
1.2	Narrative	18
2	Synergies with the US Neutrino Program	21
2.1	Key Takeaways	21
2.2	Narrative	22
3	Synergies with the Broader US Science Program	25
3.1	Key Takeaways	25
3.2	Narrative	25
4	Three-Neutrino Oscillation Physics with Reactors (NF01)	27
4.1	Key Takeaways	27
4.2	Narrative	28
5	Non-Standard Flavor Mixing Searches at Reactors (NF02)	36
5.1	Key Takeaways	36
5.2	The Reactor Antineutrino Anomaly	36
5.3	Reactor Spectrum Ratio Experiments and the Complex Current Landscape	39
5.4	The Future of Short-Baseline Reactor Experiments	41
5.5	Medium- and Long-Baseline Reactor Experiments	43
6	Probing Neutrino Properties and Unknown Particles with Reactors Neutrino Detectors (NF03, NF05)	44
6.1	Key Takeaways	44
6.2	Reactor $CE\nu NS$ and Low-Energy Processes: Theory and Experimental Limits	45
6.3	Experimental Requirements For Reactor $CE\nu NS$ Detection	47
6.4	Exotic particle searches at nuclear reactors	49
7	Improving Reactor and Nuclear Physics Knowledge Through Neutrino Measurements and Modelling (NF09)	51
7.1	Key Takeaways	51
7.2	Reactor Neutrino Flux and Spectrum Measurements	51
7.3	Modeling Reactor Antineutrino Emissions	53
7.4	Data-Model Discrepancies	54
7.5	Future Improvements in Understanding Isotopic Neutrino Emissions . . .	56
8	Priorities for Improving Reactor Antineutrino Detection (NF10)	59
8.1	Key Takeaways	59

8.2	Reactor Antineutrino Detection Technologies	59
8.3	Very Low Energy Detection	59
8.4	IBD Detection Technology Improvements	62
8.5	Synergies	65
9	Applications of Reactor Neutrinos (NF07)	66
9.1	Key Takeaways	66
9.2	Antineutrino Applications Overview	66
9.3	Potential Societal Benefits from the Application of Neutrino Detection . . .	66
9.4	Overlaps between Applications and High Energy Physics Opportunities . .	68
9.5	Overlaps With Technology Development	68
9.6	Workforce Development Pipeline and Non-traditional Career Paths	69
9.7	Realizing Synergies between Neutrino Physics and Neutrino Applications	69

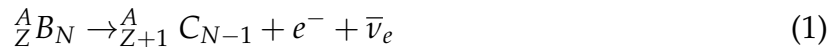
1 Introduction

1.1 Key Takeaways

- Nuclear reactors are a uniquely powerful, abundant and flavor-pure source of antineutrinos that continue to play a vital role in the US neutrino physics program.
- Neutrino physics opportunities at reactors offer strong complementarity with numerous aspects of the wider US neutrino program, including Standard Model and BSM oscillations studies and technology development.
- Reactor neutrino experiments have a direct societal impact and have become a strong workforce and technology development pipeline for DOE National Laboratories and universities.

1.2 Narrative

Nuclear reactors are a uniquely powerful, abundant, and flavor-pure source of MeV-scale antineutrinos. Electron-flavored antineutrinos ($\bar{\nu}_e$) are produced in reactors as the unstable, neutron-rich products of nuclear fission undergo beta decay reactions:



While only a few percent of the the roughly 200 MeV of excess rest mass energy from one nuclear fission is ultimately expressed as $\bar{\nu}_e$ kinetic energy, this equates to a total release of 2×10^{20} $\bar{\nu}_e$ per GW_{th} power generated. The energy spectrum of $\bar{\nu}_e$ emitted by an operating reactor core reflects the decay schemes of the decaying isotopes, whose endpoints roughly range from the sub-MeV to the 10 MeV scale, as well as the relative abundance of these isotopes in the nuclear fuel, which is driven primarily by the likelihood of their production (or yield) in the core's fission reactions [1–4].

The antineutrino emissions of dozens of nuclear reactors across three different continents have been observed with neutrino detectors. Locations of current and recent past experiments are illustrated in Figure 1; detailed reviews of these and other past experiments can be found in Refs [5–7]. Most of these have been commercial power reactors, which operate in the $\sim\text{GW}_{\text{th}}$ regime and burn fuel with a relatively low level of ${}^{235}\text{U}$ enrichment (low enriched, or LEU). These reactors' neutrino emissions are produced by a mixture of fissionable isotopes, with the dominant isotopes ${}^{235}\text{U}$ and ${}^{239}\text{Pu}$ providing $>80\%$ of all fissions, and ${}^{238}\text{U}$ and ${}^{241}\text{Pu}$ each providing less than 10%. A substantial number of experiments have been performed at research reactors operating at substantially lower power, $\sim 10\text{--}100 \text{ MW}_{\text{th}}$, than commercial LEU cores. These cores have generally been smaller in spatial extent ($<1 \text{ m}$ dimensions) than commercial ones ($>\text{m}$ dimensions), and have used fuel of substantially higher ${}^{235}\text{U}$ enrichment (highly enriched, or HEU), leading to $\bar{\nu}_e$ emissions overwhelmingly dominated by ${}^{235}\text{U}$ fission

products. While other reactor types exist that contain substantially different fuel content than these two options, such as mixed oxide [8–10] or natural uranium reactors [11], no successful measurements of these reactor types have been performed.

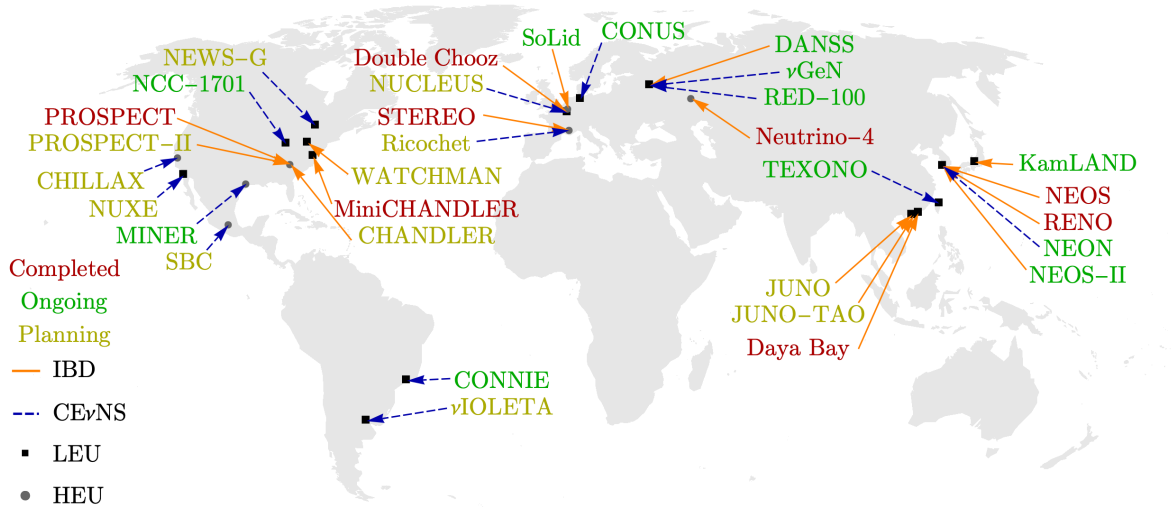


Figure 1: Map of planned, current, and completed reactor antineutrino experiments. Text color indicates experimental status, while arrow color indicates the interaction channel used by the experiment. Only completed experiments taking data after 2010 are included. Further description of these experiments are given in Tables 3 and 4.

As differing fission isotopes have differing yet overlapping fission product yields, HEU and LEU reactors modestly differ in the mean number and energy spectrum of neutrinos they release per fission. Considering the decay production mechanism in Eq. 1, predictions of HEU and LEU reactor $\bar{\nu}_e$ emissions can be composed by relying either primarily on knowledge of the produced parent and daughter nuclei, referred to as the *summation* or *ab initio* approach [2, 4, 12–14], or primarily on knowledge of the properties of the decay electron produced in concert with each $\bar{\nu}_e$, referred to as the *conversion* approach [15–18]. These prediction methods are described in further detail in Section 7.

Reactor $\bar{\nu}_e$ can be detected via multiple detection channels, including inverse beta decay (IBD) on protons or other nuclei, neutral current inelastic nuclear scattering, neutrino-electron elastic scattering, and coherent elastic neutrino-nucleus scattering [19]. The proton IBD interaction, $p + \bar{\nu}_e \rightarrow n + e^+$, represents the vast majority of all observed interactions to date. The presence of two final-state particles that can be individually and coincidentally detected in organic scintillator detectors is advantageous in achieving excellent background reduction; this channel also facilitates high-fidelity determination of $\bar{\nu}_e$ energies via reconstruction of e^+ energies. Detectors with some combination of very low background contamination, very low energy detection thresholds, and specialized

materials are required for detection of reactor $\bar{\nu}_e$ using other detection channels. As an example, detection via coherent neutrino-nucleus scattering require cryogenic detectors using semiconductors or bolometric crystals as targets, with energy detection thresholds well below 1 keV_{nr}. Figure 1 also indicates the exploited interaction channel in recent and future reactor $\bar{\nu}_e$ experiments.

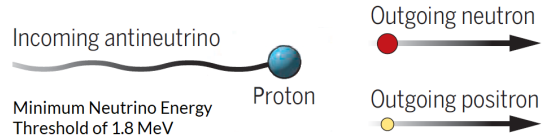
Past reactor antineutrino experiments have been critically important in the elucidation of the contemporary view of the Standard Model of particle physics (SM). Proton IBD-based reactor measurements were the first to verify the existence of neutrinos [21], and have yielded world-leading or competitive precision on three of the six SM neutrino mixing parameters [22–27]. Deuteron IBD-based reactor measurements provided early validations of weak interaction theory [28]. Reactor $\bar{\nu}_e$ -electron scattering measurements have enabled measurement of the Weinberg mixing angle and competitive limits on measurements of the magnetic moment of the neutrino [29, 30]. Reactor experiments have also enabled world-leading probes of new beyond-the-Standard-Model (BSM) physics. Short-baseline proton IBD experiments have been used to set new limits on active-sterile neutrino mixing in the eV-scale range and below [31–37]. Efforts to measure reactor-based coherent neutrino scattering, while so far unsuccessful in detecting a statistically significant quantity of neutrino interactions, have nonetheless established world-leading limits on some prospective hidden sector couplings to neutrinos [38, 39]. All of these measurements have been performed with fairly imprecise knowledge regarding the true underlying flux and spectrum of reactor $\bar{\nu}_e$ emissions.

In the coming decade, reactor-based neutrino measurements can continue to provide crucial new insights into the nature of the Standard Model and beyond. New reactor-based oscillation experiments can continue extending the boundaries of our understanding of key SM mixing parameters [40–42], while also pushing active-sterile

Common types of interactions for reactor neutrinos

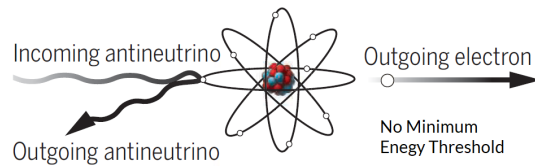
Inverse beta decay (IBD)

An incoming antineutrino exchanges charge with a proton, converting to a neutron and a positron.



Neutrino electron elastic scattering

An incoming antineutrino scatters off of an electron. The recoiling electron emerges in a direction that is very close to that of the incoming neutrino.



Coherent elastic neutrino-nucleus scattering (CEνNS)

The entire nucleus recoils as a solid body off of an incoming antineutrino.

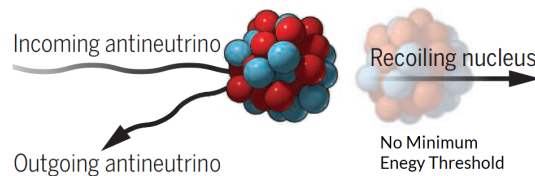


Figure 2: Illustrations of reactor $\bar{\nu}_e$ interaction mechanisms. Adapted from [20]

mixing parameter space coverage in the electron flavor sector close to the few-percent level over a wide range of mass splittings from Δm_{13}^2 to the 10s of eV^2 scale [43–47]. Both SM and BSM oscillation measurements are highly synergistic with other aspects of the US neutrino physics program, including its long-baseline and short-baseline accelerator neutrino efforts. Future high-statistics $\bar{\nu}_e$ measurements at differing reactor types can greatly improve our understanding of the absolute flux and spectrum of reactor $\bar{\nu}_e$ produced by all reactor core types, both above and below the 1.8 MeV IBD interaction threshold [48]. In addition to improving the achievable precision of some reactor-based BSM measurements, such as those performed by CEvNS experiments, these improvements are clearly synergistic with facets of the applied reactor physics, nuclear safeguards, and nuclear data communities [49–53]. The reactor $\bar{\nu}_e$ field’s comparatively low barrier to entry and small experiment scales enable it to serve as a valuable workforce and technology development pipeline while concurrently delivering world-class physics results.

The purpose of this white paper, written as part of the Snowmass 2021 community organizing exercise, is to survey the impressive range of high-impact physics that can be achieved in the coming decade with current and prospective future reactor antineutrino experiments, to highlight the large degree of synergy between this future reactor $\bar{\nu}_e$ measurement program, and to emphasize direct societal impacts of near-term investments of the HEP community in the reactor $\bar{\nu}_e$ sector. In this context, Section organization and content will be generally aligned with the boundaries of specific Neutrino Frontier Topical Groups. Sections 2 and 3 will begin by summarizing synergies between future reactor $\bar{\nu}_e$ efforts and the US neutrino program and the broader US science community, respectively. Sections 4 (directed towards Topical Group NF01) and 5 (towards NF02) highlights potential improvements in understanding of SM oscillations and current short-baseline neutrino anomalies, respectively. Section 6 (towards NF03 and NF04) discusses how future reactor measurements can improve knowledge of other SM neutrino properties and possible hidden-sector couplings. Section 7 (towards NF09) overviews potential advancements in global understanding of $\bar{\nu}_e$ emissions from various reactor types and the ability to accurately model these emissions. Finally, Sections 8 and 9 (towards NF10 and NF07, respectively) will focus on applications and detector technology developments relevant to reactor $\bar{\nu}_e$.

2 Synergies with the US Neutrino Program

2.1 Key Takeaways

- Due to their comparatively low energies and high electron flavor purity, reactor $\bar{\nu}_e$ experiments play a necessary role in a multi-faceted global effort to probe the potential BSM origins of existing short-baseline neutrino anomalies.

- High-precision reactor-based probes of active-sterile neutrino couplings are important for ensuring clear interpretations of DUNE’s long-baseline oscillation physics results.
- Reactor-based measurements of θ_{13} , θ_{12} , Δm_{31}^2 , Δm_{21}^2 and the mass hierarchy serve to expand the physics deliverables and ultimate sensitivity of DUNE and the US long-baseline neutrino program.
- Reactor $\bar{\nu}_e$ experiments continue to develop technologies well-suited for application to other areas in neutrino and particle physics, such as detection of light dark matter, geoneutrinos, solar neutrinos, and neutrinoless double beta decay.

2.2 Narrative

Reactor $\bar{\nu}_e$ data plays a variety of essential roles in performing future Standard Model and BSM oscillation measurements vital to the US neutrino community. Their power and complimentary position in the global landscape is well illustrated in Figures 3 and 4. As they sample lower neutrino energies than most other efforts (Figure 3), reactor experiments can feasibly access all Δm^2 ranges of interest in current oscillation studies with a single source type. They also sample a pure flux of electron-flavor neutrinos (Figure 4), enabling particularly clean tests of specific mixing parameters. Since lower energies in reactor experiments are also accompanied by shorter baselines, reactor-based oscillation tests are also less influenced by some commonly-studied neutrino sector BSM effects, such as non-standard matter interactions or heavy-mediator couplings between neutrinos and hidden sectors.

In the context of the today’s US neutrino program, one of reactor experiments’ most prominent roles is in testing the origin of anomalies observed by short-baseline neutrino experiments. This topic addresses two of the five Science Drivers identified in the 2014 P5 report [56]. Many of these persistent anomalies rest in the electron flavor realm, where reactor experiments, in particular, excel. For example, the BEST experiment recently confirmed the robustness of the so-called ‘Gallium Anomaly’ by detecting a $\sim 20\%$ deficit in observed interactions of sub-MeV ν_e generated by an intense radioactive source [57]. Even MicroBooNE, which primarily samples ν_μ from Fermilab’s BNB beamline, has attracted attention with weak hints of a deficit of ν_e interactions [58], prompting further theoretical examination of sterile-mediated electron-flavor disappearance [59, 60]. This recent result contrasts with long-standing MiniBooNE results showing an excess of ν_e -like events in the same beamline [61].

Future aspects of the US neutrino program, such as Fermilab SBN [62], will certainly fight in the following decade to elucidate the causes of these and other anomalies. However, when viewed in the canonical BSM framework of oscillations between three active neutrino states and one additional sterile state (3+1), it seems likely that

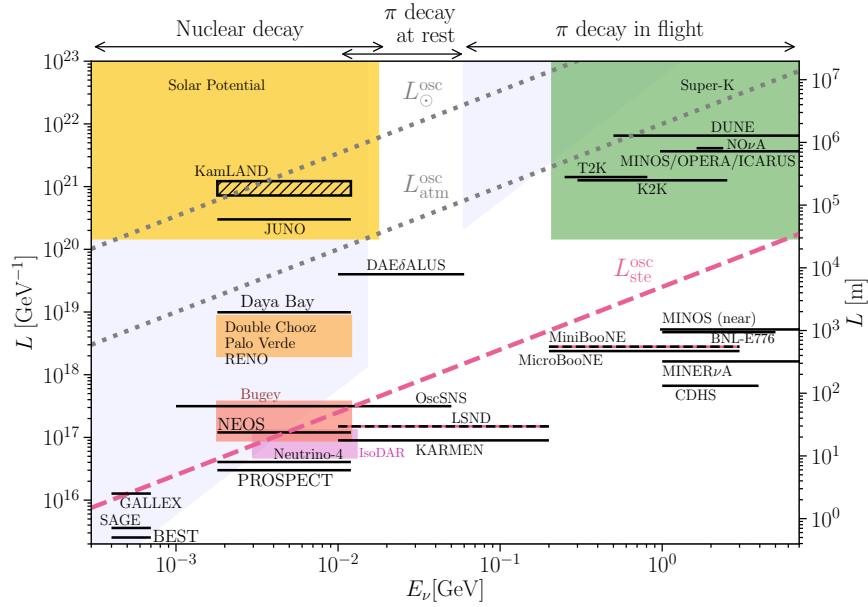


Figure 3: Overview of experimental source-detector baselines (L) and neutrino energies (E) sampled by neutrino experiments worldwide; adapted from Ref [54].

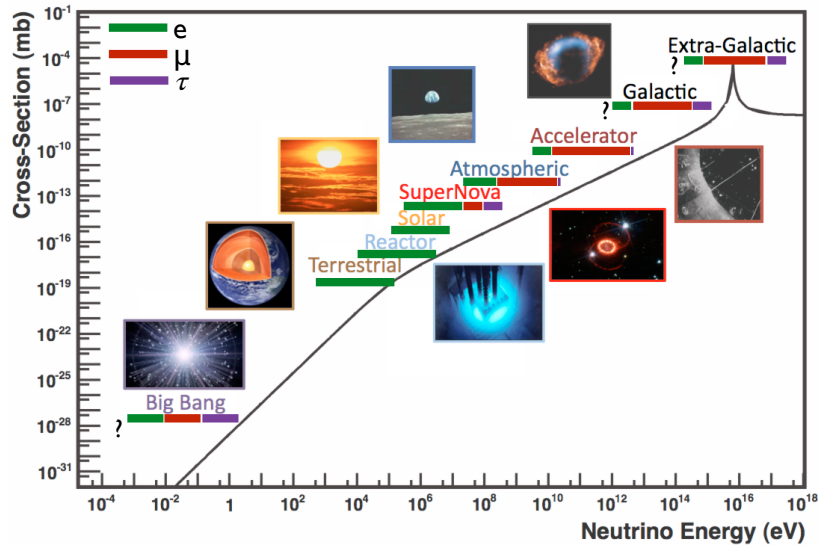


Figure 4: Approximate flavor composition of commonly discussed neutrino sources; adapted from [55]. Reactor experiments are notable in their use of lower energy neutrinos, their access to very short baselines, and their extreme electron flavor purity.

conclusively demonstrating the consonance or dissonance of these varied datasets will be a challenging task. Datasets that test, with maximal clarity, the 3+1 oscillation interpretation in specific channels and suggested phase space regions are a particularly

important ingredient in this effort. Short-baseline reactor neutrino experiments, with their well-defined flavor profile, straightforward energy reconstruction, and purely relative analysis methods, offer an ideal experimental arrangement for targeted, clear tests. For these reasons, reactor experiments are a crucial piece of a diverse future global effort capable of elucidating whether or not a 3+1 model is an acceptable solution to the various short-baseline anomalies.

It is also possible that the observed short-baseline anomalies are instead explained by a hidden sector physics scenario more complex than the canonical 3+1 model, such as one with multiple sterile neutrinos (3+N) [63], sterile neutrino decay [64, 65], NSI [66], hidden sector couplings [67], or some combination of effects [68]. If this is the case, data from diverse channels, energies, and sources will be even more crucial for disentangling the different contributing effects, as each effect may or may not manifest itself differently in specific experimental regimes. In the stable of global measurements, short-baseline reactor oscillation measurements are unique in their capability to very purely probe sterile oscillation effects. As mentioned above, this is due to the lower energies involved in interactions and decays in the reactor, which prohibits production and decay of heavier hidden-sector particles, and their very short baselines, which minimize the impact of NSI.

Short-baseline reactor experiment results also have particular relevance to upcoming measurements of Standard Model neutrino properties. Theoretical studies have pointed to specific regions of 3+1 phase space that could complicate interpretation of DUNE and other future US long-baseline neutrino measurements [69, 70]. For example, a sterile sector with specific combinations of non-zero active and sterile CP violating phases could mimic CP-conserved signatures in DUNE [71]. Parameter degeneracies can be avoided for DUNE if separate measurements are used to constrain the level of active-sterile mixing; scenarios like the one above can be avoided if limits on θ_{14} and θ_{24} can be improved to approximately the 5° ($\sin^2 2\theta = 0.03$) level [72]. θ_{14} limits meeting this stringent requirement are only accessible with intense electron-flavor sources, such as reactors and tritium decay facilities like KATRIN and Project-8 [73]. Thus, reactor $\bar{\nu}_e$ experiments play a synergistic role in enabling clear interpretations of the neutrino community's centerpiece experiment, DUNE, and its physics centerpiece, measurement of leptonic CP-violation.

Medium- and long-baseline reactor oscillation measurements are also crucial in extending the US Standard Model neutrino oscillation measurements program. It should first be emphasized that reactor-based measurements of a large θ_{13} value paved the way for DUNE by demonstrating that CP-violation measurements are feasible with conventional neutrino beams. In the near future, Daya Bay's still-improving limits on θ_{13} remain essential in current accelerator-based probes of CP-violation with T2K and NOvA [74, 75], and later, when included in DUNE fits, they will modestly enhance

DUNE’s oscillation parameter measurement precision [76]. Approached from a different perspective, comparisons of Daya Bay’s and DUNE’s independently-measured θ_{13} values can be directly compared to yield tests of unitarity in the PMNS mixing matrix [77, 78]. In the solar sector, JUNO, along with DUNE, are the primary pieces in a future program for sharpening our view of tensions in solar- and reactor-derived measurements of Δm_{21}^2 [79]; if such a discrepancy persists in these higher-precision experiments, it could provide the first clear evidence for non-standard neutrino interactions [66]. Last but not least, JUNO will measure the mass hierarchy independently of other experiments [80], providing unique information on a parameter that is extremely important across many branches of neutrino physics, including neutrinoless double beta decay and neutrino mass experiments, as well as DUNE’s long-baseline oscillation [81, 82] and supernova neutrino burst [83] physics programs.

3 Synergies with the Broader US Science Program

3.1 Key Takeaways

- *Nuclear physics:* Nuclear reactors’ antineutrinos provide a novel source of information regarding short-lived, high-Q isotopes whose properties are in some cases poorly understood.
- *Applications:* HEP-oriented reactor neutrino detector technologies and techniques are highly relevant to future antineutrino-oriented safeguards, reactor exclusion and reactor monitoring use cases, as well as neutron and gamma-ray detection.
- *US Workforce Development:* Compared with large international experiments, the relatively small size and fast timescale from design to data-taking of reactor experiments provide an inviting workforce development opportunity, enabling the realization of versatile skillsets for new generations of young nuclear and particle physicists. Additionally, antineutrino-based applications at all scales offer a unique opportunity for collaborative engagement between applications-focused and basic science-focused community members.
- *US Facility Enhancement:* Reactor neutrino experiments enable the use of crucial US facilities for purposes beyond their initially intended or envisioned scope, which strengthens the scientific interest and vitality of these facilities.

3.2 Narrative

Efforts pursuing neutrino physics goals using reactor $\bar{\nu}_e$ have many benefits to and synergies with the broader scientific community of the United States and the World. These range across the direct contribution of important scientific knowledge, development of cross-cutting technologies and facilities, enabling applications with

significant societal impact, and the development of a highly skilled workforce.

Beyond the high energy physics topics mentioned in the previous section, reactor $\bar{\nu}_e$ measurements can contribute to other fields of scientific enquiry. As described in Sec. 7, the $\bar{\nu}_e$ emissions from a reactor provide a probe of the nuclear fission process that is complementary to other techniques that measure more readily accessible particles like fission fragments, gamma-rays and neutrons. Specifically, the reactor $\bar{\nu}_e$ energy spectrum encodes information about fission product yields and the energy spectrum of beta-decays of those fission daughters. Included in the total $\bar{\nu}_e$ spectrum are contributions from short-lived, high Q-value isotopes, some of which have received limited experimental investigation. High statistics and high precision $\bar{\nu}_e$ spectrum measurements therefore have the potential to test the nuclear data evaluations that underlie many areas of nuclear physics, nuclear energy, and nuclear security. Nuclear data needs and benefits that can be addressed with reactor $\bar{\nu}_e$ have been described in recent workshops and reports [51, 53].

Advances in scientific knowledge regarding neutrino production in nuclear reactors and characterizing such nuclear systems themselves also underlie another significant societal benefit of reactor $\bar{\nu}_e$ studies. As described in Sec. 9 and Ref. [84], the $\bar{\nu}_e$ emitted by operating nuclear reactors and spent nuclear fuel may be useful for cooperative nonproliferation applications such as monitoring fissile material production in reactors, exclusion of undeclared reactors, and monitoring of spent fuel and reprocessing facilities.

A recent study focused on the potential utility of $\bar{\nu}_e$ for nuclear energy and nuclear security applications elucidates some of the relevant characteristics of these particles and potential use cases for them [52]. The highly penetrating nature of neutrinos poses detection and implementation challenges in the context of monitoring applications, but also holds promise as a non-intrusive technique that does not require direct access to complex and/or sensitive facilities. Considering user need and constraints, forthcoming advanced reactor types for which nuclear safeguards techniques are still be developed and nuclear security deals between nations were found to be promising use cases for $\bar{\nu}_e$ monitoring measurements.

Of course, potential applications of $\bar{\nu}_e$ depend heavily upon the detection tools and techniques developed by neutrino physics experiments. All application oriented demonstrations of reactor $\bar{\nu}_e$ have been enabled by the multi-decade succession of reactor $\bar{\nu}_e$ scientific experiments that have preceded them [84]. Recent advances like aboveground $\bar{\nu}_e$ detection without substantial overburden [85, 86] have greatly broadened the range of applications that can be considered. Since neutron identification is central to detection of the IBD interactions, materials and techniques developed for reactor $\bar{\nu}_e$ also have significant potential for neutron detection in support a wide range

of nuclear security applications [87].

Beyond the scope of the US neutrino oscillation physics program and potential applications, reactor $\bar{\nu}_e$ experiments continue to develop technologies well-suited for other areas in neutrino and particle physics. For example, technology being developed to enable detection of low-energy signals from coherent neutral current nuclear scattering of reactor $\bar{\nu}_e$ addresses similar challenges to those needed to seek dark matter interactions with electrons and nuclei [88–90]. Doped aqueous, plastic, or opaque scintillator technology used for reactor IBD detection may offer value in other sectors of the US neutrino physics program, such as in neutrinoless double beta decay experiments [91, 92], measurements of neutrino-induced neutron production [93], and future water-based DUNE far detector modules [94]. For these and other cases described in Section 8, synergies clearly exist between the pursuit of reactor neutrino detection and other aspects of the US particle physics program.

The training and mentoring of a skilled, creative, and diverse workforce is not only essential to the future of HEP, but it is also one of the primary societal benefits that justifies public investment in this field. Reactor $\bar{\nu}_e$ experiments are an especially effective training ground for producing highly skilled and well rounded scientists. Due to their relatively small size, they offer young scientists the rare opportunity to experience the experimental process from the idea and design stage to data taking and analysis. Experiments of order of 5 years duration offer invaluable training opportunities matched to the research timescale of postdocs (3 years) and graduate students (4-6 years). In addition, the relatively smaller size of collaborations of these experiments offer supportive and nurturing environments that are complementary to the opportunities found in large, international collaborations and reduce the threshold for early career scientists to get involved.

More broadly, antineutrino-based applications offer a unique opportunity for collaborative engagement between applications-focused and basic science-focused community members. Since a key programmatic goal of the US HEP program is workforce training for US National Laboratories, opportunities for bridging between applied and fundamental science research should be fostered wherever it is possible to do so. By engaging in antineutrino applications research, applications and fundamental physics researchers can work side by side in performing technology development, engineering and deployment, and data analysis.

4 Three-Neutrino Oscillation Physics with Reactors (NF01)

4.1 Key Takeaways

- Nuclear reactors are a powerful, abundant, cost-effective, and well-understood source of antineutrinos, and have been used to make some seminal measurements

in neutrino oscillations.

- In the next half-decade, reactor antineutrino experiments are expected to provide the world's best estimates for the foreseeable future of 4 out of 6 oscillation parameters:
 - $\sin^2 \theta_{13}$ with Daya Bay, Double Chooz and RENO.
 - Δm_{31}^2 , Δm_{21}^2 , and $\sin^2 \theta_{12}$ with JUNO (with sub-half-percent precision).
- Reactor antineutrinos in JUNO will also enable an independent measurement of the mass ordering with very different baseline, energy, backgrounds, and detector systematic uncertainties to what other experiments will do.

4.2 Narrative

In recent years, reactors have played a major role in the study of neutrino oscillations and helped establish the three-neutrino oscillation framework that still stands as the leading paradigm of this phenomenon [95, 96]. In this section, we review the theory, experiments, and prospects of three-neutrino oscillation physics with reactors.

In the Standard Model of particle physics, three neutrino flavors, ν_e , ν_μ , and ν_τ , participate in the weak interaction. However, if neutrinos have a non-zero mass, the flavor composition of a neutrino beam could change as the neutrinos propagate in space. This phenomenon is called neutrino oscillations and is a quantum mechanical effect stemming from the fact that a neutrino with a definite flavor need not have a definite mass. In fact, a neutrino flavor eigenstate can be viewed as a linear superposition of the neutrino mass eigenstates, ν_1 , ν_2 , and ν_3 :

$$\begin{pmatrix} \nu_e \\ \nu_\mu \\ \nu_\tau \end{pmatrix} = \begin{pmatrix} U_{e1} & U_{e2} & U_{e3} \\ U_{\mu1} & U_{\mu2} & U_{\mu3} \\ U_{\tau1} & U_{\tau2} & U_{\tau3} \end{pmatrix} \cdot \begin{pmatrix} \nu_1 \\ \nu_2 \\ \nu_3 \end{pmatrix}. \quad (2)$$

The unitary 3×3 mixing matrix, U , is called the Pontecorvo-Maki-Nakagawa-Sakata (PMNS) matrix and can be parameterized by three mixing angles, θ_{12} , θ_{13} , θ_{23} , and one CP-violation phase, $\delta_{CP}\ddagger$:

$$U_{\text{PMNS}} = \begin{pmatrix} 1 & 0 & 0 \\ 0 & c_{23} & s_{23} \\ 0 & -s_{23} & c_{23} \end{pmatrix} \begin{pmatrix} c_{13} & 0 & s_{13}e^{-i\delta_{CP}} \\ 0 & 1 & 0 \\ -s_{13}e^{i\delta_{CP}} & 0 & c_{13} \end{pmatrix} \begin{pmatrix} c_{12} & s_{12} & 0 \\ -s_{12} & c_{12} & 0 \\ 0 & 0 & 1 \end{pmatrix}, \quad (3)$$

where the notation $c_{ij} = \cos \theta_{ij}$, $s_{ij} = \sin \theta_{ij}$ is used.

As neutrinos travel a certain distance L in vacuum, their mass eigenstates with energy E develop a phase such that $\nu_i(L) = e^{-i\frac{m_i^2}{2E}L} \cdot \nu_i(0)$. Given the neutrino mixing formula

\ddagger There are two additional phases if neutrinos are Majorana particles, but they do not play a role in neutrino oscillation experiments.

in Eq. (2), the probability of a neutrino with flavor l transforming to a different flavor l' can be written as:

$$\begin{aligned}
P_{\nu_l \rightarrow \nu_{l'}} &= |\langle \nu_{l'}(L) | \nu_l(0) \rangle|^2 \\
&= \left| \sum_j U_{lj} U_{l'j}^* e^{-i \frac{m_j^2}{2E} L} \right|^2 \\
&= \sum_j |U_{lj} U_{l'j}^*|^2 + \sum_j \sum_{k \neq j} U_{lj} U_{l'j}^* U_{lk}^* U_{l'k} e^{i \frac{\Delta m_{jk}^2 L}{2E}}, \tag{4}
\end{aligned}$$

where $\Delta m_{jk}^2 = m_j^2 - m_k^2$ are the mass-squared differences between mass eigenstates.

Since nuclear reactors produce only electron antineutrinos, $\bar{\nu}_e$, with energy below about 9 MeV that is lower than the production threshold of a muon or a tau lepton, the experimental observation of neutrino oscillations is typically through the disappearance channel. Namely, the $\bar{\nu}_e$ neutrino flux is measured at some distance L away from the reactor, and the survival probability $P_{\bar{\nu}_e \rightarrow \bar{\nu}_e}$ is calculated by comparing to the flux near the source. Given Eq. (4), this survival probability can be expressed as:

$$\begin{aligned}
P_{\bar{\nu}_e \rightarrow \bar{\nu}_e} &= 1 - 4|U_{e1}^2| |U_{e3}^2| \sin^2 \Delta_{31} - 4|U_{e2}^2| |U_{e3}^2| \sin^2 \Delta_{32} - 4|U_{e1}^2| |U_{e2}^2| \sin^2 \Delta_{21} \\
&= 1 - \sin^2 2\theta_{13} (\cos^2 \theta_{12} \sin^2 \Delta_{31} + \sin^2 \theta_{12} \sin^2 \Delta_{32}) - \cos^4 \theta_{13} \sin^2 2\theta_{12} \sin^2 \Delta_{21}, \tag{5}
\end{aligned}$$

where the notation $\Delta_{ij} = \frac{\Delta m_{ij}^2 L}{4E}$ is used. From Eq. (5) we see that reactor antineutrino disappearance is a clean channel that is only dependent on θ_{12} , θ_{13} , Δm_{21}^2 , Δm_{31}^2 , and the neutrino mass ordering, making it ideal for precision measurements of these oscillation parameters. Fig. 5 shows the survival probability as a function of the travel distance L for a typical 4 MeV reactor $\bar{\nu}_e$. The large disappearance at ~ 60 kilometers is driven by the solar-mixing mass scale Δm_{21}^2 and its corresponding large mixing angle θ_{12} , while the smaller disappearance at ~ 2 kilometers is caused by the atmospheric-mixing mass scale $\Delta m_{31}^2 \sim \Delta m_{32}^2$ and the small mixing angle θ_{13} . The two very different Δm^2 scales benefit designs of reactor antineutrino oscillation experiments, which can isolate the parameters of interest and improve the precision of their determination by placing detectors at strategic baselines.

The first reactor antineutrino experiment that observed an evidence of neutrino oscillations is the KamLAND experiment [22], built in the early 2000s in Japan. The KamLAND experiment was prompted by the ‘‘Solar Neutrino Problem’’, which refers to the observation that the ν_e flux from the Sun is less than a half of the prediction from the Standard Solar Model [97]. The theory of neutrino oscillations provides an elegant solution to the solar neutrino problem, and can be tested on Earth using reactor antineutrinos assuming CPT invariance. The KamLAND experiment is located in the middle of Japan, surrounded by 55 Japanese reactor cores with a flux-weighted average

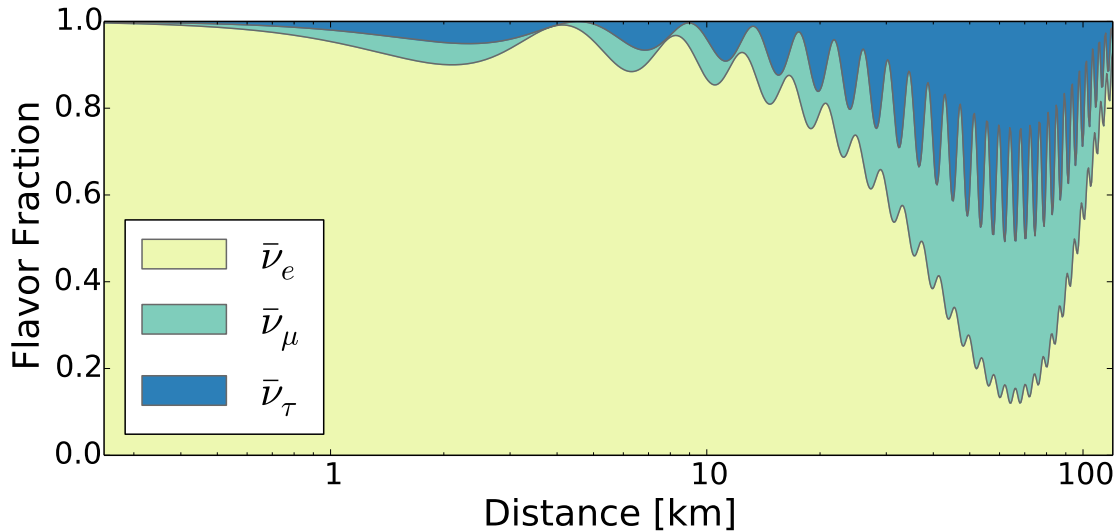


Figure 5: Expected flavor composition of the reactor antineutrino flux as a function of distance to a reactor core for neutrinos of 4 MeV energy. Figure taken from Ref. [95]. The light yellow region corresponds to the survival probability of $\bar{\nu}_e$ that reactor antineutrino experiments can measure by placing their detectors at different baselines.

baseline of ~ 180 kilometers. As shown in Fig. 5, at this baseline, the KamLAND experiment is sensitive to the solar-mixing parameters Δm_{21}^2 and θ_{12} , and benefits from a better understood neutrino source and simpler vacuum oscillation formula compared to solar neutrino experiments. The KamLAND detector uses one kiloton of liquid scintillator as the target volume, which is contained in a 13-meter-diameter transparent balloon surrounded by a mineral oil region containing 1,879 photomultiplier tubes (PMTs). The results in 2008 observed a total of 1609 events with a 2.9 kton-year exposure, which was only about 60% of the predicted signal if there were no oscillations [98]. The calculated survival probability shows a clear oscillatory pattern as a function of L/E_ν , a smoking gun evidence of the existence of neutrino oscillations. The results were also highly consistent with solar neutrino experiments. When combined with the results from SNO [99], they provided the most precise measurement of $\tan^2 \theta_{12} = 0.47^{+0.06}_{-0.05}$ and $\Delta m_{21}^2 = 7.59^{+0.21}_{-0.21} \times 10^{-5} \text{ eV}^2$ to date [98].

The first generation of reactor θ_{13} experiments, CHOOZ [100] and Palo Verde [101], did not observe $\bar{\nu}_e$ disappearance from reactors and only an upper limit of $\sin^2 2\theta_{13} < 0.10$ at 90% C.L. was set. In the 2000s, a new generation consisting of Daya Bay [102], Double Chooz [103], and RENO [25], was initiated to measure the small mixing angle θ_{13} .

Given the mass-scale Δm_{31}^2 suggested by the atmospheric neutrino experiments, the corresponding baseline for reactor antineutrino experiments is about 1–2 kilometers, as indicated in Fig. 5. All experiments adopted the strategy of performing a relative

measurement between near and far functionally identical detectors to largely suppress the reactor and detector related systematic uncertainties. After some early indications in 2011 [26, 104, 105], all three experiments reported clear evidence of $\bar{\nu}_e$ disappearance in 2012 with a few month's data taking [24, 25, 106].

Among these experiments, the Daya Bay experiment, being the most sensitive one, excluded $\theta_{13} = 0$ at 5.2σ with 55 days of data [24]. The Daya Bay experiment is located near the six reactors of the Daya Bay nuclear power plant in southern China, with a total reactor power of $17.4 \text{ GW}_{\text{th}}$. Daya Bay uses eight identical antineutrino detectors (ADs), with two ADs at $\sim 360 \text{ m}$ from the two Daya Bay reactor cores, two ADs at $\sim 500 \text{ m}$ from the four Ling Ao reactor cores, and four ADs at a far site $\sim 1580 \text{ m}$ away from the 6-reactor complex. Each AD contains 20-tons of gadolinium-loaded liquid scintillator as the target volume. Each AD's target is viewed by 192 8-inch PMTs that yield an energy resolution of $8.5\%/\sqrt{E(\text{MeV})}$, allowing a precise measurement of the reactor antineutrino energy spectrum that enables the the observation of a spectral distortion between far and near detectors as expected from neutrino oscillations. In 2018 results, Daya Bay reported detection of nearly 3.5 million reactor antineutrino events in the near detectors and 500 thousand events in the far detectors over 1958 days of data collection. The comparison of relative $\bar{\nu}_e$ event rates and energy spectra among detectors is consistent with the three-neutrino oscillation formula as introduced in Eq. (5) and yields $\sin^2 \theta_{13} = 0.0856 \pm 0.0029$ and $\Delta m_{32}^2 = 2.471_{-0.070}^{+0.068} \times 10^{-3} \text{ eV}^2$ assuming the normal mass ordering, and $\Delta m_{32}^2 = -(2.575_{-0.070}^{+0.068}) \times 10^{-3} \text{ eV}^2$ assuming the inverted mass ordering [107]. The remarkable precision makes θ_{13} the most precisely measured angle among the three neutrino mixing angles in the PMNS matrix, despite being the last known mixing angle to be non-zero. The full data set of Daya Bay from 2012–2020, with over 6 million events, is the largest library of reactor antineutrino events collected in history, and is expected to further improve the precision of $\sin^2 \theta_{13}$ and Δm_{32}^2 to better than 2.5% and 2%, respectively. Thanks to the consistent results reported by Double Chooz [108] and RENO [109], reactor experiments are providing robust and precise constraints to other experiments, including those searching for leptonic CP violation [74, 75, 81, 110].

Beyond completion of these θ_{13} experiments, reactor antineutrino experiments continue to be at the forefront of neutrino oscillation physics. The Jiangmen Underground Neutrino Observatory (JUNO) is currently under construction in southern China and is expected to come online in 2023 [80]. JUNO will be located at a baseline of $\sim 52.5 \text{ km}$ from six $2.9 \text{ GW}_{\text{th}}$ nuclear reactor cores in the Yangjiang Nuclear Power Plant (NPP) and two $4.6 \text{ GW}_{\text{th}}$ cores in the Taishan NPP. As shown in Fig. 6, JUNO's central detector (CD) will consist of 20 kilotons of liquid scintillator contained in an acrylic sphere immersed in water and surrounded by 17,612 20-inch and 25,600 3-inch PMTs providing more than 75% optical coverage. This central region will be supported by an external water

Cherenkov veto detector, and a detector-top cosmic veto tracker and calibration house.

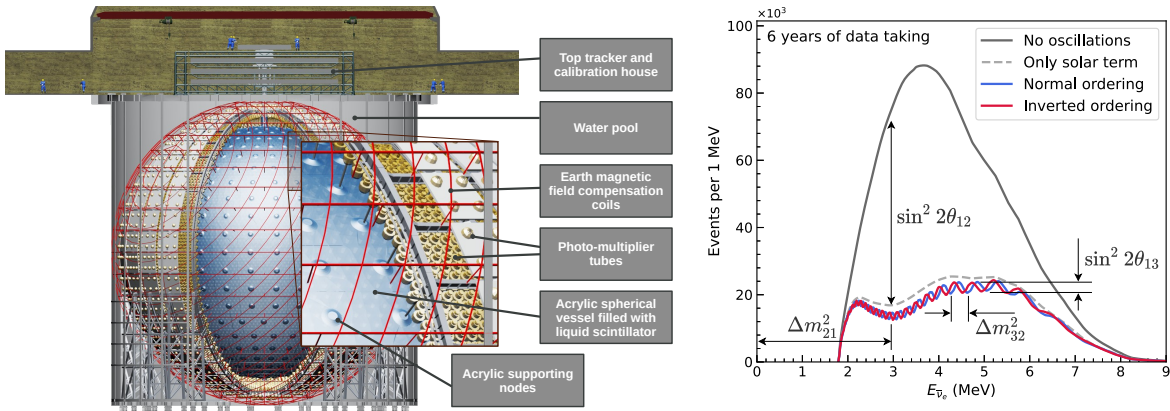


Figure 6: Left: Schematic of the JUNO detector. An acrylic sphere containing 20 kilotons of liquid scintillator serving as the $\bar{\nu}_e$ detection target is surrounded by 20-inch and 3-inch PMTs. Right: JUNO IBD spectrum with and without neutrino oscillation effects. For illustration purposes, a detector with perfect energy resolution is assumed. The gray dashed curve shows the oscillated spectrum when only the term in the disappearance probability that is modulated by $\sin^2 2\theta_{12}$ is included, whereas the blue and red curves show it when the full oscillation probability in vacuum is used assuming the normal and inverted mass orderings, respectively. Some features driven by the $\sin^2 2\theta_{12}$, $\sin^2 2\theta_{13}$, Δm_{31}^2 and Δm_{21}^2 oscillation parameters are shown pictorially. Figures obtained from Ref. [111].

JUNO will see an unparalleled amount of light for a detector of this type, amounting to over 1,300 photoelectrons per MeV. This, in combination with a comprehensive calibration program that includes the 3-inch PMT system as a handle to assess any instrumental non-linearities in the 20-inch PMT system [112], will result in an energy resolution of 3% at 1 MeV. The unprecedented detector size and energy resolution will allow to simultaneously observe the effects of both the solar and atmospheric oscillations for the first time. As illustrated on the right panel of Fig. 6, the former produces a “slow” oscillation modulated by $\sin^2 2\theta_{12}$ with frequency Δm_{21}^2 , while the latter causes a “fast” oscillation modulated by $\sin^2 2\theta_{13}$ with frequency Δm_{32}^2 . As also illustrated in Fig. 6, the oscillated spectrum changes slightly depending on the neutrino mass ordering, providing sensitivity to this parameter. This difference is caused by the interference effects that occur between the Δm_{31}^2 and Δm_{32}^2 terms in the oscillation probability of Eq. 5, which depend on the sign of Δm_{31}^2 . Knowledge of the unoscillated reactor antineutrino spectrum is important for JUNO’s physics goals, so the collaboration will deploy a satellite detector at a baseline of ~ 30 m from one of the Taishan 4.6 GW_{th} cores called the Taishan Antineutrino Observatory (JUNO-TAO) [47]. JUNO-TAO will be a 1 ton fiducial sphere of liquid scintillator loaded with gadolinium surrounded by silicon photomultipliers providing about 94% of coverage. It will be

able to measure the unoscillated reactor antineutrino spectrum with an unprecedented energy resolution $\lesssim 2\%$ at 1 MeV, thus eliminating any model dependencies in JUNO's oscillation measurements.

The conventional method to estimate JUNO's median sensitivity to the mass ordering is fitting the oscillated spectrum under the normal and inverted ordering scenarios and considering the difference in the minimum χ^2 values. Using the configuration of Ref. [42], a value of $\Delta\chi^2 = 10$ with 6 years of data taking is obtained, which corresponds to a sensitivity of about 3σ . This configuration assumes ten nuclear reactors rather than the eight that will actually be built, but also uses lower estimates of the IBD detection efficiency and the PMT detection efficiency, among others. A reassessment of the sensitivity is underway but no significant changes are expected [80].

JUNO's approach to measuring the mass ordering is orthogonal to the one to be carried out by next-generation experiments relying on atmospheric [113, 114] and accelerator [110, 115] neutrinos. The latter use neutrinos in the $\sim\text{GeV}$ energy scale traversing distances of hundreds or thousands of km, while JUNO's neutrinos will be in the $\sim\text{MeV}$ scale and will only travel for 52.5 km. Likewise, the detection technology and the backgrounds will be completely distinct. Very importantly, JUNO's measurement is completely independent of the θ_{23} mixing angle and the δ_{CP} phase. Finally, JUNO's signal arises entirely from vacuum oscillations, whereas all other experiments rely on matter effects. For all these reasons, JUNO's measurement will greatly strengthen the community's confidence in the determination of this critical parameter.

JUNO's measurement is also complementary to that of other experiments in that it will provide synergistic information beyond the pure statistical addition of results. A combined analysis of JUNO's data with those of ongoing or near term atmospheric [116, 117] or accelerator [118] experiments could yield the first determination of the neutrino mass ordering to $\geq 5\sigma$ significance. This synergy occurs primarily because of a tension in the measured values of Δm_{31}^2 that arises when the wrong ordering is assumed. As a result, the first unambiguous determination of the neutrino mass ordering could be achieved this decade.

JUNO's large-statistics measurement of the oscillated spectrum with unprecedented energy resolution will also enable determination of the four oscillation parameters that drive the disappearance of reactor antineutrinos at its 52.5 km baseline: Δm_{31}^2 , Δm_{21}^2 , $\sin^2 \theta_{12}$, and $\sin^2 \theta_{13}$. The expected sensitivities to these parameters after 6 years of data-taking are shown in Table 1. The expected relative precision is $\leq 0.5\%$ for Δm_{31}^2 , Δm_{21}^2 and $\sin^2 \theta_{12}$, and the corresponding improvement over current knowledge for those parameters is around an order of magnitude. Fig. 7 shows the expected precision as a function of running time for the four parameters. As can be seen there, the precision on Δm_{21}^2 and $\sin^2 \theta_{12}$ will already be world-leading with only ~ 100 days of data. Moreover,

the precision of the four parameters will continue to improve appreciably even after 6 years of data-taking.

	Δm_{31}^2	Δm_{21}^2	$\sin^2 \theta_{12}$	$\sin^2 \theta_{13}$
JUNO 6 years	$\sim 0.2\%$	$\sim 0.3\%$	$\sim 0.5\%$	$\sim 12\%$
PDG2020	1.4%	2.4%	4.2%	3.2%

Table 1: Expected precision of the oscillation parameters after 6 years of JUNO run time. All uncertainties are considered, and no external constraint is applied on $\sin^2 \theta_{13}$. The precision with which these parameters are currently known is shown for comparison [96]. Numbers obtained from Ref. [111].

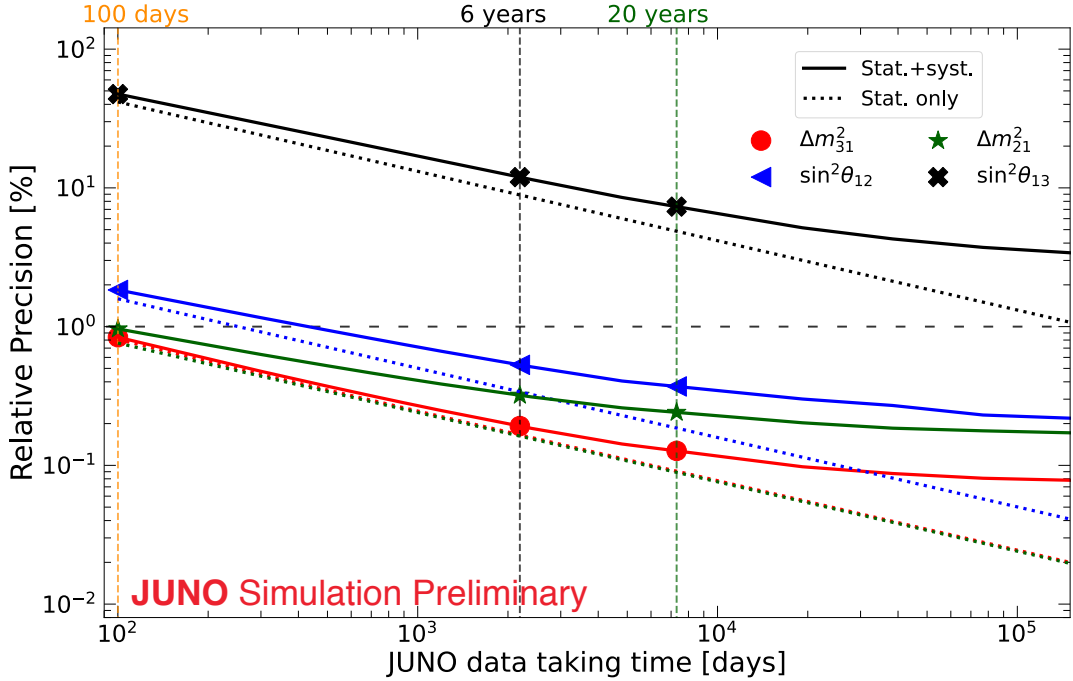


Figure 7: JUNO’s relative precision on the oscillation parameters as a function of run time. The markers and vertical lines highlight run times of 100 days, 6 years, and 20 years. The horizontal gray dashed line represents a 1% relative precision. The green dotted and red dotted lines are indistinguishable from each other since the statistical-only precision is essentially identical for the Δm_{31}^2 and Δm_{21}^2 parameters. Figure obtained from Ref. [111].

There is no confirmed experiment on the horizon that will be able to reach this precision on Δm_{31}^2 , Δm_{21}^2 and $\sin^2 \theta_{12}$, so these measurements are expected to be the best in the world for the foreseeable future. There are several ways in which they are expected to be an important input to the community:

- They will provide important constraints to present and future experiments.
- They will provide stringent inputs for neutrino masses and model building. For instance, the more precise knowledge of θ_{12} will play a prominent role, since this parameter is more sensitive to quantum corrections due to the fact that $\Delta m_{21}^2 \ll |\Delta m_{31}^2|$ and because the non-zero value of θ_{13} can induce further corrections for θ_{12} [119–121].
- They will narrow down the parameter space of the neutrinoless double beta-decay effective mass $|m_{ee}|$. In inverted mass ordering scenarios where $m_3 < 0.05$ eV, the minimal value of $|m_{ee}|$ is proportional to $\cos^2 \theta_{12}$ [122]. The better knowledge in θ_{12} will shrink the possible parameter space of $|m_{ee}|$ such that its minimum value can be increased by a factor of 2 [123]. This will make a big difference to experiments (roughly a factor of 16 in the combined product of running time, detector mass, background level, and energy resolution for a background dominated experiment) and will thus have a strong impact on when and how a conclusive test of the inverted mass ordering region can be achieved [42].
- They will play a crucial role in model-independent tests of the three-neutrino oscillation framework, most notably unitarity tests of the PMNS matrix. For example, the combination of JUNO's results with those of short-baseline reactor experiments like Daya Bay and solar experiments like SNO will enable the first such direct test of $|U_{e1}|^2 + |U_{e2}|^2 + |U_{e3}|^2 = 1$ to the few percent level [77, 78, 124]. Similarly, the combination of JUNO with muon (anti)neutrino disappearance measurements will enable tests of the mass sum rule $\Delta m_{13}^2 + \Delta m_{21}^2 + \Delta m_{32}^2 = 0$, which is another important probe of physics beyond the Standard Model such as the existence of sterile neutrinos.

In summary, reactor antineutrino experiments have played an essential role in unveiling the oscillatory behavior of the neutrino, from the first clear observation of the L/E_ν dependence of this phenomenon with terrestrial neutrinos, to the discovery of the non-zero value of θ_{13} , among other breakthroughs. The precise determination of θ_{13} by reactor experiments already underpins the world's best knowledge on CP violation, and will continue to do so for the foreseeable future. Reactor antineutrinos will continue to have a prominent role in neutrino oscillation physics, with a measurement within this decade by JUNO of the neutrino mass ordering that is independent and complementary to what atmospheric and accelerator experiments can do. Likewise, by the end of this decade, the most precise knowledge of four out of the six parameters that drive neutrino oscillation will come from reactor antineutrino experiments, namely Daya Bay and JUNO, with three of these determined to 0.5% or better. The United States has traditionally played a leading role in experimental efforts with reactor antineutrinos, but currently has only a small participation in JUNO. This experiment will begin operations

soon and thus presents an excellent opportunity to participate in the production of cutting-edge reactor antineutrino physics results before other next-generation neutrino oscillation experiments come online.

5 Non-Standard Flavor Mixing Searches at Reactors (NF02)

5.1 Key Takeaways

- While the 3+1 oscillation scenario is disfavored by a combination of diverse appearance and disappearance results, the desire to explain lingering short-baseline anomalies with new physics has not gone away.
- By performing correlated measurements of the $\bar{\nu}_e$ spectrum at multiple short baselines, reactor experiments offer a low-cost experimental method for unambiguously probing non-standard neutrino flavor transformation.
- There are plausible explanations for the Reactor Antineutrino Anomaly that do not involve sterile neutrinos. These explanations provide a better match to host of new neutrino and nuclear physics measurements and modelling studies performed in the last decade.
- New neutrino mass states enrich studies of CP violation. On one hand, non-standard oscillations can confound inferences of the standard δ_{CP} at, e.g., DUNE; on the other, they also generically introduce new sources of CP violation.

5.2 The Reactor Antineutrino Anomaly

In 2011, two independent reevaluations of the reactor antineutrino spectrum were published by Mueller et al. [12] and Huber [18]. Both concluded that the integrated antineutrino flux is $\approx 3\%$ larger than previous calculations; we defer a discussion of the details of the flux model to Sec. 7. Many of the authors of Ref. [12] would then explicitly reanalyze reactor experiments dating back to the early 1980s in Ref. [5], finding that observed interaction rates were, on average, $(5.7 \pm 2.3)\%$ less than what the new ‘Huber-Mueller’ (HM) model predicted; this disagreement was named *the Reactor Antineutrino Anomaly (RAA)*. It is pertinent to consider whether modifications to three-neutrino oscillations might be the cause of the RAA.

The SM can be extended by introducing N additional neutrino species. If these are light enough to participate in oscillations, then they must be uncharged under SM interactions, as the invisible decay width of the Z boson is consistent with there being only three light neutrinos [125]. We refer to these as *sterile neutrinos* and denote them $\{\nu_{s_1}, \nu_{s_2}, \dots, \nu_{s_N}\}$; these are accompanied by new mass eigenstates denoted $\{\nu_4, \nu_5, \dots, \nu_{3+N}\}$. The mixing relationship given in Eq. (2) can be readily generalized

to

$$\begin{pmatrix} \nu_e \\ \nu_\mu \\ \nu_\tau \\ \nu_{s_1} \\ \vdots \end{pmatrix} = \begin{pmatrix} U_{e1} & U_{e2} & U_{e3} & U_{e4} & \dots \\ U_{\mu 1} & U_{\mu 2} & U_{\mu 3} & U_{\mu 4} & \dots \\ U_{\tau 1} & U_{\tau 2} & U_{\tau 3} & U_{\tau 4} & \dots \\ U_{s_1 1} & U_{s_1 2} & U_{s_1 3} & U_{s_1 4} & \dots \\ \vdots & \vdots & \vdots & \vdots & \ddots \end{pmatrix} \cdot \begin{pmatrix} \nu_1 \\ \nu_2 \\ \nu_3 \\ \nu_4 \\ \vdots \end{pmatrix}; \quad (6)$$

the 3×3 PMNS matrix is replaced by a $(3 + N) \times (3 + N)$ analog. The sterile species, by construction, will not interact in a detector; one must infer their existence through their modifications to the oscillation probabilities of the active species. We focus on the case $N = 1$ for simplicity and replace $\nu_{s_1} \rightarrow \nu_s$. In this case, there are three unique mass-squared differences, $\{\Delta m_{21}^2, \Delta m_{31}^2, \Delta m_{41}^2\}$, and the 4×4 extended PMNS matrix may be written in terms of six mixing angles and three CP -odd phases. Here, we focus on the survival probability $P(\bar{\nu}_e \rightarrow \bar{\nu}_e) \equiv P_{\bar{e}\bar{e}}$ in the limit relevant to SBL reactor experiments. In the three-neutrino scenario, $P_{\bar{e}\bar{e}}$ does not deviate appreciably from unity for baselines $\lesssim \mathcal{O}(100)$ m at reactor energies. Therefore, any oscillations observed on $\mathcal{O}(10 - 100)$ -m length scales would be attributable only to Δm_{41}^2 . In the limit $\Delta_{21}, \Delta_{31} \approx 0$, we write

$$P_{\bar{e}\bar{e}} \approx 1 - 4|U_{e4}|^2(1 - |U_{e4}|^2) \sin^2 \Delta_{41} \equiv 1 - \sin^2 2\theta_{ee} \sin^2 \Delta_{41}; \quad (7)$$

where $\sin^2 2\theta_{ee}$ is the *effective mixing angle*. If $\sin^2 2\theta_{ee}$ is nonzero, then this can manifest as a deficit of $\bar{\nu}_e$ relative to prediction — precisely as indicated by the RAA.

In Ref. [5], rate experiments were explicitly analyzed with respect to the sterile neutrino hypothesis. It was found that the data prefer a sterile neutrino at the level $p \approx 3.5\%$; the preferred regions of parameter space were approximately $\sin^2 2\theta_{ee} \in [0.02, 0.20]$ and $\Delta m_{41}^2 \gtrsim 0.40 \text{ eV}^2$. When combined with anomalous ν_e disappearance results from the radioactive source experiments GALLEX [126, 127] and SAGE [128, 129] — the so-called Gallium Anomaly [130, 131] — these become $p \approx 0.3\%$, $\sin^2 2\theta_{ee} \in [0.05, 0.22]$ and $\Delta m_{41}^2 \gtrsim 1.45 \text{ eV}^2$.

Since Ref. [5] first appeared, new measurements of the antineutrino rate at HEU reactors were performed at Nucifer [132] and STEREO [133]. Moreover, medium-baseline experiments have also become competitive in this endeavor. Double Chooz [134], Daya Bay [135], and RENO [136] all measured time-integrated antineutrino rates consistent with the RAA. These results supported the robustness of the suggested data-model flux discrepancy and hint for sterile neutrino oscillations. On the other hand, Daya Bay [137, 138] and RENO [139] have also exploited a particular feature of LEU reactors: they can track how the $\bar{\nu}_e$ detection rate evolves with the reactor fuel composition. They observe a dependence of the RAA size on fuel content, a clear indication of flux mis-modelling of some sort.

In parallel to these experimental developments, $\bar{\nu}_e$ HM flux model has also been the subject of increased scrutiny. While modeling will be discussed in more depth in Sec. 7,

Flux Model	R	Significance	2σ Limit on $\sin^2 2\theta_{ee}$
HM	$0.930^{+0.024}_{-0.023}$	2.8σ	[0.031, 0.236]
EF	$0.975^{+0.032}_{-0.030}$	0.8σ	< 0.170
HKSS	$0.922^{+0.024}_{-0.023}$	3.0σ	[0.039, 0.259]
KI	0.970 ± 0.021	1.4σ	< 0.144
HKSS-KI	$0.960^{+0.022}_{-0.021}$	1.8σ	< 0.166

Table 2: The ratio R of measured antineutrino rates compared to the predictions from various flux models, adapted from Ref. [143]. Also shown are the corresponding statistical significances and the 2σ limit on $\sin^2 2\theta_{ee}$ in the large- Δm_{41}^2 ($\gtrsim 5 \text{ eV}^2$) region.

we quickly overview salient details. The HM flux model is largely based on the so-called *conversion method*, whereby one inverts measured isotopic fission β spectra [15–17] to infer the corresponding $\bar{\nu}_e$ spectra. One could instead calculate the spectrum by direct *summation* of available nuclear data. In 2019, two new, notable flux calculations appeared. The first [14] (hereafter ‘EF’) provided an updated summation calculation, while the second [140] (‘HKSS’) incorporated conversion techniques while accounting for shape alterations contributed by forbidden beta decays. The EF model predicted a ^{235}U flux that is 5 – 10% less than HM, whereas HKSS predicted a modest ($\approx 1 - 2\%$) excess. These models have been compared with reactor rate data in Refs. [7, 141–143]; the results of Ref. [143] are given in Table 2. Interestingly, the EF model does not indicate anomalous disappearance, whereas the HKSS model slightly enhances the RAA.

The ratio of the β spectra of ^{235}U and ^{239}Pu was recently measured at the Kurchatov Institute [144, 145]. In Ref. [145], the $\bar{\nu}_e$ spectrum for ^{235}U was rederived via β conversion assuming that the ^{239}Pu spectrum is given by the HM model; we call this “KI.” Moreover, Ref. [143] derives yet another flux model by rescaling the HKSS prediction for ^{235}U by the same multiplicative factor (1.054 ± 0.002) by which the integrated ^{235}U fluxes for HM and KI disagree; the result is named “HKSS-KI.” The experimental deficits with respect to these models are given in Table 2; they are consistent with EF in that they also do not indicate significant, anomalous disappearance.

It is too soon to consider the RAA definitively resolved by these findings. For example, if one had instead assumed that the HM ^{235}U spectrum is correct and that the ^{239}Pu one is not, then one would find *increased* evidence for anomalous disappearance [146, 147]. Still, these results indicate that the conversion and summation approaches may be converging, which is a decided improvement relative to the past decade. However, the RAA is not the only motivating factor for nonstandard oscillation searches at nuclear reactors. Anomalous $\nu_e/\bar{\nu}_e$ appearance results at LSND [148] and MiniBooNE [61, 149, 150] and Gallium Anomaly disappearance results can still be explained in terms of an eV-scale sterile neutrino [63, 151–157]. If true for LSND and MiniBooNE, then this would

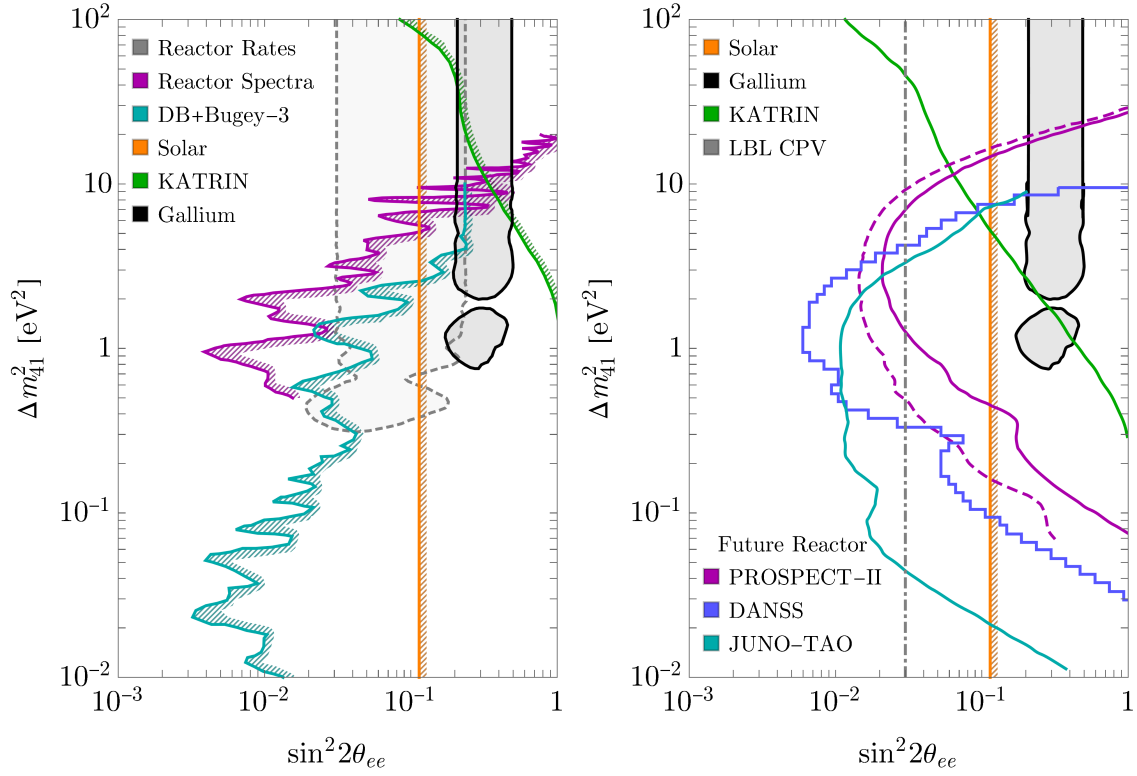


Figure 8: Left: Current constraints on a sterile neutrino from $\nu_e/\bar{\nu}_e$ disappearance. Color fillings represent preferences; hatching represents exclusions. The dashed, gray region is the fit to reactor rate deficits using the HM flux model [143], given for context. See text for more details. Right: The future sensitivities of KATRIN [158] (green; 95% C.L.), PROSPECT-II [45] (purple; 90% C.L.), DANSS (light blue; 90% CL_s) and JUNO-TAO [47] (cyan; 90% CL_s). For PROSPECT-II, two configurations are shown: two years at an HEU core (solid), and four years at an HEU core plus two years at an LEU core (dashed). The dot-dashed gray line is the CP violation disambiguation limit relevant for DUNE [72].

require nonstandard contributions to both ν_μ and ν_e disappearance. Assuming that the central value model predictions of Table 2 accurately reflect reality, flux models can still accommodate a $\sim 5 - 10\%$ change in the antineutrino rate; thus, there is still room for active-sterile mixings of modest size in the reactor sector, even without the RAA.

5.3 Reactor Spectrum Ratio Experiments and the Complex Current Landscape

If one measures the *spectrum* of antineutrinos instead of the energy-integrated rate, then one can potentially observe oscillations directly. Moreover, if one measures the spectrum at two (or more) baselines, then their *ratio* is largely insensitive to the details of the underlying flux model. Antineutrino spectra had been measured prior to the 2010s at, e.g., ILL [159, 160] and Bugey [31] – these were considered in Ref. [5] – but this

program blossomed as a result of searches for nonzero θ_{13} . Daya Bay, Double Chooz and RENO all employed detectors at multiple locations at the \sim km scale, as appropriate for Δm_{31}^2 , but these were situated at too long of baselines to probe oscillations at the eV scale. However, experiments exploiting some combination of (1) multiple detectors, (2) movable detectors, or (3) segmented detectors have been constructed at short baselines – within 25 m – to search for eV-scale oscillations. Over the past decade, SBL searches have been performed by DANSS [34], NEOS [33], Neutrino-4 [37, 161], PROSPECT [36, 85] and STEREO [35, 162]; similar searches are ongoing at NEOS-II [163] and SoLid [164]. Past global analyses of reactor spectral ratios [7, 141, 142, 154–157, 165] have inferred a preference for new oscillations as high as $\gtrsim 3\sigma$, but a combination of more data and improved statistical treatments [166–170] suggests that this is no more than $1-2\sigma$ [171, 172]. The 2σ C.L. exclusion curve from a global fit of SBL spectral measurements [172] is shown in magenta in Fig. 8 (left). In comparison, Daya Bay and Bugey-3 were studied jointly in Ref. [173]; the result (90% CL_s) is shown in cyan. § It is a triumph of experiment that the field has matured to the point of percent-level oscillation sensitivities over the course of roughly a decade.

It is pertinent to consider how reactors fit into the landscape of $\nu_e/\bar{\nu}_e$ disappearance studies, and of sterile neutrino searches more broadly. In Fig. 8 (left), we show constraints on $\sin^2 2\theta_{ee}$ from solar neutrino experiments [174] (orange; 2σ) || and from KATRIN [158] (green; 95% C.L.). The region preferred (2σ) by a combined analysis of gallium experiments [172] is shaded in gray. In addition to SAGE and GALLEX, this includes recent results from BEST [57, 176], where a $\gtrsim 5\sigma$ deficit has been reported [177]. Constraints have also been derived from ν_e scattering on ^{12}C at KARMEN and LSND [178–180], as well as from T2K [181] and MicroBooNE [59, 60]; these have been omitted for clarity. Curiously, the solar constraint and the gallium preference are in $\gtrsim 3\sigma$ tension [172]; reactor spectral measurements are compatible with either, while the compatibility between gallium and reactor rates is, as described above, flux-model dependent [143]. Moreover, there are no significant indications of anomalous ν_μ disappearance [182]; when combined with ν_e disappearance null results, this results in significant tension with the LSND and MicroBooNE anomalies [63, 156, 173]. On top of all of this, eV-scale sterile neutrinos contribute to N_{eff} and $\sum m_\nu$; cosmological observations place severe limits on nonstandard contributions to these quantities, disfavoring essentially all of the parameter space shown in Fig. 8 [183–195]. This all suggests that $3 + 1$ oscillations do not comfortably describe the data. The question becomes: Is there a compelling conventional or BSM alternative?

The next-simplest model one could invoke would be to introduce multiple species of

§ Neither of these experiments is considered in Ref. [172]; the figure is thus not double-counting reactor spectra information.

|| This constraint assumes the GS98 solar model [175]; had the AGSS09 solar model [175] been used, the resulting constraint would be modestly stronger.

sterile neutrinos. This has been studied in, e.g., Refs. [63, 157, 196, 197]; including only additional oscillation frequencies does not appreciably resolve these tensions. Other proposed scenarios include sterile neutrino decay [64, 65], the presence of nonstandard interactions among either the active or sterile neutrinos [66, 198, 199], hidden sector couplings to neutrinos [67], or some combination of multiple effects [68]. Reactor experiments will play an essential part in a necessarily diverse global program to assessing which (if any) of these scenarios are correct. As noted in Sec. 2, they provide a clean environment in which to study oscillations, owing to (1) the flavor purity of the source; (2) the low energies, which prevent heavy states from polluting the observed signal; and (3) the relative absence of matter effects. If the existing SBL anomalies persist, and are confirmed at, e.g., the SBN program at Fermilab [62] and more robust future iterations of the BEST radiochemical experiment, then reactor experiments will continue to play an important role in discriminating between possible explanations thereof. The use of multiple arms of the US neutrino program to elucidate a more complex ‘non-vanilla’ sterile sector is very well-illustrated in Ref. [68]: in this example, which envisions a 2-component sterile sector, US short-baseline reactor data is crucial for constraining active-sterile oscillation parameters, while US short-baseline accelerator experiments are best at pinning down radiative decay phenomena experienced by the heavier sterile state.

As noted below Eq. (6), introducing a sterile neutrino also introduces two new CP -violating phases, which enriches the possibilities for CP -violation studies at long-baseline accelerator experiments. On one hand, 3+1 oscillations that violate CP may be confounded with CP -conserving, 3+0 oscillations [71]; on the other, large-amplitude, CP -conserving oscillations with a sterile neutrino may generate false signals of CP violation at, e.g., DUNE [200]. While P_{ee} in Eq. (7) is necessarily CP -conserving, the sensitivity of reactors to the existence of additional neutrinos is crucial for the disambiguation of such a signature. This potential parameter degeneracy can be broken if $\sin^2 2\theta_{ee}$ can be measured at the level $\lesssim 0.03$ [72], shown by the dot-dashed line in Fig. 8.

5.4 The Future of Short-Baseline Reactor Experiments

As of 2022, at least four new short-baseline reactor neutrino detectors are in preparation or under construction, with plans to address the open questions described above. The JUNO-TAO detector, a satellite detector for JUNO, will begin taking data in 2023 at a baseline of ~ 30 m from a commercial power reactor in China [47]. The PROSPECT-II detector, a planned upgrade of the PROSPECT detector, anticipates taking a second run of data within 10 m of the HFIR reactor in the US and possibly at other sites [45]. The DANSS Collaboration is currently upgrading their detector to improve their photostatistics, and thus their energy resolution [201]. The Neutrino-4 Collaboration is also preparing an upgrade: a combination of increasing the detector volume and introducing pulse-shape discrimination is expected to triple their statistics,

Experiment	L [m]	P_{th} [MW]	Material(s)
DANSS [34]	$\sim 11 - 13$	3100	SS
MiniCHANDLER [86]	25	2900	SS
NEOS [33]	24	2800	LS
NEOS-II [33]	24	2800	LS
Neutrino-4 [161]	$\sim 6 - 12$	100	LS
PROSPECT [85]	$\sim 7 - 9$	85	LS
PROSPECT-II [44]	$\sim 7 - 9$	85	LS
SoLid [164]	$\sim 6 - 9$	40-100	SS
STEREO [162]	$\sim 9 - 11$	58	LS
JUNO-TAO [47]	~ 30	4600	LS
Daya Bay [135]	550, 1650	17,400	LS
Double Chooz [134]	400, 1050	8500	LS
RENO [136]	430, 1450	16,800	LS
JUNO [112]	52,500	26,600	LS

Table 3: A tabulation of IBD-based reactor experiments that were either performed in roughly the last decade or will be performed in the near future. Experiments are sorted into short, medium, and long-baseline categories.

though the impact on their sterile neutrino sensitivity has not yet been made public [202]. Each of these experiments will extend sensitivity to non-standard neutrino oscillation well beyond current limits, into regions of interest for the still-unresolved gallium anomaly and the continuing tension between short-baseline accelerator results. These experiments are likely to provide particularly good sensitivity in the $\sim 2\text{-}20$ eV² mass splitting region, where current limits on active-sterile mixing are comparatively weaker in the electron disappearance channel. While probing this region, JUNO-TAO, PROSPECT-II and DANSS will also be able to authoritatively address existing claims of moderate confidence-level observations of sterile neutrino oscillations at the Neutrino-4 experiment [37]. These detectors will also increase the precision of neutrino spectrum measurements, described more in Sec. 7.

As the neutrino community seeks to resolve remaining short-baseline neutrino anomalies, reactor experiments such as PROSPECT-II and JUNO-TAO provide several points of complementarity to other approaches. As shown in Fig. 8, the projected PROSPECT-II sensitivity will combine with the projected KATRIN sensitivity to fully cover the parameter space favored by the current gallium anomaly (which, as noted above, is already disfavored solar experiments) and to definitively exclude an oscillation solution to the RAA. Although the curves in Fig. 8 correspond most directly to a 3+1 sterile neutrino models, they illustrate the general point that reactor neutrinos explore

Experiment	L [m]	P_{th} [MW]	Material(s)	Technology
CHILLAX [203]	~ 25	~ 1000	LAr & LXe	Dual-Phase TPC
CONNIE [88, 204]	30	3800	Si	Skipper CCDs
CONUS [205]	17	3900	Ge	Ionization
MINER [90]	$\sim 2 - 10$	1	Ge, Si, Al ₂ O ₃	Bolometry
NCC-1701 [39]	8	2960	Ge	Ionization
NEON [206]	24	2800	NaI(Tl)	Scintillation
NEWS-G [207]	-	-	Ne	Ionization
ν GeN [208]	~ 10	3100	Ge	Ionization
NUCLEUS [209]	-	-	CaWO ₄ & Al ₂ O ₃	Bolometry
NUXE [210, 211]	~ 25	~ 3000	LXe	Ionization/Scintillation
RED-100 [212]	19	3100	LXe	Dual-Phase TPC
Ricochet [89, 213]	8.8	58	Ge & Zn	Bolometry
SBC [214]	3	1	LXe	Scintillation
TEXONO [215, 216]	28	2900	Ge	Ionization
ν IOLETA [217]	8, 12	2000	Si	Skipper CCDs

Table 4: A tabulation of CE ν NS reactor experiments, including their reactor standoff L , the reactor (thermal) power P_{th} , component material(s) and detection technology.

a flavor channel (pure ν_e) where there may not be input from other sources. They do so with relatively low cost compared to accelerator experiments, because the reactor sources are already in operation and the detector size can be on the meter-scale.

In addition to JUNO-TAO, PROSPECT-II, DANSS and Neutrino-4, which all use IBD interactions in scintillator as the detector channel, a growing number of experiments are seeking to measure CE ν NS interactions at reactor sources. Ongoing reactor CE ν NS projects are listed in Table 4. Compared to the established IBD channel, the CE ν NS signal presents a much greater experimental challenge due to high sensitivity to radiation and instrumental background. So far, the low-energy CE ν NS signal has not been detected above the large backgrounds to this approach. When it becomes visible, the CE ν NS signal will provide information about reactor neutrino fluxes and interactions below the IBD threshold and, like IBD searches, complement accelerator- and DAR-based searches for sterile neutrino oscillations. These experiments are discussed in more detail in Sections 6 and 8.

5.5 Medium- and Long-Baseline Reactor Experiments

We conclude this section by commenting on searches for nonstandard oscillations at medium- and long-baseline reactor experiments. In Fig. 8, we have already noted the combined constraint from Daya Bay and Bugey-3 [173]; the constraint is dominated by

Daya Bay below $\Delta m_{41}^2 \lesssim 0.3 \text{ eV}^2$. Similar exclusions have been derived for RENO and Double Chooz [218, 219]. Long-baseline experiments are sensitive to smaller values of Δm_{41}^2 than those shown in Fig. 8: the JUNO collaboration forecasts a sensitivity to $\sin^2 2\theta_{ee} \gtrsim 0.02$ for $3 \times 10^{-4} \lesssim \Delta m_{41}^2 \lesssim 2 \times 10^{-3}$ [42].

Neutrino oscillations are fundamentally contingent on the coherence of the neutrino wave-packet; decoherence could dramatically change the oscillation probabilities at medium and long baselines. The Daya Bay Collaboration has studied these effects in Ref. [220] and finds that they are not significant in their existing data. This is confirmed in joint analyses of Daya Bay, RENO and KamLAND in Refs. [221, 222]. The JUNO collaboration has benchmarked their sensitivities to several models of decoherence in Ref. [223] (see also Ref. [221]); they forecast approximately one order of magnitude improvement in measuring the size of the neutrino wave-packet. Decoherence effects link up with sterile neutrino searches in a nontrivial way: recent work [54] finds that these can be important in correctly assessing constraints at SBL reactor experiments for $\Delta m_{41}^2 \sim \mathcal{O}(\text{eV}^2)$. These findings again highlight the importance of robust reactor programs at both short and long baselines.

We finally briefly note the capabilities of longer-baseline reactor experiments in probing a wider variety of exotic BSM scenarios. A variety of such studies have been performed at high-statistics medium-baseline experiments, such as *CPT* and Lorentz-invariance violation searches at Daya Bay [224] and Double Chooz [225]. Other exotic studies, such as searches for large extra dimensions have also been proposed [226].

6 Probing Neutrino Properties and Unknown Particles with Reactor Neutrino Detectors (NF03, NF05)

6.1 Key Takeaways

- Reactor antineutrinos, due to their low energies, are capable of scattering coherently from all nucleons in a target nucleus, which greatly enhances the expected cross-section of this CEvNS process with respect to other interaction channels.
- For this reason, reactors offer unprecedented sensitivity in measuring the Standard Model CEvNS cross-sections at low momentum transfer, as well as data-model deviations indicative of a range of BSM physics processes.
- A range of low-threshold detection technologies currently under active development can allow access to this new low-momentum transfer regime.
- Other novel aspects of reactor-based experiments, such as their on-surface location and their proximity to large reactor-produced photon fluxes, offer promise in probing the existence of a range of hidden sector particles and interactions.

6.2 Reactor CE ν NS and Low-Energy Processes: Theory and Experimental Limits

CE ν NS is a neutral-current process that arises when the momentum transfer in the neutrino-nucleus interaction is less than the inverse of the size of the nucleus. For typical nuclei, this corresponds to neutrinos with energies $E_\nu \lesssim 50$ MeV. In the SM, the interaction is mediated by the Z-boson, with its vector component leading to the coherent enhancement. As a reference point, we first write the cross section in the form

$$\frac{d\sigma}{dT} = \frac{G_F^2 M}{4\pi} \left(1 - \frac{MT}{2E_\nu^2}\right) Q_w^2 [F_w(q^2)]^2, \quad (8)$$

where G_F is the Fermi constant, $T = E_R = q^2/(2M) = E_\nu - E'_\nu$ is the nuclear recoil energy (taking values in $[0, 2E_\nu^2/(M + 2E_\nu)]$), $F_w(q^2)$ is the weak form factor, M is the mass of the target nucleus, and E_ν (E'_ν) is the energy of the incoming (outgoing) neutrino. The tree-level weak charge is defined by

$$Q_w = Z(1 - 4\sin^2\theta_W) - N, \quad (9)$$

with proton number Z , neutron number N , and weak mixing angle $\sin^2\theta_W$. To first approximation, the weak form factor $F_w(q^2)$ depends on the nuclear density distribution of protons and neutrons. In the coherence limit $q^2 \rightarrow 0$ it is normalized to $F_w(0) = 1$, with the coherent enhancement of the cross section reflected by the scaling with N^2 via the weak charge, given the accidental suppression of the proton weak charge $Q_w^p \ll 1$. Consequently, this implies that CE ν NS is mainly sensitive to the neutron distribution in the nucleus.

Nuclear reactors have long been utilized as copious sources of electron anti-neutrinos. Neutrinos from reactors have been detected using the inverse beta decay reaction, $\bar{\nu}_e + p + 1.806 \text{ MeV} \rightarrow e^+ + n$, by observing both the outgoing positron and coincident neutron. The characteristic neutrino energy for this source is $\lesssim 1$ MeV, roughly an order of magnitude or more lower than the average energies of neutrinos produced by accelerator sources. Due to these low energies, the coherence condition for the recoil is largely preserved over the entire reactor energy regime, so that there is no dependence on the internal structure of the nucleus.

In general, the presence of any BSM physics will modify the previous cross sections, thus altering the expected number of events detected via the CE ν NS reaction in a detector. In a general fashion, we write the total cross section in the presence of BSM as

$$\frac{d\sigma}{dE_R} = \left. \frac{d\sigma}{dE_R} \right|_{\text{SM}} + \left. \frac{d\sigma}{dE_R} \right|_{\text{BSM}}, \quad (10)$$

where the first term is the SM cross section for either neutrino-electron and CE ν NS interactions, and the second is the modification created by the BSM interactions. Note

Table 5: Contributions to the neutrino-electron and CE ν NS cross-sections for the different scenarios considered here. The g_V, g_A are given by $g_V = \frac{1}{2} + 2 \sin^2 \theta_W, g_A = \frac{1}{2}$ [227].

Interaction	Non-zero couplings	$\frac{d\sigma_{\nu e}}{dE_R} \Big _{\text{BSM}}$	$\frac{d\sigma_{\text{CE}\nu\text{NS}}}{dE_R} \Big _{\text{BSM}}$
Magnetic Moment	μ_{ν_e}	$\alpha_{\text{EM}} \mu_{\nu_e}^2 \frac{E_V - E_R}{E_V E_R}$	$\alpha_{\text{EM}} \mu_{\nu_e}^2 Z^2 \frac{E_V - E_R}{E_V E_R} \mathcal{F}^2(E_R)$
Scalar	$g_{\nu, \phi}, g_{es}, g_{qs}$	$\frac{g_{\nu, \phi}^2 g_{es}^2 E_R m_e^2}{4\pi E_V^2 (2E_R m_e + m_\phi^2)^2}$	$\frac{Q_S^2 m_N^2 E_R g_{\nu\phi}^2 g_{qs}^2}{4\pi E_V^2 (2E_R m_N + m_\phi^2)^2}$
Pseudoscalar	$g_{\nu, \phi}, g_{ep}, g_{qp}$	$\frac{g_{\nu, \phi}^2 g_{ep}^2 E_R^2 m_e}{8\pi E_V^2 (2E_R m_e + m_\phi^2)^2}$	0
Vector	$g_{\nu Z'}, g_{ev}, g_{qv}$	$\frac{\sqrt{2} G_F m_e g_V g_{\nu Z'} g_{ev}}{\pi (2E_R m_e + m_{Z'}^2)}$ $+$ $\frac{g_{\nu Z'}^2 g_{ev}^2 m_e}{2\pi (2E_R m_e + m_{Z'}^2)^2}$	$-\frac{G_F m_N Q_V^{\text{SM}} Q'_V (2E_V^2 - E_R m_N)}{2\sqrt{2}\pi E_V^2 (2E_R m_N + m_{Z'}^2)}$ $+$ $\frac{Q_V^2 m_N (2E_V^2 - E_R m_N)}{4\pi E_V^2 (2E_R m_N + m_{Z'}^2)^2}$
Axial	$g_{\nu Z'}, g_{ea}, g_{qa}$	$-\frac{\sqrt{2} G_F m_e g_A g_{\nu Z'} g_{ea}}{\pi (2E_R m_e + m_{Z'}^2)}$ $+$ $\frac{g_{\nu Z'}^2 g_{ea}^2 m_e}{2\pi (2E_R m_e + m_{Z'}^2)^2}$	$\frac{G_F m_N Q_A Q'_A (2E_V^2 + E_R m_N)}{2\sqrt{2}\pi E_V^2 (2E_R m_N + m_{Z'}^2)}$ $-\frac{G_F m_N Q_V^{\text{SM}} Q'_A E_V E_R}{2\sqrt{2}\pi E_V^2 (2E_R m_N + m_{Z'}^2)}$ $+$ $\frac{Q_A^2 m_N (2E_V^2 + E_R m_N)}{4\pi E_V^2 (2E_R m_N + m_{Z'}^2)^2}$

that any possible interference effect that can appear according to the nature of the new mediators are included in the BSM cross section.

The new physics can be enhanced by light mediators. It could be the photon coupling through electromagnetic properties of the neutrino, or additional mediators having couplings to neutrinos, charged leptons and quarks. In the spirit of simplified models, we assume a Lagrangian at low energies which includes terms for the new interactions with the SM fermions without specifying the gauge invariant models at high energies as in [228]. For each scenario, the modification of both neutrino-electron and CE ν NS cross sections will have a specific shape, possibly including interference effects. In Table 5 we summarize and compile the distinct BSM contributions to the neutrino-electron and CE ν NS cross sections for each light mediator scenario, together with the non-zero couplings relevant in each case.

In the specific case of CE ν NS, there is an additional step; we need to translate the interactions from the quark to the nucleon level. The coherence factors related to the

specific mediator are given by (see e.g. Refs. [227, 229–232])

$$Q'_V = 3(N + Z)g_{\nu Z'}g_{qv}, \quad (11a)$$

$$Q'_A = 0.3S_Ng_{\nu Z'}g_{qa}, \quad (11b)$$

$$Q_A = 1.3S_N, \quad (11c)$$

$$Q_S = 14(N + Z) + 1.1Z, \quad (11d)$$

corresponding to the vector, axial, SM axial, and scalar currents, with nuclear spin S_N , and neutrino- Z' and quark vector couplings $g_{\nu Z'}$ and g_{qv} , respectively.

Figure 9 shows the sensitivity at 90% C.L. of a new light scalar mediator coupling to neutrinos and quarks (left panel) and the sensitivity to a light vector mediator coupled to neutrinos and quarks (right panel), for current experiments using accelerator neutrinos (blue area) and reactor neutrinos (green area) [38, 39]. New sensor technologies aiming to detect CEvNS at nuclear reactors have thresholds low enough to reap the benefits of the large neutrino flux of the reactor and access these new physics models. Both graphs show a better sensitivity for mediator masses below 20 MeV in reactor-based CEvNS experiments. The projected sensitivity for a 10 kg experiments using Skipper CCD [233] with silicon as the target material is also shown in both plots. The sensor allows for a energy threshold of a few eV of the equivalent ionization energy. A wide range of coupling constants is unconstrained in the parameter space for masses for light mediators [228]. Since the interaction cross sections scale with the fourth power of the coupling parameter (y-axes in the plots), the increase in sensibility of this new search is several orders of magnitude of the existing limits.

The combination of three aspects – the cross-section enhancement for nuclear interaction for the reactor neutrino energies, the very low energy threshold of new technologies to observe faint depositions, and the reactor being the most intense neutrino flux on earth – make the proposed technique a unique tool to search for dark sector candidates in new regimes.

6.3 Experimental Requirements For Reactor CEvNS Detection

The maximum nuclear recoil energy resulted from CEvNS interactions can be approximated as $2k^2/M$, and is usually at the keV level or below for reactor antineutrinos with a characteristic energy of $\lesssim 1\text{MeV}$. As illustrated in Fig. 10, with a Si/Ar/Ge/Xe target, 90% of the reactor CEvNS signals will have an energy below 0.8/0.6/0.3/0.2 keV. In addition, the majority of energy transferred from the antineutrino to a nucleus is dissipated as heat. As a result, for detector technologies that measure scintillation and/or ionization signatures from particle interactions, only a small fraction of nuclear recoil energy is observable. In Si [234], Ge [235–237] and Xe [238] the reduction factors of measurable energy (or quenching factors) have been measured down to ~ 0.3 keV, with

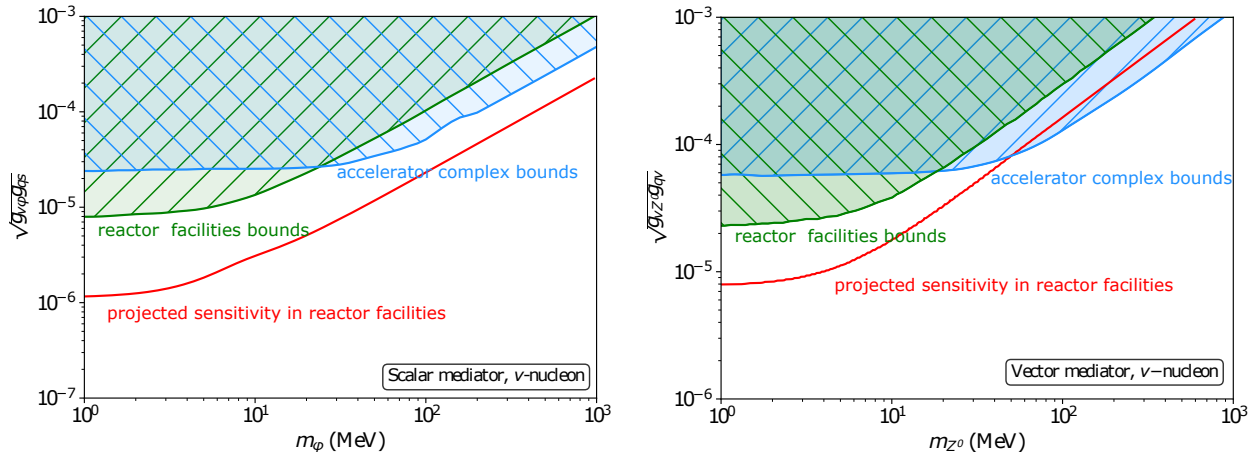


Figure 9: Current bounds and projected sensitivity bounds for new neutrino interactions with nucleons through a scalar mediator (left) and vector mediator (right). Plots show with different colors the parameter space ruled out using neutrinos from accelerator complex and neutrinos from nuclear reactor facilities. Figures taken from [228].

typical suppression values around 6–10 in this energy regime. This quenching effect, in addition to the low nuclear recoil energy, makes the detection of reactor CEvNS signals challenging.

Thanks to the progress of direct detection dark matter experiments in the last few decades, low-threshold detectors sensitive to keV-level nuclear recoils have been developed [239–242]. A typical dark matter experiment focuses on nuclear recoils from a few keV to tens of keV, and thus the detection of reactor CEvNS requires the detector thresholds to be further reduced. Several experimental efforts have been launched to advance the low-energy sensitivity of detector technologies including Si and Ge ionization detectors [204, 205, 240, 242], liquid argon and xenon scintillation/ionization detectors [203, 210, 212, 214, 239, 243], and cryogenic bolometers [90, 213, 244, 245]. Up to date, energy thresholds in the range of tens of eV to hundreds of eV have been demonstrated in bolometers and ionization detectors.

Coincidentally, at a detection threshold of ~ 200 eV, reactor CEvNS experiments using different targets are expected to observe comparable event rates per target mass (Fig. 10). Because of the near-exponential shape of the CEvNS spectra, an experiment with a 50 eV threshold will be able to collect 5–10 times more CEvNS events than those with 200 eV thresholds, demonstrating the need to develop lower-threshold detector technologies. Further, due to the low expected event rate of neutrino interactions, a detector also needs to have a large active mass to obtain sufficient statistics to study possible BSM physics associated with CEvNS. Currently available low-threshold detectors such as Skipper CCDs are limited to active masses at a hundred-gram level [242, 246], while high-mass

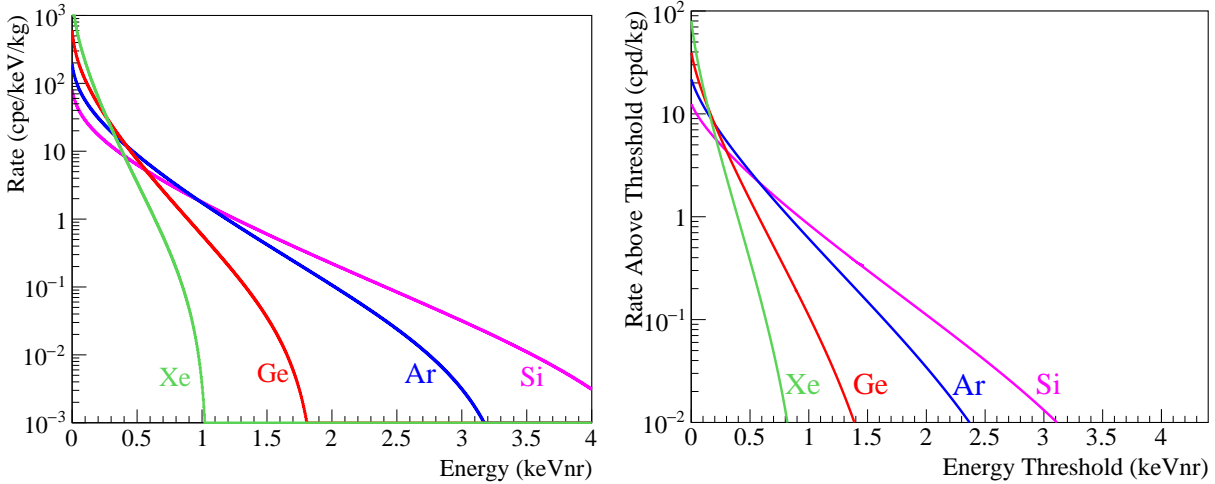


Figure 10: **Left:** The expected reactor CEvNS energy spectra in a Si/Ar/Ge/Xe target, with the assumption of 1kg target mass and 25m standoff distance from a 1GW reactor core; reactor antineutrino spectrum is taken from [3]. **Right:** Integrated CEvNS event rate in 1 kg of Si/Ar/Ge/Xe as a threshold of detector energy threshold, with the same assumption on reactor parameters as for the left figure.

detectors such as liquid argon and xenon Time Projection Chambers (TPCs) are limited to an energy threshold of hundreds of eV [239, 243, 247]. Ongoing R&D efforts are currently pursuing substantial improvements in these directions [248–251]. More R&Ds is needed in the next decade to perform a first definitive experimental observation of reactor CEvNS.

In addition to detector threshold and active mass, another important aspect to consider in reactor CEvNS detection experiments is the excess backgrounds observed in the low energy regions of different detectors [239, 243, 252–254], which operate at very different temperatures and have different signal readout schemes. Such backgrounds often manifest themselves as a fast rising event rate as the energy approaches the detector threshold, and can vary drastically in rate, temporal behavior, and other characteristics. In ionization detectors these backgrounds are suspected to arise from the trap and delayed release of electrons [243, 254] or low-energy interactions near the active volume [252], and in bolometers they are sometimes hypothesized to originate from crystal stress or accumulation of energy in the active volume [252, 253]. Much remains unstudied for these experiments to enjoy meaningful nuclear recoil sensitivities in the reactor CEvNS energy regime.

6.4 Exotic particle searches at nuclear reactors

Other novel aspects of reactor-based experiments, such as their on-surface location and their proximity to large reactor-produced photon fluxes, can be leveraged to probe the

existence of a range of hidden sector particles and interactions. Below, we illustrate with a few examples.

Nuclear reactors are also an intense source of photons and neutrons, which can interact with the materials of the reactor structure or spontaneously transform to produce hidden sector candidates that could escape from the reactor core and reach a nearby detector. This new framework of production and detection at nuclear facilities has been studied due to the large production rates obtained in reactors and the availability of new technologies to detect them [255–257]. As an example of the sensitivity of this technique Fig 11 (from [256]) shows the reach in the search for axion-like particles for different low threshold sensor technologies in nuclear reactors (different color lines) compared to other astrophysically derived constraints (shaded areas). The plot shows the parameter space of axion-like particles coupling to photons (coupling constant in the y axes and particle mass in the x axes). As the plot shows, the new technique shows unprecedented sensitivity to regions that cannot be accessed by other experiments for axion masses around 1 MeV (the so called cosmological triangle). These detectors can also similarly detect other indirectly electron- or photon-coupled hidden sector particles generated in the core, such as millicharged particles [258]. Neutron-sensitive detectors, such as those used in reactor IBD experiments, are highly capable of probing neutron-coupled hidden sector particles; a search setting world-leading limits on hidden neutrons was recently reported by the STEREO experiment [259].

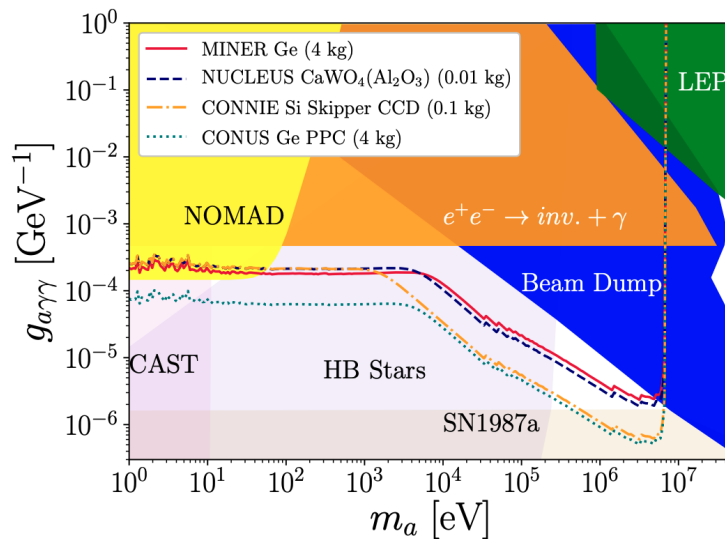


Figure 11: Comparison of sensitivity of axion like particles searches at nuclear reactor compared with existing bounds. Figures taken from [256].

Most short-baseline reactor experiments are located on-surface and lack a substantial amount of overburden. While disadvantageous from the perspective of increases in neutrino-like cosmic backgrounds, it also provides unique advantages for the

detection of high-cross-section cosmogenic dark matter particles that would be otherwise attenuated before reaching a detector [260]. The PROSPECT reactor antineutrino experiment has used its overburden-free, PSD-capable IBD detector to perform a sensitive search for single proton recoils from interactions of boosted dark matter in the sub-GeV mass regime [261]. Similar on-surface reactor-located rare event searches may also be applicable for pursuit of other BSM particle types, such as multiply-interacting massive particles (MIMPS) [262, 263] or macroscopic dark matter [264].

7 Improving Reactor and Nuclear Physics Knowledge Through Neutrino Measurements and Modelling (NF09)

7.1 Key Takeaways

- Precise knowledge of the total magnitude and energy spectrum of reactor antineutrino emissions is a vital ingredient in performing some future neutrino physics measurements.
- Recent neutrino experiments have been very successful in advancing the state of knowledge of reactor antineutrino emissions, most notably by uncovering the reactor flux and spectrum anomalies.
- The increased precision of reactor neutrino measurements has had a broader science impact by spurring investments and improvements in non-neutrino nuclear physics measurements, nuclear data, and reactor antineutrino modelling.
- Next-generation IBD and non-IBD experiments are poised to improve their reactor flux and spectrum measurement precision beyond the associated modelling uncertainties, enabling data-driven improvements to reactor and nuclear physics.

7.2 Reactor Neutrino Flux and Spectrum Measurements

Antineutrino emissions from LEU and HEU reactors have been precisely measured by a range of IBD detection experiments covering baselines from roughly 7 m to 2000 m. While some experiments have measured emissions from HEU reactors, which burn only ^{235}U , most others have sampled LEU reactors, whose neutrino emissions are contributed by the primary fissile isotopes (^{235}U , ^{238}U , ^{239}Pu , and ^{241}Pu) according to their fission fractions at a specific point in the reactor's burnup cycle. These measurements enable accurate evaluation of antineutrino yields and spectra per fission from the primary fissile isotopes, as well as providing cross-checks for antineutrino flux predictions made from nuclear databases and beta-spectra conversions.

Experiments listed in Table 6 measured the IBD detection rate from various reactors with organic scintillator targets. Using precise knowledge of the rate of reactor fission in the core and the IBD detection efficiency (see Refs. [265, 266] for details), IBD rate

Experiment	f_{235}	f_{238}	f_{239}	f_{241}	Measurements
Bugey-3	0.614	0.074	0.274	0.03	flux/spect
Bugey-4	0.614	0.074	0.274	0.03	flux
Daya Bay	0.630-0.511	0.075-0.077	0.253-0.345	0.042-0.068	flux/evol/spect
RENO	0.62-0.527	0.072-0.074	0.262-0.333	0.046-0.066	flux/evol/spect
Double CHOOZ	0.520	0.087	0.333	0.060	flux/spect
ILL	1	0	0	0	flux
Savannah River	1	0	0	0	flux
STEREO	1	0	0	0	flux/spect
PROSPECT	1	0	0	0	spect

Table 6: Examples of IBD experiments’ measurement of reactor neutrino flux, spectrum, and evolution, with different reactor compositions.

measurements can be converted to a measure of IBD yield, or antineutrino flux times the well-known IBD cross-section [267]. Time-averaged IBD yield measurements made by most experiments provided a first global picture of a family of uncorrelated or modestly correlated data points from different baselines and fissile isotope compositions [5, 268]. Among the example experiments in Table 6, Bugey-4, Daya Bay, RENO and Double CHOOZ measured the IBD rate from corresponding reactors with experimental uncertainties of 1.4%, 1.5%, 2.1%, and 1.0%, respectively [134, 139, 266, 269]. The examples on HEU produced IBD rate includes the ILL, Savannah River, and STEREO measurements with uncertainty of 9.1%, 2.9%, and 2.5%, respectively [133, 159, 270]. From this dataset, IBD yields of ^{235}U could be tightly constrained using HEU measurements, while constraints on the yields of the remaining isotopes remained quite loose [271].

Beyond time-integrated yields, the Daya Bay and RENO experiments more recently reported IBD yields measured at various points in their reactors’ fuel cycles with the same reactor-detector configuration [137, 139], yielding a set of highly-correlated data points capable of substantially improving direct knowledge of ^{239}Pu and ^{238}U yields [147, 272, 273]. Best-fit isotopic IBD yields provided by time-integrated and so-called ‘flux evolution’ datasets are shown in Figure 12.

As overviewed in Table 6, many of these reactor experiments have also reported the differential spectrum of IBD positron energies detected per fission, while others have further unfolded this IBD positron spectrum into an interacting antineutrino energy spectrum per fission. Meaningful measurements of this type require detectors with positron energy resolutions roughly of order 20% or better. While first high-statistics absolute spectrum measurements at LEU reactors first became available in the mid-

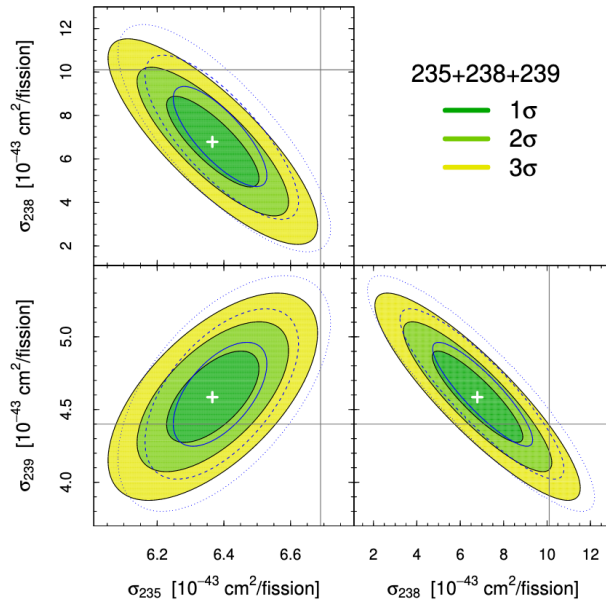


Figure 12: Allowed regions for isotopic IBD yields of ^{235}U , ^{239}Pu , and ^{238}U provided by a fit of time-integrated and ‘flux evolution’ IBD yield datasets. For this fit, sterile neutrino oscillations are assumed to be negligible. From Ref [147].

1990s [274], available precision greatly improved with the θ_{13} experiments of the 2010’s [135, 136, 275]. Precision HEU spectra only become available very recently with the PROSPECT and STEREO experiments [276, 277]. The interacting neutrino spectrum per fission for ^{235}U and ^{239}Pu was reported by Daya Bay measuring spectra at different points in its reactors’ fuel cycles [138, 278]. Measured ^{235}U isotopic spectra have been demonstrated to be generally consistent between Daya Bay, PROSPECT, and STEREO [279, 280].

7.3 Modeling Reactor Antineutrino Emissions

Two complementary methods are available for modelling the per-experiment or isotopic IBD yields and spectra per fission reported in the previous section [3]. The first is the ‘summation’ or ‘*ab-initio*’ method in which the flux and spectra are directly calculated from tabulated fission yields and branching ratios. This method uses nuclear databases, such as JEFF [281], to account the fission yields, as well as data on beta-unstable isotopes from ENSDF databases [282] to sum the theoretical beta spectra of hundreds of fission products and thousands of beta branches. Uncertainties in the summation method are contributed by missing information of beta-unstable isotopes and uncertainties of beta decay branching and fission product yields. Until very recently, tabulations also did not account for correlations in fission yield and decay uncertainties between isotopes and branches, meaning that uncertainty envelopes, even when provided, are

ill-defined. Recently, cataloguing of fission yield correlations [283, 284] and addition of improved decay data using total absorption spectroscopy (TAGS) techniques [285–294] has provided the promise of reducing and better understanding summation uncertainties.

The second method, generally considered to be more precise, performs the conversion of measured aggregate post-fission beta decay spectra into antineutrino spectra through the fitting of a limited number of individual beta branches [5, 18]. The universally used aggregate beta decay datasets underlying this method were measured by neutron-induced fission of ^{235}U [295], ^{239}Pu [296], and ^{241}Pu [297] at the ILL reactor. Beta-branches are fitted to the cumulative beta spectra such that the sum of branches is the best-fit to measured beta spectrum. This data-driven approach has the advantage of being immune to uncertainties from unknown or unmeasured beta decay spectra. However, the fitted branches do not fully represent the ~ 1000 fission-produced beta branches actually present in the spectrum. Theoretical corrections, including forbidden transitions [140, 298] and weak magnetism corrections [299], which add additional uncertainties. Flux prediction of neutrinos from ^{238}U , and other non-fissile isotopes in reactor facilities, still rely on other experimental data or nuclear database summation.

These two methods have complementary, largely uncorrelated uncertainties, and efforts have been taken in recent years to compare their outcomes. While the conversion and summation spectral predictions had been initially thought to be in conflict [300, 301], more recent studies using up-to-date database and decay information have found striking spectral shape agreement between prediction methods [14]. On the other hand, all recent studies have found discrepancies between the methods' predicted energy-integrated fluxes, both in overall magnitude and in the relative offset between ^{235}U and ^{239}Pu yields [7, 14, 302]. Flux model offsets are illustrated in Figure 13 as the difference between blue and orange/cyan circle data points.

7.4 Data-Model Discrepancies

With improvements in reliability of the models and precision of IBD yield and spectrum measurement in the last decade, a variety of data-model discrepancies have emerged. First, the global average of measured reactor neutrino fluxes were found to be offset with respect to the more-precise conversion prediction [5] – the ‘reactor antineutrino anomaly’ described in some detail in Section 5. This discrepancy is visible as the diagonal offset between the red and orange ellipses in Figure 13. More recently, the flux evolution datasets from Daya Bay and RENO have elucidated that, absent neutrino oscillations, this flux anomaly can be more accurately interpreted as an offset in measured and predicted ^{235}U IBD yields, visible as a horizontal offset between the purple and orange ellipses in Figure 13. Moreover, the consonance between flux evolution datasets, summation predictions, and recent conversion predictions using new

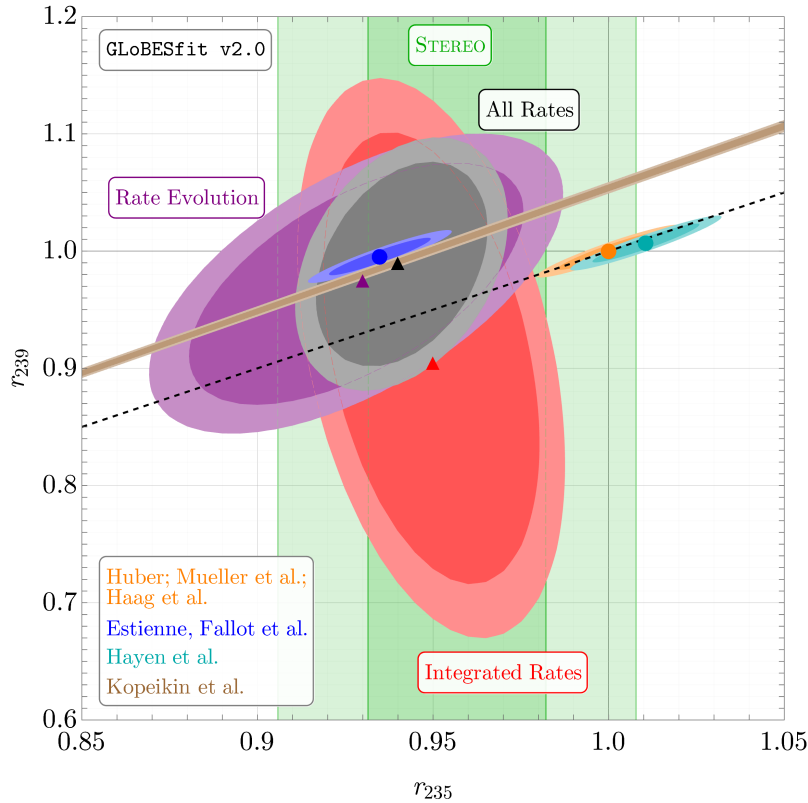


Figure 13: The 95% C.L. (dark) and 99% C.L. (light) contours in r_{235} - r_{239} plane for integrated rate (red), fuel evolution (purple) and all reactor experiments (black), where r_X is the ratio of the flux predicted/measured for isotope X over its HM prediction. The result from STEREO [133] is shown in green; the bands represent the 1σ (dark) and 2σ (light) regions for one degree of freedom. The orange, blue and cyan ellipses represent the expectations from the HM, EF and HKSS flux models, respectively; 1σ (2σ) is shown in dark (light) shades. The brown bands represent the 1σ (dark) and 2σ (light) determination of the $^{239}\text{Pu}/^{235}\text{U}$ ratio from the Kurchatov Institute [144, 145]. The black, dashed line represents the line along which $r_{235} = r_{239}$. The triangles represent the best-fit values for the three fits, and the circles show the central values for the flux models. Figure and caption adapted from Ref. [7].

fission beta measurements [144] indicates that ILL-measured beta spectrum inputs to the conversion approach may be largely to blame for IBD yield data-model discrepancies. Historical reactor decay heat measurements have also been recently investigated towards this end [303].

Recent measurements of the antineutrino energy spectra at LEU and HEU reactors also demonstrate discrepancies between data and predictions. As demonstrated in Figure 14, there is most notably an excess of events observed at approximately 5 MeV which

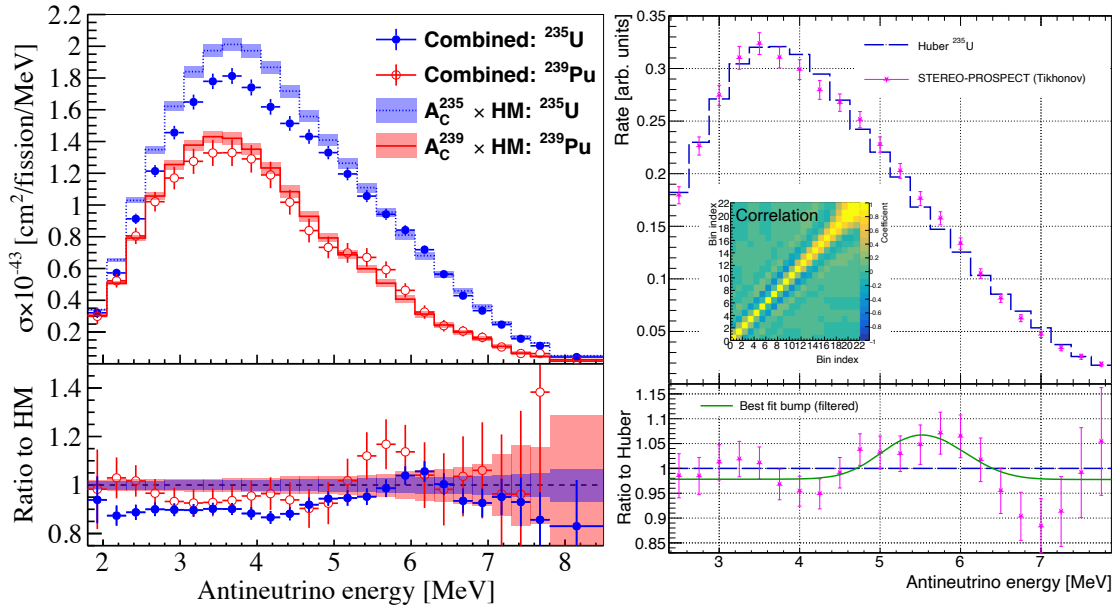


Figure 14: Joint unfolded interacting antineutrino energy spectrum of ^{235}U and ^{239}Pu from Daya Bay and PROSPECT (left) and of ^{235}U from STEREO and PROSPECT (right). Comparisons to the Huber-Mueller model are given in both cases. From [279] and [280].

is not matched by theoretical models. This so-called ‘bump’ has been the focus of much interest in the neutrino as well as the nuclear physics community, since there are only a small number of high- Q isotopes which contribute the majority of neutrinos in this region [4]. While this spectral deviation was first observed at LEU reactors, short-baseline measurements by PROSPECT and STEREO have observed a similar-sized effect in the spectrum of ^{235}U , indicating a common mis-modelling of the interacting antineutrino energy spectrum of multiple fissile isotopes [36, 277, 280]. This spectral data-model discrepancy appears to be common across all prediction types, even after the introduction of updated fission yield and nuclear structure datasets [14]. The universality of this problem indicates an issue with an input common to both prediction techniques, such as the assumed theoretical shape of the beta spectra used in both calculations [304].

7.5 Future Improvements in Understanding Isotopic Neutrino Emissions

A range of ongoing and future experimental IBD-based efforts offer the promise of improving the precision of isotopic antineutrino flux and spectrum measurements. Most recently, the NEOS-II experiment was deployed in Sep, 2018, and just completed a ~ 500 -day reactor-on data taking period encompassing the entire fuel cycle of a single 2.8 GW commercial LEU core at the YoungKwang Hanbit nuclear power plant. The experiment aims to measure the IBD rate and energy spectrum of this reactor core at 24 m

baseline and perform an analysis of antineutrino spectrum and flux evolution. While its IBD statistics are unlikely to approach those provided by Daya Bay, its single-core measurement enables it to observe a broader range of reactor fuel content, potentially enabling isotopic measurements comparable to Daya Bay and RENO. Plausible gains in isotopic IBD yield measurement precision achievable in a single-core LEU experiment are overviewed in Ref. [273].

Beyond this, a pair of proposed future high-precision short-baseline reactor experiments aim to build on recent successes utilizing neutrinos to enhance understanding of nuclear data. The PROSPECT collaboration has proposed a follow-up measurement with an improved detector called PROSPECT-II to be deployed at 7-9 m from the High Flux Isotope Reactor at Oak Ridge National Lab [44]. The proposed run plan will increase its acquired IBD dataset by more than a factor of five over PROSPECT's first run, alongside an increased signal-to-background ratio. Additionally, PROSPECT plans a new measurement of the absolute flux of neutrinos from ^{235}U reaching a $\sim 2.5\%$ precision primarily limited by knowledge of the HFIR reactor core's thermal power. These measurements will provide an important test of theoretical models in a simple system primarily composed of a single fissile isotope, ^{235}U . The expected ^{235}U spectrum measurement uncertainties of PROSPECT-II uncertainty are shown in figure 15: its ^{235}U precision will substantially exceed Daya Bay, and will rival that of the theoretical models. Subsequent deployment of PROSPECT-II at an LEU reactor would allow correlated flux measurements between core types, further enhancing knowledge of individual isotopic contributions, again outlined in Ref. [273].

In southern China, a high-resolution ($<2\%/\sqrt{E \text{ (MeV)}}$) satellite detector for the JUNO project, called JUNO-TAO, is in the development phase and will be deployed at ~ 25 m from one LEU reactor at the Taishan nuclear power plant [47]. JUNO-TAO will collect a large (millions) IBD dataset with excellent energy resolution over multiple fuel cycles, which should enable searches for sub-structure in the neutrino spectrum from individual beta-decays, as shown in Figure 15. When analyzed in combination with a high-precision HEU experiment, such as that provided by PROSPECT-II, these datasets should enable major improvements in knowledge of the antineutrino spectrum produced after ^{239}Pu and ^{238}U fissions.

Data-model discrepancies have been authoritatively demonstrated by recent high-precision reactor antineutrino measurements. A resolution of this picture will likely require not just improvements in IBD datasets, but also the advancement of a variety of non-IBD nuclear physics and neutrino datasets. An overview of relevant recommendations for improving non-IBD datasets can be found in Refs. [51, 53].

On the conversion prediction side, recent Russian measurements of aggregate beta spectrum/yield ratios have cast doubt on the accuracy of the original ILL datasets [144,

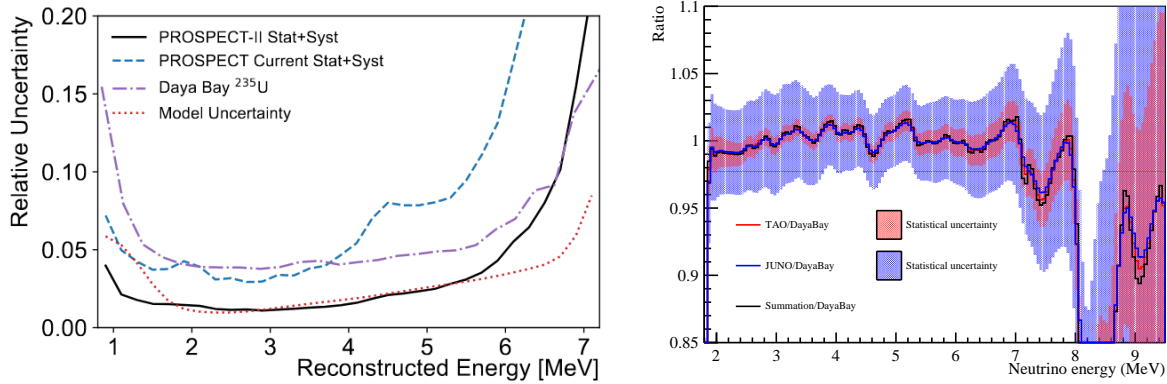


Figure 15: Left: PROSPECT-II ^{235}U spectrum measurement uncertainties after two years of data-taking. From [45]. Right: Comparison of projected JUNO-TAO and JUNO measurements and uncertainties with Daya Bay measurements, assuming that the true LEU reactor spectrum measured by JUNO-TAO and JUNO is given by Ref. [14]; JUNO-TAO’s sensitivity to fine structure in the LEU reactor antineutrino spectrum is clearly illustrated. From Ref. [47].

145]. To authoritatively resolve this issue, a high-precision aggregate beta spectrum measurement using modern neutron facilities and measurement techniques should be performed for all major and minor fission isotopes; such a measurement should be achievable at a number of US-based neutron facilities. The robustness of both conversion and summation predictions could be enhanced via measurement of beta spectrum shapes for a few forbidden beta decay transitions of high- Q isotopes that provide a dominant contribution to the high-energy reactor antineutrino spectrum. Such a measurement would verify this key theoretical input to both calculations. For summation predictions, continuation of total absorption gamma spectroscopy (TAGS) measurements should be carried out to further minimize the incidence of Pandemonium-affected data in the nuclear data.

Up to this point, direct antineutrino measurements have been unable to test the accuracy of summation modelling below the 1.8 MeV proton IBD interaction threshold. High-precision measurements of recoil spectra from the threshold-free $\text{CE}\nu\text{NS}$ interaction at reactors offer the promise of addressing this current weakness in the global antineutrino flux picture.

8 Priorities for Improving Reactor Antineutrino Detection (NF10)

8.1 Key Takeaways

- A broad range of detection technologies are required to cover the full range of physics topics accessible via detection of reactor neutrinos using coherent-neutrino nucleus scattering.
- Small short baseline and large medium baseline reactor neutrino experiments require improvements in particle identification, light collection, and/or target composition to achieve future fundamental and applied physics goals.
- Technology used in reactor neutrino physics overlaps with those used in direct dark matter searches and in a range of neutrino physics topics, such as long-baseline beam neutrino oscillations, neutrinoless double beta decay, solar neutrino physics, geoneutrino detection, and more.

8.2 Reactor Antineutrino Detection Technologies

The reactor neutrino sub-field has been particularly prolific within the broader scope of neutrino physics in recent years. However, persistent tensions between the results of multiple short baseline experiments, together with the yet to-be realized detection of $\text{CE}\nu\text{NS}$ using reactor neutrinos, are strong reasons to continue improving on current techniques and developing new enabling technologies. To ensure a broad range for known and unknown physics with reactor neutrinos, it is necessary that new experiments and development efforts cover a wide range of detection principles. In this Section, we provide a condensed description of the many current initiatives in pursuit of low-threshold and/or MeV-scale reactor antineutrino detection.

8.3 Very Low Energy Detection

Coherent scattering of neutrinos off nuclei has become a growing field of interest in reactor neutrino physics and neutrino physics in general. For coherent scattering, the neutrino energy transfer occurs with the entire nucleus rather than a single nucleon, meaning that energy transfer has to be very low. In addition, a large fraction of transferred energy is released as heat or lost due to quenching effects. While coherent scattering was already discovered at high energy spallation neutron sources, fully coherent scattering would happen only at low reactor energies and thus very sensitive new detector technologies are required. These detectors need to offer a low threshold and low noise levels. In addition, those detectors require a thick shielding and overburden as they are running close to a continuous reactor, as opposed to have an accelerator-based timing reference signal to suppress background.

The use of low-threshold detectors for performing novel non-standard physics searches

was described previously in Sections 5 and 6. Since coherent scattering detectors in reactor neutrino physics are sensitive to very low energies, implemented technologies also offer promise beyond reactor neutrino detection. For example, such a technology would also be useful in probing the scattering of low-mass dark matter. First results have already been delivered on these topics [305]. In the following, different types of low energy detectors in the context of coherent neutrino nucleus scattering are discussed.

P-type High Purity Germanium Detectors. These detectors belong to the class of ionization detectors. Opposed to conventional n-type point contact technology, p-type point contact permits high purity Ge detectors to bypass the characteristic limited charge collection efficiency and degraded energy resolution. This results in reduced capacitance while offering a large detector volume of about 1 kg per detector unit. The small value of the capacitance results in low electronic noise and allows to lower the detection threshold to values between 200 and 300 eVee. A mechanical cooling is commonly used and shielding is either employed via sandwiches of lead, copper, polyethylene or active vetoing through scintillation crystals. There are four major experiments at the commissioning or data-taking stage that could reveal a positive detection of reactor neutrino CE ν NS in the near future: CONUS [306], NuGEN [208], TEXONO [307] and the NCC-1701 vessel at Dresden-II nuclear reactor [39].

Skipper Si CCD. In the most general sense, the interaction principle of Charge-Coupled Device (CCD) is based on the photoelectric effect, where incident photons are absorbed in a silicon substrate generating as a consequence one or more electron-hole pairs. In conventional scientific CCDs, low-frequency readout noise results in variations in the measured charge per pixel creating a fundamental limitation on precise single-photon counting. Some initiatives like CONNIE [308] have been applying CCDs to neutrino detection for many years, providing an upper limit for reactor CE ν NS event rate.

However, in the recent years, a new noise-reduction technique has emerged based in the use of a floating gate output stage to perform repeated charge measurements for each pixel. This multiple readout technique was implemented in the form of a Skipper-CCD achieving ultra-low readout noise that stood several orders of magnitude below values obtained with conventional CCD detection [309]. The application of this novel technology is expected to bring unprecedented detection precision down to the eV energy scale. CONNIE recently upgraded to Skipper-CCDs [246] showing preliminary stable and very low values of readout noise. Another new initiative called ν IOLETA has taken the chance to join the efforts for building a kg-scale experiment based on Skipper-CCDs projecting a 90% C.L observation of CE ν NS in 1.5 days of data taking.

Besides allowing high precision measurements of the SM at low energies, Skipper-CCD might enable a unique exploration of any physics hiding beyond that. Light-boson

mediated interactions, neutrino magnetic moment or dark matter searches are strong candidates to be investigated.

Noble Element Detectors. Noble element detectors, especially liquid xenon (LXe) and liquid argon (LAr) detectors, have been developed during the last decade mainly for direct dark matter searches. One of their main advantages is the extremely low detection threshold, a feature that makes noble element technology an excellent candidate to observe $CE\nu NS$. By means of time projection chambers filled with the aforementioned noble elements, low energy interactions like these have been sought by analyzing ionization signals, but to date the sensitivity in the few-electron region has been compromised by backgrounds. The most recognizable effort trying to observe $CE\nu NS$ using this technology is the RED collaboration [212]. This experiment uses a dual phase xenon detector of 100 kg fiducial volume. Ionization electrons created in the liquid phase are extracted through electric fields and amplified in the gaseous phase. The scintillation light of about 30 photons per electron in the gaseous phase is then detected by photosensors. This experiment has achieved a low background rate down to 4 ionization electrons while operating at the surface level. R&D efforts to reduce the single-and-few electrons background in noble liquid detectors are being pursued in the NUXE program [210, 211], which plans to use a 30 kg LXe active target to detect reactor neutrino $CE\nu NS$ events with signals down to single ionization electrons.

Synergies with dark matter searches using similar technologies exist. More concretely, the observation of $CE\nu NS$ using noble gases will provide valuable input for a precise signal and background modeling for next-generation LAr and LXe based dark matter experiments. Finally, it could present a new way to monitor the nuclear fuel cycle using neutrinos for nuclear safeguarding applications.

Bolometers. Bolometers are designed as heat detectors and measure phonons created by nuclear recoils. Operating at mK temperatures, these detectors are able to achieve very low thresholds down to 20 eV. Three collaborations, NUCLEUS [209, 245], Ricochet [213], and MINER [90], are following this strategy. NUCLEUS uses $CaWO_4$ and Al_2O_3 crystals, while Ricochet and MINER use Ge/Zn and Ge/Si targets, respectively. To ensure a reasonable energy resolution, the detector crystals in use have to be kept small, in the order of 10 g. An exception is MINER with a detector at the order of 1 kg, since they detect charged particles through phonons created by the charged particles in high field regions of the detector. Their detector therefore belongs rather to the class of ionization detectors. Besides MINER, also Ricochet can exploit ionization and heat signals. This allows them, from the comparison of these signals, to perform particle identification and therefore background rejection.

Crystal Scintillator Detectors. An alternative form of scintillation-based detectors revolves around crystal scintillators. One of the main advantages of this technology is

the high yield of photons produced by scintillator crystals while producing low amounts of background. The crystals are also relatively accessible and permit for the use of large and relatively inexpensive pieces. The NEON collaboration [310] uses short 15 kg NaI crystals to improve the light collection efficiency. Crystals are read out by PMTs on both ends. They achieve a 220 eV energy threshold. An active liquid scintillator veto is surrounding the target crystal. Data taking has started from December 2020 which includes 1 month reactor-off period.

Color Center Passive Detectors. Crystal defects have been identified as candidate for the detection of low energy nuclear recoils. Recently, it was proposed to use materials where these defects act as color centers and to use modern microscopic techniques, specifically selective plane illumination microscopy, to image individual radiation induced color centers in bulk volumes [311]. This technology could provide passive detectors for reactor CEvNS, both for basic science and also nuclear security applications.

8.4 IBD Detection Technology Improvements

Unlike the previously discussed very low energy detection of coherent neutrino nucleus scattering, reactor neutrino detection via inverse beta decay is well established. To improve the scalability and/or background rejection performance of IBD detectors, novel detector media are currently being investigated. These developments may improve the achievable physics precision of IBD-based detectors and increase their capability or versatility as reactor monitoring instruments.

^6Li -doped Organic Scintillators. The study of reactor antineutrinos has traditionally pivoted around organic scintillators. Among common requirements like high scintillation light yield and good optical transmission, organic scintillators need to provide excellent particle identification for fast neutrons and neutron captures in order to properly identify IBD interactions. To successfully fulfill these criteria organic scintillator compounds can be mixed with PSD-capabilities in mind and then doped with a neutron-catcher isotope like ^6Li .

Liquid PSD-capable scintillators with ^6Li -doping (LiLS) have already been produced and used in experiments like PROSPECT at the ton-scale [43]. Besides its PSD-capabilities, LiLS production is easily scalable which permits larger proton-rich targets with long-term stability at standard temperatures. A complementary alternative to LiLS that permits readily transportation and flexibility comes from ^6Li -doped plastic scintillators (LiPS). While historically plastics have been found to exhibit much poorer discrimination properties, in the recent years significant progress has been made in synthesizing stable PSD-capable plastic scintillators [312], even with dissolved ^6Li [313]. Some initiatives like the ROADSTR near-field working group [314] and SANDD [315] are currently developing novel prototypes for readily mobile reactor antineutrino detectors using PSD-

capable LiPS.

Water-based Liquid Scintillators. Monolithic optical detectors have a long history of success in neutrino physics via IBD or ES, from water Cherenkov detectors to liquid scintillator detectors. As new experiments push current limits into previously unexplored regions of phase space, a priority are advanced detection techniques for particle identification and background rejection. A promising new approach is given by exploiting Cherenkov and scintillation signals simultaneously using water-based organic liquid scintillators, i.e water is loaded with $\sim 10\%$ liquid scintillator [316, 317]. This technology is foreseen in the Eos experiment and could be deployed in planned experiments for reactor monitoring like AIT-NEO [318]. There are also potential synergies with future kilo-ton experiments like Theia [319] which will have a rich physics program including topics in high-energy, nuclear, geo, and astrophysics such as neutrino mass ordering, CP-violation in the leptonic sector, solar neutrinos, diffuse supernova neutrinos, neutrinos from supernova bursts, neutrinos from the Earth's crust, nucleon decay, and neutrinoless double beta decay with sensitivity towards normal neutrino mass ordering.

Powerful aspects are the particle identification (PID) capabilities offered from the Cherenkov/scintillation ratio [320]. This PID has the potential to significantly improve signal/background discrimination of alpha/beta and beta/gamma particles and arises from two sources: the time profile of scintillation light emitted in response to a recoiling proton may differ from electron-like events due to quenching effects and the ratio of Cherenkov to scintillation light will differ between heavier and lighter particles. Additionally, recent developments have demonstrated the capability to identify neutron/gamma particles through the pulse shape discrimination of the scintillation light [321].

Mixed and Slow Liquid Scintillators. Alternative approaches to improve discrimination power via the time profile of scintillation light exists. This can be achieved by using compound scintillators blended from two or more scintillator components. In addition, varying the concentration of fluors allows to slow down the scintillation pulse time profile. This allows in particular to distinguish between nuclear and electronic recoils. The recoil protons excite more triplet states of the solvent molecules than electrons or positrons, therefore leading to a different magnitude of quenching. These triplet states have longer decay times increasing the charge ratio in the tail of the scintillation pulse. Blended scintillators were successfully exploited for PID in the past [322, 323].

Opaque Scintillator. LiquidO is a detection approach relying on opaque scintillators that represents a departure from conventional scintillation detectors. The main principle resides in stochastically confining light around the production point by reducing the

scattering length of photons to below the cm level, while keeping the absorption length high enough to ensure a good light output [92]. The localised detection of trapped photons provides imaging of topological energy depositions that translates into superior event-by-event identification and position reconstruction. In order to capture the confined light, the detector is traversed by a tight array of optical wave-shifting fibers that collect the light at the interaction point and transport it to photodetectors, typically SiPMs, located at the end of each fiber. While LiquidO can have multiple fiber orientations running simultaneously to reach 3D imaging, it is possible to use timing, if the resolution is good enough, to infer the projected position along the fiber. The LiquidO detection technique is not limited to the use of scintillation. In fact, Cherenkov light can and has been detected this way. However, the use of scintillation is key for low energy neutrino detection. In addition to its imaging capabilities, the opaque medium of LiquidO offers unique opportunities for heavy loading (in the order of 10% or more), as the lack of a transparency requirement relaxes the constraints on the optical model.

An experimental proof-of-concept was successfully run in 2018, called Micro-LiquidO, with an active volume of 0.2 L. Its successor, called Mini-LiquidO, is currently in operation and completing data taking with a volume of 7.5 L. The first opaque scintillating medium used in both LiquidO detectors was NoWaSH [324], an admixture from LAB and PPO as the scintillator and paraffin wax to provide the opacity. This compound has displayed below-cm scattering lengths while keeping a high profile of photons per MeV. Above 40°C it mixes homogeneously with ease, while becoming highly viscous when cooling to room temperature. Preliminary studies of NoWaSH also support the possibility of metal loading into the admixture, a feature much needed for different physics goals. Other solutions for possible opaque scintillators exist [325] and are in the early stages of R&D within the LiquidO scientific consortium.

In the context of reactor antineutrino IBD detection, LiquidO could have the ability to separate positrons from electrons and gammas on an event-by-event basis, enabling a major improvement of the signal-to-background ratio and reducing the reliance on overburden. LiquidO's native muon-tracking capability with sub-cm precision is also expected to enable a tight control of cosmogenically produced backgrounds. A full 5 ton reactor neutrino program detector has been funded by the EIC-Pathfinder-2021 European program and will start construction in early 2023. LiquidO technology is also actively being considered for the detection of solar neutrinos using indium, geoneutrinos, accelerator neutrinos, and double beta decay [92].

Gd-doped Water Gadolinium-doping has long been recognized as a key advance in the context of enhancing sensitivity to neutrons and thus antineutrinos in IBD detectors. The Super-Kamiokande gadolinium upgrade [326] reflects the importance of this technological enhancement for fundamental neutrino physics at the MeV scale. Similarly, Gd-doping presents the opportunity to improve sensitivity to reactors in large-

scale detectors, especially for mid-to-far-field monitoring and exclusion applications. Detectors such as the proposed kiloton-scale AIT-NEO detector [318] will permit exploration of further enhancements to the sensitivity of gadolinium-doped water detectors in both domains. For example the use of smaller and/or faster photosensors offers the prospect of improved vertex resolution compared to SK-Gd, with beneficial effects on fiducialization and background rejection. The scale of the detector also permits detailed experimental validation of the performance of technologies such as wavelength shifting plates, and new methods for in-situ characterization of water attenuation in doped media. Reconstruction of supernova directionality through the electron scatter channel may be achievable by tagging IBD events using the gadolinium dopant. AIT-NEO can also be used to study the combined benefits of the essential gadolinium dopant with those coming from alternative media such as water-based liquid scintillator.

8.5 Synergies

Given the technology overlap between reactor neutrinos and other rare event detection fields like dark matter or neutrinoless double-beta decay allow for interesting synergies that could be exploited. We discuss here some of these synergies, leaving the broader picture of potential applications to the next section.

- High Purity Ge detectors: low threshold detection allows for $0\nu\beta\beta$ decay, gamma and x-ray spectroscopy.
- Plastic Scintillators: their flexibility could be practical for reactor monitoring purposes through readily mobile neutrino detectors (see Sec. 9).
- Skipper CCD: nuclear spectroscopy, massive multiplexed optical/near-infrared cosmic surveys to study the dark sector, direct DM searches.
- Bolometers: their sensitivity to nuclear recoil make them ideal for dark matter/axion searches or probing the structure of nuclei.
- Noble liquids: accurate signal and background modeling for the next generation of dark matter experiments.
- Water-based scintillators: strong PID capabilities and broad energy range would allow multi-disciplinary research, including BSM physics like $0\nu\beta\beta$ decay or proton decay.
- Opaque scintillators: background suppression and flexible doping allow for multiple types of neutrino research, like $0\nu\beta\beta$ or solar neutrinos.

9 Applications of Reactor Neutrinos (NF07)

9.1 Key Takeaways

- Neutrino measurements for fundamental physics and nonproliferation applications require strongly overlapping technology and workforce capabilities.
- There are strong synergies between the future scientific goals, nuclear data needs, and technology pathways of both fields.
- Stakeholders for both fundamental and applied neutrino physics programs would benefit from coordination of investments in reactor-based experiments and demonstrations.

9.2 Antineutrino Applications Overview

Measurement of antineutrinos can provide information about the operation of a nuclear reactor as well as addressing important science goals for the Neutrino Physics community. Application of reactor antineutrino detection technology, the development of which has largely been motivated by the pursuit of fundamental scientific discovery, enables remote monitoring of nuclear reactors which has the potential to address nuclear energy and security problems. Conversely, engagement and support from these application communities could provide additional impetus for investments in improving reactor antineutrino flux predictions and detection technology, benefiting scientific efforts at such facilities.

Here, we describe mutual benefits that the scientific and application communities could enjoy from strong and enduring engagement.

9.3 Potential Societal Benefits from the Application of Neutrino Detection

The preceding sections of this white paper describe the scientific case for using reactor neutrinos to help understand properties of the Standard Model and BSM physics. In addition, neutrinos from reactors can be leveraged to gain information on the reactor itself or nuclear science at large. Currently, there are over 400 commercial and 200 research reactors operating worldwide, the former of which produce approximately 10% of the globe's electricity. Nuclear reactors present a viable clean energy source which can help combat the effects of climate change, and more reactors are projected to be constructed every year. However, concern over the misuse of nuclear technologies and materials is one of the several impediments to the widespread adoption of this power source. Antineutrino detection can potentially support the safe and peaceful use of nuclear energy as a non-intrusive, remote measurement method to increase confidence and transparency by verifying that reactors are being used in a manner consistent with their declared purpose. Furthermore, reactor neutrino emissions are inherently coupled

to underlying nuclear data such as fission yields and the characteristics of short-lived beta-unstable isotopes, and neutrino measurements can help to improve our knowledge of these parameters [53].

Neutrino physicists have proposed several uses of neutrino detection to monitor reactors and spent nuclear fuel, as well as completing several demonstrations close to reactors [84]. The monitoring concepts proposed can roughly be grouped into two categories, near-field and far-field. Near-field monitoring concepts typically involve ton-scale detectors that are located within ~ 100 m of a reactor core. Ideally, such a system would be able to operate with limited overburden to provide more flexibility and avoid the need for modifications to a facility or the fortunate circumstance of an existing deployment location that provides substantial cosmic background attenuation. Near-field systems can potentially determine reactor status (on/off), power level, and fissile content. Far-field monitoring concepts typically involve below-ground detectors of hundred ton to several hundred kiloton scale, located well beyond the facility boundary ($\sim 2 - 200$ km from the reactor core). Demonstration of these concepts has been encouraged by an enduring NNSA strategic goal to demonstrate the capability to remotely monitor nuclear reactors using antineutrinos. Potential benefits include a reduction in intrusiveness from the perspective of the country being monitored, the elimination of any potential for interference with facility operations, and the ability to exclude the possibility of reactor operations over radii as large as ~ 200 km. Cost and practicality must also be carefully assessed due to the rapid fall-off in antineutrino flux with increasing standoff, which of necessity implies larger detector sizes for timely signal accumulation and increasing overburden for background suppression.

The Nu Tools study [52], commissioned by the National Nuclear Security Administration (NNSA) Office of Defense Nuclear Nonproliferation Research & Development (DNN R&D), identified current and future areas of utility for neutrinos in nuclear energy and security via end-user engagement through over 40 interviews with potential stakeholders. The study identified several promising applications in which neutrino technology can service nuclear energy and security needs. The two most promising use case applications identified by the study were advanced reactor safeguards and future nuclear deals. Some forthcoming advanced reactor design are not amenable to existing safeguards techniques and neutrino detection might be able to play a role. Applications to safeguards of spent fuel and nuclear accident response show some promise, although further study is needed. Notably, application of neutrino detection to the current fleet of nuclear reactors operated under safeguards overseen by the International Atomic Energy Agency was not found to be promising.

9.4 Overlaps between Applications and High Energy Physics Opportunities

The pursuit of fundamental discovery often motivates technology development that then enables new applications; however, in the context of neutrino physics there is the opportunity for the converse to also occur. For example, detectors with the ability to deploy above-ground and packaged for mobility have been identified as attractive by potential antineutrino monitoring end-users. As described in [84], applications-focused technology R&D in this direction informed the successful design efforts of the current generation of short baseline sterile neutrino searches at reactors which must also operate with limited overburden. Looking towards future possibilities, the deployment of monitoring detectors at different reactor types could provide information to further constrain and improve flux and spectrum predictions. To give a specific example, an antineutrino-based power diagnostic for the forthcoming Versatile Test Reactor could support the materials science mission of that facility, while also measuring the antineutrino emissions from a reactor with exotic fuel types and fast neutron spectra [327]. As discussed elsewhere in this whitepaper, precision flux and spectrum predictions could enable BSM physics searches using reactor neutrinos.

Mobile detectors able to measure spectra with common systematic uncertainties would be especially beneficial and have evident appeal for applications. Finally, if antineutrino detection is adopted as a means to monitor reactors at 10-100km standoff, this may present an opportunity for oscillation measurements at unique baselines that could reduce uncertainties on neutrino mixing parameters. Furthermore, such detectors could contribute to the Supernova early warning system.

9.5 Overlaps With Technology Development

Fundamental and applied neutrino science can both benefit from advances in detection technology. Cooperation on common goals and techniques can enable new physics probes and expand the application space of neutrino detection. Methods to reduce backgrounds and improve the energy resolution and efficiency of detectors utilizing Inverse Beta Decay (IBD) would improve the sensitivity of short baseline sterile neutrino searches and application observables. Detection of coherent elastic neutrino-nucleus scattering (CEvNS) at reactors is challenging, but if achieved with low enough threshold could provide unique measurements below the IBD threshold for applications as well as a rich physics program. Finally, directional neutrino detection would be another advance with strong mutual benefits. This capability would mitigate declared reactor backgrounds for far-field detection of undeclared facilities, enhance searches for the diffuse supernova background and geoneutrinos, and provide the source direction for optical observations of a core collapse supernova. Improvements in light collection, photo-detection, and fast inexpensive readout systems would also be of benefit to both science and applications.

9.6 Workforce Development Pipeline and Non-traditional Career Paths

The training early career HEP physicists receive in graduate programs related to neutrino physics experiments greatly benefits applied antineutrino research for nuclear safeguards. Alternatively, the relatively small scale of most application efforts often provides students and postdocs the opportunity to contribute to all aspects of an experimental particle physics project. Such opportunities ameliorate the ability of early career physicists to develop their own research programs and maintain a workforce pipeline. Institutions that focus on nuclear energy and safeguards technology provide an additional career option that enables physicists to continue to develop HEP relevant technical skills and make important societal contributions.

9.7 Realizing Synergies between Neutrino Physics and Neutrino Applications

As recommended by the Nu Tools study, stakeholders for both fundamental neutrino physics and applications would benefit from taking advantage of these overlaps and coordinating investments for detectors deployed at reactors [52]. Additionally, researchers in both fields would benefit from coordination within the community to identify key overlaps between goals through workshops, community engagements, and attending targeted conference series. Such organization could reduce redundancies in parallel technology development efforts and foster stronger interactions between experts across the wide range of neutrino science and its applications.

References

- [1] Way K and Wigner E 1948 *Phys. Rev.* **73** 1318
- [2] Vogel P, Schenter G K, Mann F M and Schenter R E 1981 Reactor Anti-neutrino Spectra and Their Application to Anti-neutrino Induced Reactions. 2. *Phys. Rev. C* **24** 1543–1553
- [3] Hayes A and Vogel P 2016 Reactor Neutrino Spectra *Ann. Rev. Nucl. Part. Sci.* **66** 219–244 (*Preprint arXiv:1605.02047*)
- [4] Sonzogni A, Johnson T and McCutchan E 2015 Nuclear structure insights into reactor antineutrino spectra *Phys. Rev. C* **91** 011301
- [5] Mention G, Fechner M, Lasserre T, Mueller T, Lhuillier D, Cribier M and Letourneau A 2011 The Reactor Antineutrino Anomaly *Phys. Rev. D* **83** 073006 (*Preprint arXiv:1101.2755*)
- [6] Abazajian K *et al* 2012 Light Sterile Neutrinos: A White Paper (*Preprint arXiv:1204.5379*)
- [7] Berryman J M and Huber P 2021 Sterile Neutrinos and the Global Reactor Antineutrino Dataset *JHEP* **01** 167 (*Preprint arXiv:2005.01756*)
- [8] Jaffke P and Huber P 2017 Determining reactor fuel type from continuous antineutrino monitoring *Phys. Rev. Applied* **8** 034005 (*Preprint arXiv:1612.06494*)
- [9] Bernstein A, Bowden N S and Erickson A S 2018 Reactors as a source of antineutrinos: the effect of fuel loading and burnup for mixed oxide fuels *Phys. Rev. Applied* **9** 014003 (*Preprint arXiv:1612.00540*)
- [10] Behera S P, Mishra D K and Pant L M 2020 Active-sterile neutrino mixing constraints using reactor antineutrinos with the ISMRAN setup *Phys. Rev. D* **102** 013002 (*Preprint arXiv:2007.00392*)
- [11] Carroll J, Coleman J, Lockwood M, Metelko C, Murdoch M, Schnellbach Y, Touramanis C, Mills R, Davies G and Roberts A 2018 Monitoring Reactor Anti-Neutrinos Using a Plastic Scintillator Detector in a Mobile Laboratory (*Preprint arXiv:1811.01006*)
- [12] Mueller T A *et al* 2011 Improved Predictions of Reactor Antineutrino Spectra *Phys. Rev. C* **83** 054615
- [13] Fallot M *et al* 2012 New antineutrino energy spectra predictions from the summation of beta decay branches of the fission products *Phys. Rev. Lett.* **109** 202504 (*Preprint arXiv:1208.3877*)

- [14] Estienne M *et al* 2019 Updated Summation Model: An Improved Agreement with the Daya Bay Antineutrino Fluxes *Phys. Rev. Lett.* **123** 022502 (*Preprint* arXiv:1904.09358)
- [15] Schreckenbach K, Colvin G, Gelletly W and Von Feilitzsch F 1985 Determination of the antineutrino spectrum from U-235 thermal neutron fission products up to 9.5 MeV *Phys. Lett. B* **160** 325–330
- [16] Von Feilitzsch F, Hahn A A and Schreckenbach K 1982 Experimental beta-spectra from Pu-239 and U-235 thermal neutron fission products and their correlated antineutrino spectra *Phys.Lett.* **B118** 162–166
- [17] Hahn A A *et al* 1989 Anti-neutrino Spectra From ^{241}Pu and ^{239}Pu Thermal Neutron Fission Products *Phys.Lett.* **B218** 365–368
- [18] Huber P 2011 On the determination of anti-neutrino spectra from nuclear reactors *Phys. Rev. C* **84** 024617 [Erratum: *Phys.Rev.C* 85, 029901 (2012)] (*Preprint* arXiv:1106.0687)
- [19] Qian X and Peng J C 2019 Physics with Reactor Neutrinos *Rept. Prog. Phys.* **82** 036201 (*Preprint* arXiv:1801.05386)
- [20] Link J M 2017 Scattering neutrinos caught in the act *Science* **357** 1098–1099 URL <https://www.science.org/doi/abs/10.1126/science.aao4050>
- [21] Reines F and Cowan C L 1959 Free anti-neutrino absorption cross-section. 1: Measurement of the free anti-neutrino absorption cross-section by protons *Phys. Rev.* **113** 273–279
- [22] Eguchi K *et al* (KamLAND) 2003 First results from KamLAND: Evidence for reactor anti-neutrino disappearance *Phys. Rev. Lett.* **90** 021802 (*Preprint* arXiv:hep-ex/0212021)
- [23] Araki T *et al* (KamLAND) 2005 Measurement of neutrino oscillation with KamLAND: Evidence of spectral distortion *Phys. Rev. Lett.* **94** 081801 (*Preprint* arXiv:hep-ex/0406035)
- [24] An F *et al* (Daya Bay) 2012 Observation of electron-antineutrino disappearance at Daya Bay *Phys. Rev. Lett.* **108** 171803 (*Preprint* arXiv:1203.1669)
- [25] Ahn J *et al* (RENO Collaboration) 2012 *Phys. Rev. Lett.* **108** 191802
- [26] Abe Y *et al* (Double Chooz) 2012 Indication of Reactor $\bar{\nu}_e$ Disappearance in the Double Chooz Experiment *Phys. Rev. Lett.* **108** 131801 (*Preprint* arXiv:1112.6353)
- [27] An F *et al* (Daya Bay) 2014 Spectral measurement of electron antineutrino

- oscillation amplitude and frequency at Daya Bay *Phys. Rev. Lett.* **112** 061801 (Preprint arXiv:1310.6732)
- [28] Pasierb E, Gurr H S, Lathrop J, Reines F and Sobel H W 1979 Detection of Weak Neutral Current Using Fission $\bar{\nu}_e$ on Deuterons *Phys. Rev. Lett.* **43** 96
- [29] Reines F, Gurr H S and Sobel H W 1976 Detection of anti-electron-neutrino e Scattering *Phys. Rev. Lett.* **37** 315–318
- [30] Deniz M *et al* (TEXONO) 2010 Measurement of $\bar{\nu}_e$ -Electron Scattering Cross-Section with a CsI(Tl) Scintillating Crystal Array at the Kuo-Sheng Nuclear Power Reactor *Phys. Rev. D* **81** 072001 (Preprint arXiv:0911.1597)
- [31] Declais Y *et al* 1995 Search for neutrino oscillations at 15-meters, 40-meters, and 95-meters from a nuclear power reactor at Bugey *Nucl. Phys. B* **434** 503–534
- [32] An F P *et al* (Daya Bay) 2016 Improved Search for a Light Sterile Neutrino with the Full Configuration of the Daya Bay Experiment *Phys. Rev. Lett.* **117** 151802 (Preprint arXiv:1607.01174)
- [33] Ko Y *et al* (NEOS) 2017 Sterile Neutrino Search at the NEOS Experiment *Phys. Rev. Lett.* **118** 121802 (Preprint arXiv:1610.05134)
- [34] Alekseev I *et al* (DANSS) 2018 Search for sterile neutrinos at the DANSS experiment *Phys. Lett. B* **787** 56–63 (Preprint arXiv:1804.04046)
- [35] Almazán H *et al* (STEREO) 2020 Improved sterile neutrino constraints from the STEREO experiment with 179 days of reactor-on data *Phys. Rev. D* **102** 052002 (Preprint arXiv:1912.06582)
- [36] Andriamirado M *et al* (PROSPECT) 2021 Improved short-baseline neutrino oscillation search and energy spectrum measurement with the PROSPECT experiment at HFIR *Phys. Rev. D* **103** 032001 (Preprint arXiv:2006.11210)
- [37] Serebrov A *et al* (Neutrino-4) 2021 Search for sterile neutrinos with the neutrino-4 experiment and measurement results *Phys. Rev. D* **104**(3) 032003 URL <https://link.aps.org/doi/10.1103/PhysRevD.104.032003>
- [38] Aguilar-Arevalo A *et al* (CONNIE) 2020 Search for light mediators in the low-energy data of the CONNIE reactor neutrino experiment *JHEP* **04** 054 (Preprint arXiv:1910.04951)
- [39] Colaresi J, Collar J I, Hossbach T W, Kavner A R L, Lewis C M, Robinson A E and Yocum K M 2021 First results from a search for coherent elastic neutrino-nucleus scattering at a reactor site *Phys. Rev. D* **104** 072003 (Preprint arXiv:2108.02880)
- [40] Littlejohn B, Luk K B and Ochoa-Ricoux J P , Snowmass 2021 Letter of Interest

- [41] Ochoa-Ricoux J P, Wang W, Wen L and Wurm M [The JUNO Experiment](#), Snowmass 2021 Letter of Interest
- [42] An F *et al* (JUNO) 2016 Neutrino Physics with JUNO *J. Phys. G* **43** 030401 (*Preprint arXiv:1507.05613*)
- [43] PROSPECT Collaboration [Forthcoming Science from the PROSPECT-I Data Set](#) Snowmass 2021 Letter of Interest
- [44] PROSPECT Collaboration [The Expanded Physics Reach of PROSPECT-II](#) Snowmass 2021 Letter of Interest
- [45] Andriamirado M *et al* 2021 PROSPECT-II Physics Opportunities (*Preprint arXiv:2107.03934*)
- [46] Cao G, Ochoa-Ricoux J P, Wang W, Wen L, Wurm M and Zhan L [The JUNO-TAO Experiment](#), Snowmass 2021 Letter of Interest
- [47] Abusleme A *et al* (JUNO) 2020 TAO Conceptual Design Report: A Precision Measurement of the Reactor Antineutrino Spectrum with Sub-percent Energy Resolution (*Preprint arXiv:2005.08745*)
- [48] Conant A J and Surukuchi P T [Prediction and Measurement of the Reactor Neutrino Flux and Spectrum](#), Snowmass 2021 Letter of Interest
- [49] PROSPECT Collaboration [PROSPECT: a Case Study of Neutrino Physics Research providing Enabling Capabilities for Nuclear Security Applications](#) Snowmass 2021 Letter of Interest
- [50] Akindele O A and Zhang X [Mutual Benefits derived from the Application of Neutrino Physics to Nuclear Energy & Safeguards](#), Snowmass 2021 Letter of Interest
- [51] 2019 'antineutrino spectra and their applications' IAEA Report INDC(NDS)-0786 <https://www-nds.iaea.org/publications/indc/indc-nds-0786.pdf>
- [52] Akindele O *et al* 2021 Nu Tools: Exploring Practical Roles for Neutrinos in Nuclear Energy and Security (*Preprint arXiv:2112.12593*)
- [53] Romano C *et al* 2022 Nuclear Data to Reduce Uncertainties in Reactor Antineutrino Measurements: Summary Report of the Workshop on Nuclear Data for Reactor Antineutrino Measurements (WoNDRAM) <https://www.osti.gov/servlets/purl/1842423/>
- [54] Argüelles C A, Bertólez-Martínez T and Salvado J 2022 Impact of Wave Package Separation in Low-Energy Sterile Neutrino Searches (*Preprint arXiv:2201.05108*)

- [55] Formaggio J A and Zeller G P 2012 From eV to EeV: Neutrino Cross Sections Across Energy Scales *Rev. Mod. Phys.* **84** 1307–1341 (*Preprint* arXiv:1305.7513)
- [56] Ritz S *et al* (HEPAP Subcommittee) 2014 [Building for Discovery: Strategic Plan for U.S. Particle Physics in the Global Context](#)
- [57] Barinov V V *et al* 2021 Results from the Baksan Experiment on Sterile Transitions (BEST) (*Preprint* arXiv:2109.11482)
- [58] Abratenko P *et al* (MicroBooNE) 2021 Search for an Excess of Electron Neutrino Interactions in MicroBooNE Using Multiple Final State Topologies (*Preprint* arXiv:2110.14054)
- [59] Denton P B 2021 Sterile Neutrino Searches with MicroBooNE: Electron Neutrino Disappearance (*Preprint* arXiv:2111.05793)
- [60] Argüelles C A, Esteban I, Hostert M, Kelly K J, Kopp J, Machado P A N, Martinez-Soler I and Perez-Gonzalez Y F 2021 MicroBooNE and the ν_e Interpretation of the MiniBooNE Low-Energy Excess (*Preprint* arXiv:2111.10359)
- [61] Aguilar-Arevalo A A *et al* (MiniBooNE) 2021 Updated MiniBooNE neutrino oscillation results with increased data and new background studies *Phys. Rev. D* **103** 052002 (*Preprint* arXiv:2006.16883)
- [62] Antonello M *et al* (MicroBooNE, LAr1-ND, ICARUS-WA104) 2015 A Proposal for a Three Detector Short-Baseline Neutrino Oscillation Program in the Fermilab Booster Neutrino Beam (*Preprint* arXiv:1503.01520)
- [63] Kopp J, Machado P A N, Maltoni M and Schwetz T 2013 Sterile Neutrino Oscillations: The Global Picture *JHEP* **05** 050 (*Preprint* arXiv:1303.3011)
- [64] Dentler M, Esteban I, Kopp J and Machado P 2020 Decaying Sterile Neutrinos and the Short Baseline Oscillation Anomalies *Phys. Rev. D* **101** 115013 (*Preprint* arXiv:1911.01427)
- [65] de Gouvêa A, Peres O, Prakash S and Stenico G 2020 On The Decaying-Sterile Neutrino Solution to the Electron (Anti)Neutrino Appearance Anomalies *JHEP* **07** 141 (*Preprint* arXiv:1911.01447)
- [66] 2019 *Neutrino Non-Standard Interactions: A Status Report* vol 2 (*Preprint* arXiv:1907.00991)
- [67] Batell B, Pospelov M and Ritz A 2009 Exploring Portals to a Hidden Sector Through Fixed Targets *Phys. Rev. D* **80** 095024 (*Preprint* arXiv:0906.5614)
- [68] Moss Z, Moulai M H, Argüelles C A and Conrad J M 2018 Exploring a nonminimal

- sterile neutrino model involving decay at IceCube *Phys. Rev. D* **97** 055017 (Preprint arXiv:1711.05921)
- [69] Klop N and Palazzo A 2015 Imprints of CP violation induced by sterile neutrinos in T2K data *Phys. Rev. D* **91** 073017 (Preprint arXiv:1412.7524)
- [70] de Gouvêa A, Kelly K J and Kobach A 2015 CP-invariance violation at short-baseline experiments in 3+1 neutrino scenarios *Phys. Rev. D* **91** 053005 (Preprint arXiv:1412.1479)
- [71] Gandhi R, Kayser B, Masud M and Prakash S 2015 The impact of sterile neutrinos on CP measurements at long baselines *JHEP* **11** 039 (Preprint arXiv:1508.06275)
- [72] Dutta D, Gandhi R, Kayser B, Masud M and Prakash S 2016 Capabilities of long-baseline experiments in the presence of a sterile neutrino *JHEP* **11** 122 (Preprint arXiv:1607.02152)
- [73] Aker M *et al* (KATRIN) 2021 Bound on 3+1 Active-Sterile Neutrino Mixing from the First Four-Week Science Run of KATRIN *Phys. Rev. Lett.* **126** 091803 (Preprint arXiv:2011.05087)
- [74] Acero M A *et al* (NOvA) 2021 An Improved Measurement of Neutrino Oscillation Parameters by the NOvA Experiment (Preprint arXiv:2108.08219)
- [75] Abe K *et al* (T2K) 2021 Improved constraints on neutrino mixing from the T2K experiment with 3.13×10^{21} protons on target *Phys. Rev. D* **103** 112008 (Preprint arXiv:2101.03779)
- [76] Bass M *et al* 2015 Baseline Optimization for the Measurement of CP Violation, Mass Hierarchy, and θ_{23} Octant in a Long-Baseline Neutrino Oscillation Experiment *Phys. Rev. D* **91** 052015 (Preprint arXiv:1311.0212)
- [77] Qian X, Zhang C, Diwan M and Vogel P 2013 Unitarity Tests of the Neutrino Mixing Matrix (Preprint arXiv:1308.5700)
- [78] Ellis S A R, Kelly K J and Li S W 2020 Leptonic Unitarity Triangles *Phys. Rev. D* **102** 115027 (Preprint arXiv:2004.13719)
- [79] Capozzi F, Li S W, Zhu G and Beacom J F 2019 DUNE as the Next-Generation Solar Neutrino Experiment *Phys. Rev. Lett.* **123** 131803 (Preprint arXiv:1808.08232)
- [80] 2022 JUNO physics and detector *Prog. Part. Nucl. Phys.* **123** 103927
- [81] Abi B *et al* (DUNE) 2020 Long-baseline neutrino oscillation physics potential of the DUNE experiment *Eur. Phys. J. C* **80** 978 (Preprint arXiv:2006.16043)

- [82] Abud A A *et al* (DUNE) 2021 Low exposure long-baseline neutrino oscillation sensitivity of the DUNE experiment (*Preprint arXiv:2109.01304*)
- [83] Abi B *et al* (DUNE) 2021 Supernova neutrino burst detection with the Deep Underground Neutrino Experiment *Eur. Phys. J. C* **81** 423 (*Preprint arXiv:2008.06647*)
- [84] Bernstein A, Bowden N, Goldblum B L, Huber P, Jovanovic I and Mattingly J 2020 Colloquium: Neutrino detectors as tools for nuclear security *Rev. Mod. Phys.* **92** 011003 (*Preprint arXiv:1908.07113*)
- [85] Ashenfelter J *et al* (PROSPECT) 2018 First search for short-baseline neutrino oscillations at HFIR with PROSPECT *Phys. Rev. Lett.* **121** 251802 (*Preprint arXiv:1806.02784*)
- [86] Haghghat A, Huber P, Li S, Link J M, Mariani C, Park J and Subedi T 2020 Observation of Reactor Antineutrinos with a Rapidly-Deployable Surface-Level Detector *Phys. Rev. Applied* **13** 034028 (*Preprint arXiv:1812.02163*)
- [87] Runkle R C, Bernstein A and Vanier P E 2010 Securing special nuclear material: Recent advances in neutron detection and their role in nonproliferation *Journal of Applied Physics* **108** 111101 (*Preprint arXiv:https://doi.org/10.1063/1.3503495*)
URL <https://doi.org/10.1063/1.3503495>
- [88] Aguilar-Arevalo A *et al* (CONNIE) 2019 Exploring low-energy neutrino physics with the Coherent Neutrino Nucleus Interaction Experiment *Phys. Rev. D* **100** 092005 (*Preprint arXiv:1906.02200*)
- [89] Billard J *et al* 2017 Coherent Neutrino Scattering with Low Temperature Bolometers at Chooz Reactor Complex *J. Phys. G* **44** 105101 (*Preprint arXiv:1612.09035*)
- [90] Agnolet G *et al* (MINER) 2017 Background Studies for the MINER Coherent Neutrino Scattering Reactor Experiment *Nucl. Instrum. Meth. A* **853** 53–60 (*Preprint arXiv:1609.02066*)
- [91] Albanese V *et al* (SNO+) 2021 The SNO+ experiment *JINST* **16** P08059 (*Preprint arXiv:2104.11687*)
- [92] Cabrera A *et al* 2021 Neutrino Physics with an Opaque Detector *Commun. Phys.* **4** 273 (*Preprint arXiv:1908.02859*)
- [93] Back A R *et al* (ANNIE) 2017 Accelerator Neutrino Neutron Interaction Experiment (ANNIE): Preliminary Results and Physics Phase Proposal (*Preprint arXiv:1707.08222*)

- [94] Askins M *et al* (Theia) 2020 THEIA: an advanced optical neutrino detector *Eur. Phys. J. C* **80** 416 (*Preprint* arXiv:1911.03501)
- [95] Vogel P, Wen L and Zhang C 2015 Neutrino Oscillation Studies with Reactors *Nature Commun.* **6** 6935 (*Preprint* arXiv:1503.01059)
- [96] Zyla P A *et al* (Particle Data Group) 2020 Review of Particle Physics *PTEP* **2020** 083C01
- [97] Davis R, Harmer D and Hoffman K 1968 *Phys. Rev. Lett.* **20** 1205
- [98] Abe S *et al* (KamLAND) 2008 Precision Measurement of Neutrino Oscillation Parameters with KamLAND *Phys. Rev. Lett.* **100** 221803 (*Preprint* arXiv:0801.4589)
- [99] Ahmad Q *et al* (SNO) 2002 Direct evidence for neutrino flavor transformation from neutral current interactions in the Sudbury Neutrino Observatory *Phys. Rev. Lett.* **89** 011301 (*Preprint* arXiv:nucl-ex/0204008)
- [100] Apollonio M *et al* (CHOOZ) 1999 Limits on neutrino oscillations from the CHOOZ experiment *Phys. Lett. B* **466** 415–430 (*Preprint* arXiv:hep-ex/9907037)
- [101] Boehm F *et al* 2001 Final results from the Palo Verde neutrino oscillation experiment *Phys. Rev. D* **64** 112001 (*Preprint* arXiv:hep-ex/0107009)
- [102] An F P *et al* (Daya Bay) 2016 The Detector System of The Daya Bay Reactor Neutrino Experiment *Nucl. Instrum. Meth. A* **811** 133–161 (*Preprint* arXiv:1508.03943)
- [103] de Kerret H *et al* (Double Chooz) 2022 The Double Chooz antineutrino detectors (*Preprint* arXiv:2201.13285)
- [104] Abe K *et al* (T2K) 2011 Indication of Electron Neutrino Appearance from an Accelerator-produced Off-axis Muon Neutrino Beam *Phys. Rev. Lett.* **107** 041801 (*Preprint* arXiv:1106.2822)
- [105] Adamson P *et al* (MINOS) 2011 Improved search for muon-neutrino to electron-neutrino oscillations in MINOS *Phys. Rev. Lett.* **107** 181802 (*Preprint* arXiv:1108.0015)
- [106] Abe Y *et al* (Double Chooz) 2012 Reactor electron antineutrino disappearance in the Double Chooz experiment *Phys. Rev. D* **86** 052008 (*Preprint* arXiv:1207.6632)
- [107] Adey D *et al* (Daya Bay) 2018 Measurement of the Electron Antineutrino Oscillation with 1958 Days of Operation at Daya Bay *Phys. Rev. Lett.* **121** 241805 (*Preprint* arXiv:1809.02261)

- [108] Abrahão T *et al* (Double Chooz) 2021 Reactor rate modulation oscillation analysis with two detectors in Double Chooz *JHEP* **01** 190 (*Preprint* arXiv:2007.13431)
- [109] Bak G *et al* (RENO) 2018 Measurement of Reactor Antineutrino Oscillation Amplitude and Frequency at RENO *Phys. Rev. Lett.* **121** 201801 (*Preprint* arXiv:1806.00248)
- [110] Abe K *et al* (Hyper-Kamiokande) 2018 Hyper-Kamiokande Design Report (*Preprint* arXiv:1805.04163)
- [111] Navas Nicolas D 2021 Neutrino oscillation physics in junos presentation at the 22nd International Workshop on Neutrinos from Accelerators (NuFact) URL [urllinktotalkabstractifany](#)
- [112] Abusleme A *et al* (JUNO) 2021 Calibration Strategy of the JUNO Experiment *JHEP* **03** 004 (*Preprint* arXiv:2011.06405)
- [113] Aartsen M G *et al* (IceCube) 2017 PINGU: A Vision for Neutrino and Particle Physics at the South Pole *J. Phys. G* **44** 054006 (*Preprint* arXiv:1607.02671)
- [114] Adrian-Martinez S *et al* (KM3Net) 2016 Letter of intent for KM3NeT 2.0 *J. Phys. G* **43** 084001 (*Preprint* arXiv:1601.07459)
- [115] Abi B *et al* (DUNE) 2020 Deep Underground Neutrino Experiment (DUNE), Far Detector Technical Design Report, Volume II: DUNE Physics (*Preprint* arXiv:2002.03005)
- [116] Aartsen M G *et al* (IceCube-Gen2) 2020 Combined sensitivity to the neutrino mass ordering with JUNO, the IceCube Upgrade, and PINGU *Phys. Rev. D* **101** 032006 (*Preprint* arXiv:1911.06745)
- [117] Chau N, Athayde Marcondes de André J P, Van Elewyck V, Kouchner A, Kalousis L and Dracos M (KM3NeT, JUNO) 2021 Neutrino mass ordering determination through combined analysis with JUNO and KM3NeT/ORCA *JINST* **16** C11007
- [118] Cabrera A *et al* 2020 Earliest Resolution to the Neutrino Mass Ordering? (*Preprint* arXiv:2008.11280)
- [119] Harrison P F, Perkins D H and Scott W G 2002 Tri-bimaximal mixing and the neutrino oscillation data *Phys. Lett. B* **530** 167 (*Preprint* arXiv:hep-ph/0202074)
- [120] Xing Z z 2002 Nearly tri bimaximal neutrino mixing and CP violation *Phys. Lett. B* **533** 85–93 (*Preprint* arXiv:hep-ph/0204049)
- [121] He X G and Zee A 2003 Some simple mixing and mass matrices for neutrinos *Phys. Lett. B* **560** 87–90 (*Preprint* arXiv:hep-ph/0301092)

- [122] Lindner M, Merle A and Rodejohann W 2006 Improved limit on θ_{13} and implications for neutrino masses in neutrino-less double beta decay and cosmology *Phys. Rev. D* **73** 053005 (Preprint arXiv:hep-ph/0512143)
- [123] Ge S F and Rodejohann W 2015 JUNO and Neutrinoless Double Beta Decay *Phys. Rev. D* **92** 093006 (Preprint arXiv:1507.05514)
- [124] Fong C S, Minakata H and Nunokawa H 2017 A framework for testing leptonic unitarity by neutrino oscillation experiments *JHEP* **02** 114 (Preprint arXiv:1609.08623)
- [125] Schael S *et al* (ALEPH, DELPHI, L3, OPAL, SLD, LEP Electroweak Working Group, SLD Electroweak Group, SLD Heavy Flavour Group) 2006 Precision electroweak measurements on the Z resonance *Phys. Rept.* **427** 257–454 (Preprint arXiv:hep-ex/0509008)
- [126] Hampel W *et al* (GALLEX) 1998 Final results of the ^{51}Cr neutrino source experiments in GALLEX *Phys. Lett. B* **420** 114–126
- [127] Kaether F, Hampel W, Heusser G, Kiko J and Kirsten T 2010 Reanalysis of the GALLEX solar neutrino flux and source experiments *Phys. Lett. B* **685** 47–54 (Preprint arXiv:1001.2731)
- [128] Abdurashitov J N *et al* (SAGE) 1999 Measurement of the response of the Russian-American gallium experiment to neutrinos from a ^{51}Cr source *Phys. Rev. C* **59** 2246–2263 (Preprint arXiv:hep-ph/9803418)
- [129] Abdurashitov J N *et al* 2006 Measurement of the response of a Ga solar neutrino experiment to neutrinos from an ^{37}Ar source *Phys. Rev. C* **73** 045805 (Preprint arXiv:nucl-ex/0512041)
- [130] Acero M A, Giunti C and Laveder M 2008 Limits on ν_e and $\bar{\nu}_e$ disappearance from Gallium and reactor experiments *Phys. Rev. D* **78** 073009 (Preprint arXiv:0711.4222)
- [131] Giunti C and Laveder M 2011 Statistical significance of the gallium anomaly *Phys. Rev. C* **83**(6) 065504 URL <https://link.aps.org/doi/10.1103/PhysRevC.83.065504>
- [132] Boireau G *et al* (NUCIFER) 2016 Online Monitoring of the Osiris Reactor with the Nucifer Neutrino Detector *Phys. Rev. D* **93** 112006 (Preprint arXiv:1509.05610)
- [133] Almazán H *et al* (STEREO) 2020 Accurate Measurement of the Electron Antineutrino Yield of ^{235}U Fissions from the STEREO Experiment with 119 Days of Reactor-On Data *Phys. Rev. Lett.* **125** 201801 (Preprint arXiv:2004.04075)

- [134] de Kerret H *et al* (Double Chooz) 2020 Double Chooz θ_{13} measurement via total neutron capture detection *Nature Phys.* **16** 558–564 (*Preprint arXiv:1901.09445*)
- [135] An F P *et al* (Daya Bay) 2016 Measurement of the Reactor Antineutrino Flux and Spectrum at Daya Bay *Phys. Rev. Lett.* **116** 061801 [Erratum: *Phys.Rev.Lett.* 118, 099902 (2017)] (*Preprint arXiv:1508.04233*)
- [136] Choi J *et al* (RENO) 2016 Observation of Energy and Baseline Dependent Reactor Antineutrino Disappearance in the RENO Experiment *Phys. Rev. Lett.* **116** 211801 (*Preprint arXiv:1511.05849*)
- [137] An F *et al* (Daya Bay) 2017 Evolution of the Reactor Antineutrino Flux and Spectrum at Daya Bay *Phys. Rev. Lett.* **118** 251801 (*Preprint arXiv:1704.01082*)
- [138] Adey D *et al* (Daya Bay) 2019 Extraction of the ^{235}U and ^{239}Pu Antineutrino Spectra at Daya Bay *Phys. Rev. Lett.* **123** 111801 (*Preprint arXiv:1904.07812*)
- [139] Bak G *et al* (RENO) 2019 Fuel-composition dependent reactor antineutrino yield at RENO *Phys. Rev. Lett.* **122** 232501 (*Preprint arXiv:1806.00574*)
- [140] Hayen L, Kostensalo J, Severijns N and Suhonen J 2019 First-forbidden transitions in the reactor anomaly *Phys. Rev. C* **100** 054323 (*Preprint arXiv:1908.08302*)
- [141] Berryman J M and Huber P 2020 Reevaluating Reactor Antineutrino Anomalies with Updated Flux Predictions *Phys. Rev. D* **101** 015008 (*Preprint arXiv:1909.09267*)
- [142] Giunti C, Li Y and Zhang Y 2020 KATRIN bound on 3+1 active-sterile neutrino mixing and the reactor antineutrino anomaly *JHEP* **05** 061 (*Preprint arXiv:1912.12956*)
- [143] Giunti C, Li Y F, Ternes C A and Xin Z 2021 Reactor antineutrino anomaly in light of recent flux model refinements (*Preprint arXiv:2110.06820*)
- [144] Kopeikin V I, Panin Y N and Sabelnikov A A 2021 Measurement of the Ratio of Cumulative Spectra of Beta Particles from ^{235}U and ^{239}Pu Fission Products for Solving Problems of Reactor-Antineutrino Physics *Phys. Atom. Nucl.* **84** 1–10
- [145] Kopeikin V, Skorokhvatov M and Titov O 2021 Reevaluating reactor antineutrino spectra with new measurements of the ratio between U235 and Pu239 β spectra *Phys. Rev. D* **104** L071301 (*Preprint arXiv:2103.01684*)
- [146] Giunti C, Ji X, Laveder M, Li Y and Littlejohn B 2017 Reactor Fuel Fraction Information on the Antineutrino Anomaly *JHEP* **10** 143 (*Preprint arXiv:1708.01133*)
- [147] Giunti C, Li Y, Littlejohn B and Surukuchi P 2019 Diagnosing the Reactor Antineutrino Anomaly with Global Antineutrino Flux Data *Phys. Rev. D* **99** 073005 (*Preprint arXiv:1901.01807*)

- [148] Aguilar A *et al* (LSND Collaboration) 2001 Evidence for neutrino oscillations from the observation of $\bar{\nu}_e$ appearance in a $\bar{\nu}_\mu$ beam *Phys. Rev. D* **64**(11) 112007 URL <https://link.aps.org/doi/10.1103/PhysRevD.64.112007>
- [149] Aguilar-Arevalo A A *et al* (MiniBooNE) 2013 Improved Search for $\bar{\nu}_\mu \rightarrow \bar{\nu}_e$ Oscillations in the MiniBooNE Experiment *Phys. Rev. Lett.* **110** 161801 (*Preprint* arXiv:1303.2588)
- [150] Aguilar-Arevalo A *et al* (MiniBooNE Collaboration) 2018 Significant Excess of Electronlike Events in the MiniBooNE Short-Baseline Neutrino Experiment *Phys. Rev. Lett.* **121**(22) 221801 URL <https://link.aps.org/doi/10.1103/PhysRevLett.121.221801>
- [151] Maltoni M and Schwetz T 2007 Sterile neutrino oscillations after first MiniBooNE results *Phys. Rev. D* **76** 093005 (*Preprint* arXiv:0705.0107)
- [152] Giunti C and Laveder M 2010 Short-Baseline $\bar{\nu}_\mu \rightarrow \bar{\nu}_e$ Oscillations *Phys. Rev. D* **82** 093016 (*Preprint* arXiv:1010.1395)
- [153] Giunti C and Laveder M 2011 3+1 and 3+2 Sterile Neutrino Fits *Phys. Rev. D* **84** 073008 (*Preprint* arXiv:1107.1452)
- [154] Gariazzo S, Giunti C, Laveder M and Li Y 2017 Updated Global 3+1 Analysis of Short-BaseLine Neutrino Oscillations *JHEP* **06** 135 (*Preprint* arXiv:1703.00860)
- [155] Dentler M, Hernández-Cabezudo A, Kopp J, Maltoni M and Schwetz T 2017 Sterile neutrinos or flux uncertainties? — Status of the reactor anti-neutrino anomaly *JHEP* **11** 099 (*Preprint* arXiv:1709.04294)
- [156] Dentler M, Hernández-Cabezudo A, Kopp J, Machado P A, Maltoni M, Martinez-Soler I and Schwetz T 2018 Updated Global Analysis of Neutrino Oscillations in the Presence of eV-Scale Sterile Neutrinos *JHEP* **08** 010 (*Preprint* arXiv:1803.10661)
- [157] Diaz A, Argüelles C, Collin G, Conrad J and Shaevitz M 2020 Where Are We With Light Sterile Neutrinos? *Phys. Rept.* **884** 1–59 (*Preprint* arXiv:1906.00045)
- [158] Aker M *et al* (KATRIN) 2022 Improved eV-scale Sterile-Neutrino Constraints from the Second KATRIN Measurement Campaign (*Preprint* arXiv:2201.11593)
- [159] Kwon H, Boehm F, Hahn A, Henrikson H, Vuilleumier J, Cavaignac J, Koang D, Vignon B, Von Feilitzsch F and Mossbauer R 1981 Search for Neutrino Oscillations at a Fission Reactor *Phys. Rev. D* **24** 1097–1111
- [160] Hoummada A, Lazrak Mikou S, Avenier M, Bagieu G, Cavaignac J and Holm Koang D 1995 Neutrino oscillations I.L.L. experiment reanalysis *Applied Radiation*

- and Isotopes* **46** 449 – 450 ISSN 0969-8043 URL <http://www.sciencedirect.com/science/article/pii/0969804395000488>
- [161] Serebrov A *et al* 2018 The first observation of effect of oscillation in Neutrino-4 experiment on search for sterile neutrino (*Preprint* arXiv:1809.10561)
- [162] Almazán H *et al* (STEREO) 2018 Sterile Neutrino Constraints from the STEREO Experiment with 66 Days of Reactor-On Data *Phys. Rev. Lett.* **121** 161801 (*Preprint* arXiv:1806.02096)
- [163] Y J Ko 2016 Status of NEOS-II Neutrino 2020: XXIX International Conference on Neutrino Physics and Astrophysics URL <http://doi.org/10.5281/zenodo.4140230>
- [164] Abreu Y *et al* (SoLid) 2017 A novel segmented-scintillator antineutrino detector *JINST* **12** P04024 (*Preprint* arXiv:1703.01683)
- [165] Gariazzo S, Giunti C, Laveder M and Li Y 2018 Model-independent $\bar{\nu}_e$ short-baseline oscillations from reactor spectral ratios *Phys. Lett. B* **782** 13–21 (*Preprint* arXiv:1801.06467)
- [166] Feldman J and Cousins R 1998 *Phys. Rev. D* **57** 3873
- [167] Agostini M and Neumair B 2020 Statistical Methods Applied to the Search of Sterile Neutrinos *Eur. Phys. J. C* **80** 750 (*Preprint* arXiv:1906.11854)
- [168] Andriamirado M *et al* (PROSPECT, STEREO) 2020 Note on arXiv:2005.05301, 'Preparation of the Neutrino-4 experiment on search for sterile neutrino and the obtained results of measurements' (*Preprint* arXiv:2006.13147)
- [169] Coloma P, Huber P and Schwetz T 2021 Statistical interpretation of sterile neutrino oscillation searches at reactors *Eur. Phys. J. C* **81** 2 (*Preprint* arXiv:2008.06083)
- [170] Giunti C, Li Y F, Ternes C A and Zhang Y Y 2021 Neutrino-4 anomaly: oscillations or fluctuations? *Phys. Lett. B* **816** 136214 (*Preprint* arXiv:2101.06785)
- [171] Giunti C 2020 Statistical Significance of Reactor Antineutrino Active-Sterile Oscillations *Phys. Rev. D* **101** 095025 (*Preprint* arXiv:2004.07577)
- [172] Berryman J M, Coloma P, Huber P, Schwetz T and Zhou A 2021 Statistical significance of the sterile-neutrino hypothesis in the context of reactor and gallium data (*Preprint* arXiv:2111.12530)
- [173] Adamson P *et al* (MINOS+, Daya Bay) 2020 Improved Constraints on Sterile Neutrino Mixing from Disappearance Searches in the MINOS, MINOS+, Daya Bay, and Bugey-3 Experiments *Phys. Rev. Lett.* **125** 071801 (*Preprint* arXiv:2002.00301)

- [174] Goldhagen K, Maltoni M, Reichard S and Schwetz T 2021 Testing sterile neutrino mixing with present and future solar neutrino data (*Preprint arXiv:2109.14898*)
- [175] Vinyoles N, Serenelli A M, Villante F L, Basu S, Bergström J, Gonzalez-Garcia M C, Maltoni M, Peña Garay C and Song N 2017 A new Generation of Standard Solar Models *Astrophys. J.* **835** 202 (*Preprint arXiv:1611.09867*)
- [176] Barinov V V *et al* 2022 A Search for Electron Neutrino Transitions to Sterile States in the BEST Experiment (*Preprint arXiv:2201.07364*)
- [177] Barinov V and Gorbunov D 2021 BEST Impact on Sterile Neutrino Hypothesis (*Preprint arXiv:2109.14654*)
- [178] Armbruster B *et al* 1998 KARMEN limits on $\nu_e \rightarrow \nu_\tau$ oscillations in $2 - \nu$ and $3 - \nu$ mixing schemes *Phys. Rev. C* **57** 3414–3424 (*Preprint arXiv:hep-ex/9801007*)
- [179] Auerbach L B *et al* (LSND) 2001 Measurements of charged current reactions of ν_e on ^{12}C *Phys. Rev. C* **64** 065501 (*Preprint arXiv:hep-ex/0105068*)
- [180] Conrad J M and Shaevitz M H 2012 Limits on Electron Neutrino Disappearance from the KARMEN and LSND ν_e - Carbon Cross Section Data *Phys. Rev. D* **85** 013017 (*Preprint arXiv:1106.5552*)
- [181] Abe K *et al* (T2K) 2015 Search for short baseline ν_e disappearance with the T2K near detector *Phys. Rev. D* **91** 051102 (*Preprint arXiv:1410.8811*)
- [182] Adamson P *et al* (MINOS+) 2020 Precision Constraints for Three-Flavor Neutrino Oscillations from the Full MINOS+ and MINOS Dataset *Phys. Rev. Lett.* **125** 131802 (*Preprint arXiv:2006.15208*)
- [183] Enqvist K, Kainulainen K and Thomson M J 1992 Stringent cosmological bounds on inert neutrino mixing *Nucl. Phys. B* **373** 498–528
- [184] Melchiorri A, Mena O, Palomares-Ruiz S, Pascoli S, Slosar A and Sorel M 2009 Sterile Neutrinos in Light of Recent Cosmological and Oscillation Data: A Multi-Flavor Scheme Approach *JCAP* **01** 036 (*Preprint arXiv:0810.5133*)
- [185] Hannestad S, Tamborra I and Tram T 2012 Thermalisation of light sterile neutrinos in the early universe *JCAP* **07** 025 (*Preprint arXiv:1204.5861*)
- [186] Archidiacono M, Fornengo N, Giunti C, Hannestad S and Melchiorri A 2013 Sterile neutrinos: Cosmology versus short-baseline experiments *Phys. Rev. D* **87** 125034 (*Preprint arXiv:1302.6720*)
- [187] Mirizzi A, Mangano G, Saviano N, Borriello E, Giunti C, Miele G and Pisanti O 2013 The strongest bounds on active-sterile neutrino mixing after Planck data *Phys. Lett. B* **726** 8–14 (*Preprint arXiv:1303.5368*)

- [188] Gariazzo S, Giunti C and Laveder M 2013 Light Sterile Neutrinos in Cosmology and Short-Baseline Oscillation Experiments *JHEP* **11** 211 (*Preprint arXiv:1309.3192*)
- [189] Bridle S, Elvin-Poole J, Evans J, Fernandez S, Guzowski P and Soldner-Rembold S 2017 A Combined View of Sterile-Neutrino Constraints from CMB and Neutrino Oscillation Measurements *Phys. Lett. B* **764** 322–327 (*Preprint arXiv:1607.00032*)
- [190] Feng L, Zhang J F and Zhang X 2017 A search for sterile neutrinos with the latest cosmological observations *Eur. Phys. J. C* **77** 418 (*Preprint arXiv:1703.04884*)
- [191] Knee A M, Contreras D and Scott D 2019 Cosmological constraints on sterile neutrino oscillations from Planck *JCAP* **07** 039 (*Preprint arXiv:1812.02102*)
- [192] Berryman J M 2019 Constraining Sterile Neutrino Cosmology with Terrestrial Oscillation Experiments *Phys. Rev. D* **100** 023540 (*Preprint arXiv:1905.03254*)
- [193] Gariazzo S, de Salas P F and Pastor S 2019 Thermalisation of sterile neutrinos in the early Universe in the 3+1 scheme with full mixing matrix *JCAP* **07** 014 (*Preprint arXiv:1905.11290*)
- [194] Adams M, Bezrukov F, Elvin-Poole J, Evans J J, Guzowski P, Fearraigh B O and Söldner-Rembold S 2020 Direct comparison of sterile neutrino constraints from cosmological data, ν_e disappearance data and $\nu_\mu \rightarrow \nu_e$ appearance data in a 3 + 1 model *Eur. Phys. J. C* **80** 758 (*Preprint arXiv:2002.07762*)
- [195] Hagstotz S, de Salas P F, Gariazzo S, Gerbino M, Lattanzi M, Vagnozzi S, Freese K and Pastor S 2021 Bounds on light sterile neutrino mass and mixing from cosmology and laboratory searches *Phys. Rev. D* **104** 123524 (*Preprint arXiv:2003.02289*)
- [196] Kopp J, Maltoni M and Schwetz T 2011 Are There Sterile Neutrinos at the eV Scale? *Phys. Rev. Lett.* **107** 091801 (*Preprint arXiv:1103.4570*)
- [197] Conrad J M, Ignarra C M, Karagiorgi G, Shaevitz M H and Spitz J 2013 Sterile Neutrino Fits to Short Baseline Neutrino Oscillation Measurements *Adv. High Energy Phys.* **2013** 163897 (*Preprint arXiv:1207.4765*)
- [198] Liao J, Marfatia D and Whisnant K 2019 MiniBooNE, MINOS+ and IceCube data imply a baroque neutrino sector *Phys. Rev. D* **99** 015016 (*Preprint arXiv:1810.01000*)
- [199] Denton P B, Farzan Y and Shoemaker I M 2019 Activating the fourth neutrino of the 3+1 scheme *Phys. Rev. D* **99** 035003 (*Preprint arXiv:1811.01310*)
- [200] de Gouvêa A and Kelly K J 2016 False Signals of CP-Invariance Violation at DUNE (*Preprint arXiv:1605.09376*)
- [201] Danilov M New results from the danss experiment Presented at EPS-HEP

- 2021 Virtual Conference, (July 27, 2021) [<https://indico.desy.de/event/28202/contributions/105957/>]
- [202] Fomin A Monte carlo simulation of neutrino-4 experiment Presented at Twentieth Lomonosov Conference, (August 20, 2021) [https://lomcon.ru/files/20LomCon/presentations/20Au_A/Fomin.pdf]
- [203] Xu J 2021 Status of the CHILLAX detector development Presented at Magnificent CE ν NS 2021 URL https://indico.cern.ch/event/1075677/contributions/4556726/attachments/2324669/3959372/M7_2021.pdf
- [204] Aguilar-Arevalo A *et al* (CONNIE) 2021 Search for coherent elastic neutrino-nucleus scattering at a nuclear reactor with CONNIE 2019 data (*Preprint* arXiv:2110.13033)
- [205] Bonet H *et al* (CONUS) 2021 Constraints on Elastic Neutrino Nucleus Scattering in the Fully Coherent Regime from the CONUS Experiment *Phys. Rev. Lett.* **126** 041804 (*Preprint* arXiv:2011.00210)
- [206] Choi J J, Park B J, Ha C, Kim K W, Kim S K, Kim Y D, Ko Y J, Lee H S, Lee S H and Olsen S L 2020 Improving the light collection using a new NaI(Tl) crystal encapsulation *Nucl. Instrum. Meth. A* **981** 164556 (*Preprint* arXiv:2006.02573)
- [207] Vidal M 2020 NEWS-G: Status Presented at Magnificent CE ν NS 2020 URL https://indico.cern.ch/event/943069/contributions/4104017/attachments/2146855/3618845/CEvNS_2020_MVidal.pdf
- [208] Belov V, Brudanin V, Egorov V, Filosofov D, Fomina M, Gurov Y, Korotkova L, Lubashevskiy A, Medvedev D, Pritula R, Rozova I, Rozov S, Sandukovsky V, Timkin V, Yakushev E, Yurkowski J and Zhitnikov I 2015 The nugen experiment at the kalinin nuclear power plant *Journal of Instrumentation* **10** P12011–P12011 URL <https://doi.org/10.1088/1748-0221/10/12/p12011>
- [209] Angloher G *et al* (NUCLEUS) 2019 Exploring CE ν NS with NUCLEUS at the Chooz nuclear power plant *Eur. Phys. J. C* **79** 1018 (*Preprint* arXiv:1905.10258)
- [210] Ni K 2020 Feasibility of a Liquid Xenon Detector for Reactor Neutrino Detection via CE ν NS Presented at Magnificent CE ν NS 2020 URL <https://indico.cern.ch/event/943069/contributions/4103991/attachments/2144259/3613800/Ni-CEvNS2020-Xe.pdf>
- [211] Ni K, Qi J, Shockley E and Wei Y 2021 Sensitivity of a Liquid Xenon Detector to Neutrino–Nucleus Coherent Scattering and Neutrino Magnetic Moment from Reactor Neutrinos *Universe* **7** 54

- [212] Akimov D *et al* 2017 Status of the RED-100 experiment *Journal of Instrumentation* **12** C06018–C06018 URL <https://doi.org/10.1088/1748-0221/12/06/c06018>
- [213] Augier C *et al* (Ricochet) 2021 Ricochet Progress and Status *19th International Workshop on Low Temperature Detectors (Preprint arXiv:2111.06745)*
- [214] Flores L J *et al* (SBC, CEvNS Theory Group at IF-UNAM) 2021 Physics reach of a low threshold scintillating argon bubble chamber in coherent elastic neutrino-nucleus scattering reactor experiments *Phys. Rev. D* **103** L091301 (*Preprint arXiv:2101.08785*)
- [215] Kerman S, Sharma V, Deniz M, Wong H T, Chen J W, Li H B, Lin S T, Liu C P and Yue Q (TEXONO) 2016 Coherency in Neutrino-Nucleus Elastic Scattering *Phys. Rev. D* **93** 113006 (*Preprint arXiv:1603.08786*)
- [216] Sharma V *et al* (TEXONO) 2021 Studies of quantum-mechanical coherency effects in neutrino-nucleus elastic scattering *Phys. Rev. D* **103** 092002 (*Preprint arXiv:2010.06810*)
- [217] Moroni G F 2021 Installing a Skipper-CCD sensor in Atucha 2 power reactor: current status Presented at Magnificent CEvNS 2021 URL https://indico.cern.ch/event/1075677/contributions/4556812/attachments/2324496/3959008/magnificent_cevns_2021%20%282%29.pdf
- [218] Abrahão T *et al* (Double Chooz) 2021 Search for signatures of sterile neutrinos with Double Chooz *Eur. Phys. J. C* **81** 775 (*Preprint arXiv:2009.05515*)
- [219] Choi J H *et al* (RENO) 2020 Search for Sub-eV Sterile Neutrinos at RENO *Phys. Rev. Lett.* **125** 191801 (*Preprint arXiv:2006.07782*)
- [220] An F P *et al* (Daya Bay) 2017 Study of the wave packet treatment of neutrino oscillation at Daya Bay *Eur. Phys. J. C* **77** 606 (*Preprint arXiv:1608.01661*)
- [221] de Gouvea A, de Romeri V and Ternes C A 2020 Probing neutrino quantum decoherence at reactor experiments *JHEP* **08** 018 (*Preprint arXiv:2005.03022*)
- [222] de Gouvêa A, De Romeri V and Ternes C A 2021 Combined analysis of neutrino decoherence at reactor experiments *JHEP* **06** 042 (*Preprint arXiv:2104.05806*)
- [223] Wang J *et al* (JUNO) 2021 Damping signatures at JUNO, a medium-baseline reactor neutrino oscillation experiment (*Preprint arXiv:2112.14450*)
- [224] Adey D *et al* (Daya Bay) 2018 Search for a time-varying electron antineutrino signal at Daya Bay *Phys. Rev. D* **98** 092013 (*Preprint arXiv:1809.04660*)
- [225] Abe Y *et al* (Double Chooz) 2012 First Test of Lorentz Violation with a Reactor-based Antineutrino Experiment *Phys. Rev. D* **86** 112009 (*Preprint arXiv:1209.5810*)

- [226] Basto-Gonzalez V S, Forero D V, Giunti C, Quiroga A A and Ternes C A 2021 Short-baseline oscillation scenarios at JUNO and TAO (*Preprint* arXiv:2112.00379)
- [227] Cerdeno D G, Fairbairn M, Jubb T, Machado P A N, Vincent A C and Boehm C 2016 Physics from solar neutrinos in dark matter direct detection experiments *JHEP* **05** 118 [Erratum: *JHEP* 09, 048 (2016)] (*Preprint* arXiv:1604.01025)
- [228] Fernandez-Moroni G, Harnik R, Machado P A N, Martinez-Soler I, Perez-Gonzalez Y F, Rodrigues D and Rosauero-Alcaraz S 2021 The physics potential of a reactor neutrino experiment with skipper-ccds: Searching for new physics with light mediators (*Preprint* arXiv:2108.07310)
- [229] Alarcon J M, Martin Camalich J and Oller J A 2012 The chiral representation of the πN scattering amplitude and the pion-nucleon sigma term *Phys. Rev. D* **85** 051503 (*Preprint* arXiv:1110.3797)
- [230] Alarcon J M, Geng L S, Martin Camalich J and Oller J A 2014 The strangeness content of the nucleon from effective field theory and phenomenology *Phys. Lett. B* **730** 342–346 (*Preprint* arXiv:1209.2870)
- [231] Cirelli M, Del Nobile E and Panci P 2013 Tools for model-independent bounds in direct dark matter searches *JCAP* **10** 019 (*Preprint* arXiv:1307.5955)
- [232] Hill R J and Solon M P 2015 Standard Model anatomy of WIMP dark matter direct detection II: QCD analysis and hadronic matrix elements *Phys. Rev. D* **91** 043505 (*Preprint* arXiv:1409.8290)
- [233] Tiffenberg J, Sofo-Haro M, Drlica-Wagner A, Essig R, Guardincerri Y, Holland S, Volansky T and Yu T T 2017 Single-electron and single-photon sensitivity with a silicon Skipper CCD *Phys. Rev. Lett.* **119** 131802 (*Preprint* arXiv:1706.00028)
- [234] Chavarria A E, Collar J I, Peña J R, Privitera P, Robinson A E, Scholz B, Sengul C, Zhou J, Estrada J, Izraelevitch F, Tiffenberg J, de Mello Neto J R T and Torres Machado D 2016 Measurement of the ionization produced by sub-keV silicon nuclear recoils in a ccd dark matter detector *Phys. Rev. D* **94**(8) 082007 URL <https://link.aps.org/doi/10.1103/PhysRevD.94.082007>
- [235] Jones K W and Kraner H W 1975 Energy lost to ionization by 254-eV ^{73}Ge atoms stopping in Ge *Phys. Rev. A* **11**(4) 1347–1353 URL <https://link.aps.org/doi/10.1103/PhysRevA.11.1347>
- [236] Scholz B J, Chavarria A E, Collar J I, Privitera P and Robinson A E 2016 Measurement of the low-energy quenching factor in germanium using an $^{88}\text{Y}/\text{Be}$ photoneutron source *Phys. Rev. D* **94**(12) 122003 URL <https://link.aps.org/doi/10.1103/PhysRevD.94.122003>

- [237] Bonhomme A *et al* 2022 Direct measurement of the ionization quenching factor of nuclear recoils in germanium in the keV energy range (*Preprint* arXiv:2202.03754)
- [238] Lenardo B G, Xu J, Pereverzev S, Akindele O A, Naim D, Kingston J, Bernstein A, Kazkaz K, Tripathi M, Awe C, Li L, Runge J, Hedges S, An P and Barbeau P S 2019 Low-energy physics reach of xenon detectors for nuclear-recoil-based dark matter and neutrino experiments *Phys. Rev. Lett.* **123**(23) 231106 URL <https://link.aps.org/doi/10.1103/PhysRevLett.123.231106>
- [239] Aprile E *et al* (XENON Collaboration) 2019 Light dark matter search with ionization signals in xenon1t *Phys. Rev. Lett.* **123**(25) 251801 URL <https://link.aps.org/doi/10.1103/PhysRevLett.123.251801>
- [240] Amaral D W *et al* 2020 Constraints on low-mass, relic dark matter candidates from a surface-operated supercdms single-charge sensitive detector *Phys. Rev. D* **102**(9) 091101 URL <https://link.aps.org/doi/10.1103/PhysRevD.102.091101>
- [241] Aguilar-Arevalo A *et al* (DAMIC Collaboration) 2020 Results on low-mass weakly interacting massive particles from an 11 kg d target exposure of damic at snolab *Phys. Rev. Lett.* **125**(24) 241803 URL <https://link.aps.org/doi/10.1103/PhysRevLett.125.241803>
- [242] Barak L *et al* (SENSEI Collaboration) 2020 Sensei: Direct-detection results on sub-gev dark matter from a new skipper ccd *Phys. Rev. Lett.* **125**(17) 171802 URL <https://link.aps.org/doi/10.1103/PhysRevLett.125.171802>
- [243] Agnes P *et al* (DarkSide Collaboration) 2018 Low-mass dark matter search with the darkside-50 experiment *Phys. Rev. Lett.* **121**(8) 081307 URL <https://link.aps.org/doi/10.1103/PhysRevLett.121.081307>
- [244] Abdelhameed A H *et al* (CRESST Collaboration) 2019 First results from the cresst-iii low-mass dark matter program *Phys. Rev. D* **100**(10) 102002 URL <https://link.aps.org/doi/10.1103/PhysRevD.100.102002>
- [245] Strauss R *et al* 2017 The ν -cleus experiment: A gram-scale fiducial-volume cryogenic detector for the first detection of coherent neutrino-nucleus scattering *Eur. Phys. J. C* **77** 506 (*Preprint* arXiv:1704.04320)
- [246] Nasteva I (CONNIE) 2021 Low-energy reactor neutrino physics with the CONNIE experiment (*Preprint* arXiv:2110.13620)
- [247] Akerib D S *et al* (LUX Collaboration) 2021 Improving sensitivity to low-mass dark matter in lux using a novel electrode background mitigation technique *Phys. Rev. D* **104**(1) 012011 URL <https://link.aps.org/doi/10.1103/PhysRevD.104.012011>

- [248] Settimo M 2020 Search for low-mass dark matter with the DAMIC experiment *arXiv e-prints* arXiv:2003.09497 (*Preprint* arXiv:2003.09497)
- [249] Estrada J 2020 (accessed September 23, 2021) *Observatory of Skipper CCDs Unveiling Recoiling Atoms* <https://astro.fnal.gov/science/dark-matter/oscura/>
- [250] Agnes P *et al* (DarkSide Collaboration) 2021 Calibration of the liquid argon ionization response to low energy electronic and nuclear recoils with darkside-50 *Phys. Rev. D* **104**(8) 082005 URL <https://link.aps.org/doi/10.1103/PhysRevD.104.082005>
- [251] Lenardo B G, Xu J, Pereverzev S, Akindede O A, Naim D, Kingston J, Bernstein A, Kazkaz K, Tripathi M, Awe C, Li L, Runge J, Hedges S, An P and Barbeau P S 2019 Low-energy physics reach of xenon detectors for nuclear-recoil-based dark matter and neutrino experiments *Phys. Rev. Lett.* **123**(23) 231106 URL <https://link.aps.org/doi/10.1103/PhysRevLett.123.231106>
- [252] Fuss A, Kaznacheeva M, Reindl F, Wagner F *et al* 2022 EXCESS workshop: Descriptions of rising low-energy spectra (*Preprint* arXiv:2202.05097)
- [253] Workshop E 2021 EXCESS Workshop 2021 URL <https://indico.cern.ch/event/1013203/>
- [254] Akerib D S *et al* 2020 Investigation of background electron emission in the lux detector *Phys. Rev. D* **102**(9) 092004 URL <https://link.aps.org/doi/10.1103/PhysRevD.102.092004>
- [255] Sierra D A, De Romeri V, Flores L J and Papoulias D K 2021 Axionlike particles searches in reactor experiments *Journal of High Energy Physics* **2021** 294 ISSN 1029-8479 URL [https://doi.org/10.1007/JHEP03\(2021\)294](https://doi.org/10.1007/JHEP03(2021)294)
- [256] Dent J B, Dutta B, Kim D, Liao S, Mahapatra R, Sinha K and Thompson A 2020 New directions for axion searches via scattering at reactor neutrino experiments *Phys. Rev. Lett.* **124**(21) 211804 URL <https://link.aps.org/doi/10.1103/PhysRevLett.124.211804>
- [257] Danilov M, Demidov S and Gorbunov D 2019 Constraints on hidden photons produced in nuclear reactors *Phys. Rev. Lett.* **122**(4) 041801 URL <https://link.aps.org/doi/10.1103/PhysRevLett.122.041801>
- [258] Singh L *et al* (TEXONO) 2019 Constraints on millicharged particles with low threshold germanium detectors at Kuo-Sheng Reactor Neutrino Laboratory *Phys. Rev. D* **99** 032009 (*Preprint* arXiv:1808.02719)
- [259] Almazán H *et al* 2022 Searching for Hidden Neutrons with a Reactor Neutrino

- Experiment: Constraints from the STEREO Experiment *Phys. Rev. Lett.* **128** 061801 (Preprint arXiv:2111.01519)
- [260] Cappiello C and Beacom J F 2019 Strong New Limits on Light Dark Matter from Neutrino Experiments *Phys. Rev.* **D100** 103011 (Preprint arXiv:1906.11283)
- [261] Andriamirado M *et al* (PROSPECT) 2021 Limits on Sub-GeV Dark Matter from the PROSPECT Reactor Antineutrino Experiment (Preprint arXiv:2104.11219)
- [262] Bramante J, Broerman B, Lang R F and Raj N 2018 Saturated Overburden Scattering and the Multiscatter Frontier: Discovering Dark Matter at the Planck Mass and Beyond *Phys. Rev. D* **98** 083516 (Preprint arXiv:1803.08044)
- [263] Bramante J, Broerman B, Kumar J, Lang R F, Pospelov M and Raj N 2019 Foraging for dark matter in large volume liquid scintillator neutrino detectors with multiscatter events *Phys. Rev. D* **99** 083010 (Preprint arXiv:1812.09325)
- [264] Bai Y and Berger J 2020 Nucleus Capture by Macroscopic Dark Matter *JHEP* **05** 160 (Preprint arXiv:1912.02813)
- [265] An F P *et al* (Daya Bay) 2017 Improved Measurement of the Reactor Antineutrino Flux and Spectrum at Daya Bay *Chin. Phys. C* **41** 013002 (Preprint arXiv:1607.05378)
- [266] Adey D *et al* (Daya Bay) 2019 Improved Measurement of the Reactor Antineutrino Flux at Daya Bay *Phys. Rev. D* **100** 052004 (Preprint arXiv:1808.10836)
- [267] Vogel P and Beacom J F 1999 Angular distribution of neutron inverse beta decay *Phys. Rev. D* **60** 053003
- [268] Zhang C, Qian X and Vogel P 2013 Reactor Antineutrino Anomaly with known θ_{13} *Phys. Rev. D* **87** 073018
- [269] Declais Y *et al* 1994 Study of reactor anti-neutrino interaction with proton at Bugey nuclear power plant *Phys. Lett. B* **338** 383–389
- [270] Greenwood Z *et al* 1996 Results of a two position reactor neutrino oscillation experiment *Phys. Rev. D* **53** 6054–6064
- [271] Giunti C 2017 Precise determination of the ^{235}U reactor antineutrino cross section per fission *Phys. Lett. B* **764** 145–149 (Preprint arXiv:1608.04096)
- [272] Giunti C 2017 Improved Determination of the ^{235}U and ^{239}Pu Reactor Antineutrino Cross Sections per Fission *Phys. Rev. D* **96** 033005 (Preprint arXiv:1704.02276)
- [273] Gebre Y, Littlejohn B and Surukuchi P 2018 Prospects for Improved Understanding of Isotopic Reactor Antineutrino Fluxes *Phys. Rev. D* **97** 013003 (Preprint arXiv:1709.10051)

- [274] Achkar B *et al* 1996 Comparison of anti-neutrino reactor spectrum models with the Bugey-3 measurements *Phys. Lett. B* **374** 243–248
- [275] Abe Y *et al* (Double Chooz) 2014 Improved measurements of the neutrino mixing angle θ_{13} with the Double Chooz detector *JHEP* **10** 086 [Erratum: *JHEP* 02, 074 (2015)] (Preprint arXiv:1406.7763)
- [276] Ashenfelter J *et al* (PROSPECT) 2019 Measurement of the Antineutrino Spectrum from ^{235}U Fission at HFIR with PROSPECT *Phys. Rev. Lett.* **122** 251801 (Preprint arXiv:1812.10877)
- [277] Almazán Molina H *et al* (STEREO) 2021 First antineutrino energy spectrum from ^{235}U fissions with the STEREO detector at ILL *Journal of Physics G* **48** 075107 (Preprint arXiv:2010.01876) URL <http://doi.org/10.1088/1361-6471/abd37a>
- [278] An F P *et al* (Daya Bay) 2021 Antineutrino Energy Spectrum Unfolding Based on the Daya Bay Measurement and Its Applications (Preprint arXiv:2102.04614)
- [279] An F P *et al* (PROSPECT, Daya Bay) 2021 Joint Determination of Reactor Antineutrino Spectra from ^{235}U and ^{239}Pu Fission by Daya Bay and PROSPECT (Preprint arXiv:2106.12251)
- [280] Almazán H *et al* (PROSPECT, STEREO) 2021 Joint Measurement of the ^{235}U Antineutrino Spectrum by Prospect and Stereo (Preprint arXiv:2107.03371)
- [281] Plompen A *et al* 2020 The joint evaluated fission and fusion nuclear data library, jeff-3.3. *Eur. Phys. J. A* **56** 181
- [282] Tuli J 1996 *Nucl. Inst. Meth. A* **506** 506
- [283] Matthews E F, Bernstein L A and Younes W 2021 Stochastically estimated covariance matrices for independent and cumulative fission yields in the endf/b-viii.0 and jeff-3.3 evaluations *Atomic Data and Nuclear Data Tables* **140C** 101441 ISSN 0092-640X URL <https://www.sciencedirect.com/science/article/pii/S0092640X21000279>
- [284] Fiorito L, Diez C, Cabellos O, Stankovskiy A, Van den Eynde G and Labeau P 2014 Fission yield covariance generation and uncertainty propagation through fission pulse decay heat calculation *Annals of Nuclear Energy* **69** 331–343 ISSN 0306-4549 URL <https://www.sciencedirect.com/science/article/pii/S0306454914000565>
- [285] Greenwood R, Helmer R, Putnam M and Watts K 1997 Measurement of beta-decay intensity distributions of several fission-product isotopes using a total absorption gamma-ray spectrometer *Nucl. Inst. Meth. A* **390** 95–154 ISSN 0168-9002 URL <https://www.sciencedirect.com/science/article/pii/S0168900297003562>

- [286] Algora A *et al* 2010 Reactor decay heat in ^{239}Pu : Solving the γ discrepancy in the 4–3000-s cooling period *Phys. Rev. Lett.* **105**(20) 202501 URL <https://link.aps.org/doi/10.1103/PhysRevLett.105.202501>
- [287] Fijałkowska A *et al* 2017 *Phys. Rev. Lett.* **119**(5) 052503 URL <https://link.aps.org/doi/10.1103/PhysRevLett.119.052503>
- [288] Rasco B *et al* 2016 Decays of the Three Top Contributors to the Reactor $\bar{\nu}_e$ High-Energy Spectrum, ^{92}Rb , $^{96\text{gs}}\text{Y}$, and ^{142}Cs , Studied with Total Absorption Spectroscopy *Phys. Rev. Lett.* **117** 092501
- [289] Valencia E *et al* 2017 Total Absorption γ -Ray Spectroscopy of β -Delayed Neutron Emitters ^{87}Br , ^{88}Br and ^{94}Rb *Phys. Rev. C* **95** 024320 (Preprint arXiv:1609.06128)
- [290] Guadilla V *et al* 2019 Total absorption γ -ray spectroscopy of niobium isomers *Phys. Rev. C* **100** 024311 (Preprint arXiv:1904.07036)
- [291] Guadilla V *et al* 2019 Large Impact of the Decay of Niobium Isomers on the Reactor $\bar{\nu}_e$ Summation Calculations *Phys. Rev. Lett.* **122** 042502
- [292] Zakari-Issoufou A *et al* (IGISOL) 2015 Total Absorption Spectroscopy Study of ^{92}Rb Decay: A Major Contributor to Reactor Antineutrino Spectrum Shape *Phys. Rev. Lett.* **115** 102503 (Preprint arXiv:1504.05812)
- [293] Rice S *et al* 2017 Total absorption spectroscopy study of the β decay of ^{86}Br and ^{91}Rb *Phys. Rev. C* **96** 014320 (Preprint arXiv:1704.01915)
- [294] Guadilla V *et al* 2019 Total absorption γ -ray spectroscopy of the β -delayed neutron emitters ^{137}I and ^{95}Rb *Phys. Rev. C* **100** 044305 (Preprint arXiv:1907.02748)
- [295] Schreckenbach K, Colvin G, Gelletly W and Von Feilitzsch F 1985 Determination of the antineutrino spectrum from ^{235}U thermal neutron fission products up to 9.5 meV *Physics Letters B* **160** 325–330 ISSN 0370-2693 URL <https://www.sciencedirect.com/science/article/pii/0370269385913371>
- [296] von Feilitzsch F, Hahn A and Schreckenbach K 1982 Experimental beta-spectra from ^{239}Pu and ^{235}U thermal neutron fission products and their correlated antineutrino spectra *Physics Letters B* **118** 162–166 ISSN 0370-2693 URL <https://www.sciencedirect.com/science/article/pii/0370269382906220>
- [297] Hahn A, Schreckenbach K, Gelletly W, von Feilitzsch F, Colvin G and Krusche B 1989 Antineutrino spectra from ^{241}Pu and ^{239}Pu thermal neutron fission products *Physics Letters B* **218** 365–368 ISSN 0370-2693 URL <https://www.sciencedirect.com/science/article/pii/0370269389915980>
- [298] Hayes A, Friar J, Garvey G, Jungman G and Jonkmans G 2014 Systematic

- Uncertainties in the Analysis of the Reactor Neutrino Anomaly *Phys. Rev. Lett.* **112** 202501 (Preprint arXiv:1309.4146)
- [299] Wang X B, Friar J L and Hayes A C 2016 Nuclear Zemach moments and finite-size corrections to allowed β decay *Phys. Rev. C* **94** 034314 (Preprint arXiv:1607.02149)
- [300] Dwyer D and Langford T 2015 Spectral Structure of Electron Antineutrinos from Nuclear Reactors *Phys. Rev. Lett.* **114** 012502 (Preprint arXiv:1407.1281)
- [301] Hayes A, Friar J, Garvey G, Ibeling D, Jungman G, Kawano T and Mills R W 2015 Possible origins and implications of the shoulder in reactor neutrino spectra *Phys. Rev. D* **92** 033015 (Preprint arXiv:1506.00583)
- [302] Hayes A C, Jungman G, McCutchan E, Sonzogni A A, Garvey G T and Wang X 2018 Analysis of the Daya Bay Reactor Antineutrino Flux Changes with Fuel Burnup *Phys. Rev. Lett.* **120** 022503 (Preprint arXiv:1707.07728)
- [303] Sonzogni A A, Lorek R J, Mattera A and McCutchan E A 2022 Can decay heat measurements tell us something about the Reactor Antineutrino Anomaly? (Preprint arXiv:2203.02382)
- [304] Sonzogni A, McCutchan E and Hayes A 2017 Dissecting Reactor Antineutrino Flux Calculations *Phys. Rev. Lett.* **119** 112501
- [305] Bonet H *et al* (CONUS) 2021 Novel constraints on neutrino physics beyond the standard model from the CONUS experiment (Preprint arXiv:2110.02174)
- [306] Bonet H *et al* 2021 Large-size sub-keV sensitive germanium detectors for the CONUS experiment *Eur. Phys. J. C* **81** 267 (Preprint arXiv:2010.11241)
- [307] Soma A K *et al* (TEXONO) 2016 Characterization and Performance of Germanium Detectors with sub-keV Sensitivities for Neutrino and Dark Matter Experiments *Nucl. Instrum. Meth. A* **836** 67–82 (Preprint arXiv:1411.4802)
- [308] Aguilar-Arevalo A, Bertou X, Bonifazi C, Butner M, Cancelo G, Vazquez A, Vergara B, Chavez C, Motta H, D’Olivo J, Anjos J, Estrada J, Fernandez Moroni G, Ford R, Foguel A, Torres K, Izraelevitch F, Kavner A, Kilminster B and Wagner S 2016 The connie experiment *Journal of Physics: Conference Series* **761** 012057
- [309] Tiffenberg J, Sofo-Haro M, Drlica-Wagner A, Essig R, Guardincerri Y, Holland S, Volansky T and Yu T T 2017 Single-electron and single-photon sensitivity with a silicon skipper ccd *Phys. Rev. Lett.* **119**(13) 131802 URL <https://link.aps.org/doi/10.1103/PhysRevLett.119.131802>
- [310] Choi J 2020 Neutrino elastic-scattering observation with nai[tl](neon) 047
- [311] Cogswell B K, Goel A and Huber P 2021 Passive Low-Energy Nuclear-Recoil

- Detection with Color Centers *Phys. Rev. Applied* **16** 064060 (Preprint arXiv:2104.13926)
- [312] Zaitseva N, Glenn A, Paul Martinez H, Carman L, Pawełczak I, Faust M and Payne S 2013 Pulse shape discrimination with lithium-containing organic scintillators *Nucl. Inst. Meth. A* **729** 747–754 ISSN 0168-9002 URL <https://www.sciencedirect.com/science/article/pii/S0168900213011741>
- [313] Zaitseva N, Rupert B L, Pawełczak I, Glenn A, Martinez H P, Carman L, Faust M, Cherepy N and Payne S 2012 Plastic scintillators with efficient neutron/gamma pulse shape discrimination *Nucl. Inst. Meth. A* **668** 88–93 ISSN 0168-9002 URL <https://www.sciencedirect.com/science/article/pii/S0168900211021395>
- [314] ROADSTR Near-Field Working Group ROADSTR: a Mobile Antineutrino Detector Platform for enabling Multi-Reactor Spectrum, Oscillation, and Application Measurements Snowmass 2021 Letter of Interest URL https://www.snowmass21.org/docs/files/summaries/NF/SNOWMASS21-NF9_NF7_ROADSTR_Mobile_Antineutrino-184.pdf
- [315] Li V A, Classen T M, Dazeley S A, Duvall M J, Jovanovic I, Mabe A N, Reedy E T and Sutanto F 2019 A prototype for sandd: A highly-segmented pulse-shape-sensitive plastic scintillator detector incorporating silicon photomultiplier arrays *Nucl. Inst. Meth. A* **942** 162334 ISSN 0168-9002 URL <https://www.sciencedirect.com/science/article/pii/S0168900219309209>
- [316] Yeh M, Hans S, Beriguete W, Rosero R, Hu L, Hahn R L, Diwan M V, Jaffe D E, Kettell S H and Littenberg L 2011 A new water-based liquid scintillator and potential applications *Nucl. Instrum. Meth. A* **660** 51–56
- [317] Caravaca J, Land B J, Yeh M and Orebi Gann G D 2020 Characterization of water-based liquid scintillator for Cherenkov and scintillation separation *Eur. Phys. J. C* **80** 867 (Preprint arXiv:2006.00173)
- [318] Askins M *et al* (WATCHMAN) 2015 The Physics and Nuclear Nonproliferation Goals of WATCHMAN: A WATER Cherenkov Monitor for ANTINEUTRINOS (Preprint arXiv:1502.01132)
- [319] Askins M *et al* (Theia) 2020 THEIA: an advanced optical neutrino detector *Eur. Phys. J. C* **80** 416 (Preprint arXiv:1911.03501)
- [320] Caravaca J, Descamps F B, Land B J, Yeh M and Orebi Gann G D 2017 Cherenkov and Scintillation Light Separation in Organic Liquid Scintillators *Eur. Phys. J. C* **77** 811 (Preprint arXiv:1610.02011)
- [321] Ford M, Zaitseva N P, Carman M L, Dazeley S A, Bernstein A, Glenn A

- and Akindele O A 2022 Pulse-shape discrimination in water-based scintillators (*Preprint* arXiv:2202.07625)
- [322] Buck C, Gramlich B, Lindner M, Roca C and Schoppmann S 2019 Production and Properties of the Liquid Scintillators used in the Stereo Reactor Neutrino Experiment *JINST* **14** P01027 (*Preprint* arXiv:1812.02998)
- [323] Kim B R *et al* 2015 Pulse shape discrimination capability of metal-loaded organic liquid scintillators for a short-baseline reactor neutrino experiment *Phys. Scripta* **90** 055302
- [324] Buck C, Gramlich B and Schoppmann S 2019 Novel opaque scintillator for neutrino detection *Journal of Instrumentation* **14** P11007–P11007 (*Preprint* arXiv:1908.03334) URL <https://doi.org/10.1088/1748-0221/14/11/p11007>
- [325] Wagner S, Grassi M and Cabrera A 2018 A hybrid organic/inorganic scintillator for high performance measurements (*Preprint* arXiv:1807.00628)
- [326] Abe K *et al* (Super-Kamiokande) 2022 First gadolinium loading to Super-Kamiokande *Nucl. Instrum. Meth. A* **1027** 166248 (*Preprint* arXiv:2109.00360)
- [327] Hill A 2019 Applied Antineutrino Physics 2018 Proceedings (*Preprint* arXiv:1911.06834)